Aus dem

Institut für Medizinische Psychologie

Institut der Universität München

Kommissarischer Vorstand: Prof. Dr. Maria del Sagrario Robles Martinez

Spatiotemporal regularities in the Brain: using endogenous stimuli in Functional Magnetic Resonance Imaging Studies.

Dissertation

zum Erwerb des Doktorgrades der Humanbiologie

an der Medizinischen Fakultät der

Ludwig-Maximilians-Universität zu München

vorgelegt von

Yu Gu

aus

Peking, China

Jahr

2024

Mit Genehmigung der Medizinischen Fakultät
der Universität München

Berichterstatter:	**Prof. Dr. Dr. h.c. mult. Ernst Pöppel**
Mitberichterstatter:	**PD Dr. Paul Reidler**
	Prof. Dr. Kathrin Koch
	PD Dr. Evgeny Gutyrchik
Mitbetreuung durch den promovierten Mitarbeiter:	**Dr. med. Marco Paolini**
Dekan:	**Prof. Dr. Thomas Gudermann**

Tag der mündlichen Prüfung: 29.11.2024

Table of Contents

Zusammenfassung

Die funktionelle Magnet-Resonanz-Tomographie (fMRT, oder fMRI) ist zu einer wesentlichen Methode in den Neurowissenschaften geworden. Es ist zum Beispiel möglich geworden, miteinander verschiedene neuronale Aktivierungs-Muster zu vergleichen wie etwa der Ruheaktivität mit verschiedenen Episoden von Gedächtnisinhalten. Viele Studien mit fMRI sind fokussiert auf neuronale Aktivierungen als Reaktion auf exogene Reize. Die Möglichkeit, auch endogene Reize zu nutzen ist in fMRI-Studien noch nicht hinreichend überprüft worden. Exogene Reize repräsentieren einen „bottom-up“ -Ansatz, um neuronale Charakteristiken in bestimmten experimentellen Situationen mit fMRI zu untersuchen. Im Gegensatz dazu sind endogene Reize eher mit „top-down“ -Regulationen assoziiert; diese werden vor allem in Verhaltens-Studien angewandt, um beispielsweise interkulturelle Unterschiede besser zu verstehen. In dieser Dissertation habe ich die Brauchbarkeit endogener Reize als experimentelles Paradigma in fMRI-Studien untersucht. Es ist die Absicht zu zeigen, dass endogene Reize verlässliche Charakteristiken raumzeitlicher Regulationen bei neuronalen Aktivierungen anzeigen. Es wird ein Rahmen („pipeline“) von Methoden vorgeschlagen, die einen Vergleich neuronaler Muster erlauben, indem eine Kombination von Methoden einschließlich „machine learning“ und verschiedener statistischer Verfahren mit und ohne endogener Reize eingesetzt wird. Zwei verschiedene Studienprotokolle, jede mit einer Einzelfall- und einer Gruppen-Studie, wurden analysiert. In diesen Studien hatten die Versuchspersonen die Aufgabe, bestimmte mentale Zustände unter endogener Kontrolle zu generieren. In einer Einzelfall-Studie wurde die morgendliche Routine von Aktivierungen analysiert; in einer anderen Einzelfall-Studie stand musikalische Imagination mit unterschiedlichen Tempi im Fokus; in einer Gruppen-Studie wurden positive und negative emotionale Szenarien im Detail betrachtet; in einer weiteren Gruppen-Studie wurden neuronale Muster bei der Herstellung von Zufallsfolgen von Zahlen und Wörtern aufgedeckt. Die Analysen zeigen, dass endogene Reize konsistente Unterschiede in der neurokognitiven Maschinerie anzeigen, wenn sie bei episodischen Gedächtnis-Studien eingesetzt werden. Es wird auch gezeigt, dass innere endogene Stimuli ähnliche Muster der neuronalen Aktivierung auslösen wie äußere exogene Reize. Die Ergebnisse legen nahe, dass das Paradigma endogener Reize bei kontrollierten Bedingungen als zuverlässig angesehen werden kann. Es wird darüber hinaus gezeigt, dass der vorgeschlagene Rahmen („pipeline“) der Methoden brauchbar ist, um raumzeitliche Muster in fMRI-Studien zu identifizieren.

Abstract

Functional magnetic resonance imaging (fMRI) is now an essential method in neurosciences. It has become possible to compare different neural activation patterns for instance between the resting state and different memory episodes. Many fMRI studies are focused on brain activities being a response to external stimuli. The feasibility and potential usefulness of endogenous stimuli has not been widely explored in fMRI studies. Exogenous stimuli provide a “bottom-up” approach for exploring neural characteristics for specific experimental situations in fMRI studies. On the contrary endogenous stimuli can be said to be associated more with “top-down” regulations; they are often applied in behavioral studies to better understand for instance intercultural differences. In this study, I explore the feasibility of endogenous stimuli in fMRI research as an experimental paradigm. It is intended to show that endogenous stimuli can elicit reliable characteristics in spatiotemporal regularities of neural activities. A pipeline of methods is suggested to allow comparisons of neural patterns with and without endogenous stimuli through a combination of methods including machine learning and various statistical tools. Two sets of studies, each containing one single case study and one group study were analyzed. The subjects were instructed in these experiments to generate specific mental conditions under endogenous subjective control. In a single-case study the morning routine of activities was analyzed; in another single-case study musical imagery with different tempi was in the focus; in a group study positive and negative emotional scenarios were looked at in detail; in another group study on random number and word generation different neural activation patterns were disclosed. The analyses indicate that endogenous stimuli can create consistent differences in the neurocognitive machinery when employed in episodic memory studies. It is also shown that internal, i.e., endogenous stimuli can elicit similar neural response patterns as external, i.e., exogenous stimuli. The results suggest that the paradigm using endogenous stimuli under controlled conditions can be considered to be reliable. Furthermore, it is indicated that the pipeline approach is a useful tool for identifying specific spatiotemporal patterns in fMRI studies.

List of abbreviations

fMRI = Functional Magnetic Resonance Imaging
EEG = Electroencephalogram
MEG = Magnetoencephalography
NIRS = Near-Infrared Spectroscopy
MRI = Magnetic Resonance Imaging
PET = Positron emission tomography
CT = Computed Tomography
DTI = Diffusion Tensor Imaging
BOLD =Blood-oxygen-level-dependent
DCM = Dynamic Causal Modeling
GLM = General Linear Model
GEE = Generalized Estimating Equations
HRF = Hemodynamic Response Function
ANOVA = Analysis of Variance
SPM = Statistical Parametric Mapping
MVPA = Multivariate Voxel Pattern Analysis
GNB = Gaussian Naïve Bayes
FLD = Fisher Linear Discriminant
RSA = Representational Similarity Analysis
RDM = Representational Dissimilarity Matrix
FCA = Functional Connectivity Analysis
DFC = Dynamic Functional Connectivity
ICA = Independent Component Analysis
PCA = Principal Component Analysis
LDA = Linear Discriminant Analysis
GMM = Greedy Modularity Maximization
EC = Effective Connectivity
GC = Granger Causality
MD = Mahalanobis Distance
DTW = Dynamic Time Warping
PnP = Pöppel-Non-Parametric
VTS = Virtual Typical Subject
GA = Group Analysis
AICHA = Atlas of Intrinsic Connectivity of Homotopic Areas
HOC = Harvard-Oxford Cortical
BL = Blindlady

AI = Artificial Intelligence
DNN = Deep Neural Network
RNN = Recurrent Neural Network
LSTM = Long-Short Term Memory
SVM = Support Vector Machine

AM = Autobiographical Memory
EM = Episodic Memory
ESK = Event Specific Knowledge
PTSD = Post-Traumatic Stress Disorder
ROI = Regions of Interest
DMN = Default Mode Network
PCC = Posterior Cingulate Cortex
mPFC = Medial Prefrontal Cortex
HF = Hippocampus
PHC = Para-Hippocampus
RSC = Retrosplenial Cortex
DLPFC = Dorsolateral Prefrontal Cortex
MTG = Middle Temporal Gyrus
SMG = Supramarginal Gyrus
AG = Angular Gyrus
LOC = Lateral Occipital Complex
rTP = Right Temporal Pole
PFC = Prefrontal Cortex

1. Introduction

For thousands of years, humans have wondered about the function and power of the brain. From ancient Greek mythology to modern sciences, from Egypt to Mesoamerica, human efforts to understand the brain and its internal functions have transcended time and space. The ever-evolving technologies of our times have aided the investigation of this beautiful yet mysterious organ within our body even further. Our perception and understanding of the brain have changed significantly over the years as technology advances. From early phrenology to imaging techniques like fMRI, EEG, MEG or NIRS, we have established increasingly accurate descriptions of the brains. The increasing computational powers over the past decades have also unlocked unprecedented possibilities for analysis by applying artificial intelligence to the computational neuroscience domain.

In the past decade, one particular domain of interest has been resting state fMRI (Raichle et al., 2001). Since then researchers have identified various complex brain networks like the default mode network (Bullmore & Sporns, 2009) which is thought to be involved in episodic memories and various other functions (Andrews-Hanna, 2012). While these studies have focused on the internal world of our brain, the feasibility of incorporating purely endogenous stimuli in fMRI studies has not been fully explored. Of over 100 million articles sourced on google scholar and various libraries, only a handful of studies discuss the application of endogenous stimuli in episodic memories with fMRI. More so, most of these studies focus on attention tasks using exogenous and endogenous stimuli (Franklin et al., 2005). However, as the definition of episodic memory goes, endogenous (internal) stimuli are inseparable from the concept. Hence I want to explore whether endogenous stimuli can be reliably used in neuroimaging studies - in the scope of episodic memory and beyond.

It should be noted that a great deal of understanding comes from comparison - comparing the signals from different conditions, the results from different tasks, and the patterns of the brain at different time points. If significant and robust differences can be identified, I can then draw conclusions through comparative methods. In this spirit, I sought to examine whether I can identify significant and robust results among the various endogenous-based episodic memory studies and beyond. The spatiotemporal pattern of the brain plays a vital role in understanding brain functionality and mechanics and is, therefore, the natural focus. Through fMRI technology, I could extract the patterns from the brain across time and examine the data from a combination of proven analytical tools. Here I created a flexible analysis pipeline that utilizes the power of machine learning, statistics, graph theory, non- parametric statistics, dissimilarity measures, and temporal pattern analysis tools to examine potential regularities and changes that may surface through the comparison of various conditions.

The studies, including two sets of single case and group study, were constructed and analyzed around the central topic of examining the feasibility of endogenous stimuli in fMRI studies. The investigation begins by examining the use and validity of endogenous stimuli in episodic memory-based paradigms with different task duration and types of stimuli. It then examines the possibility of combining the endogenous stimuli paradigm with semantic memory and information modification in conjunction with exogenous stimuli, extending the analysis to non-episodic memory studies that incorporate both endogenous and exogenous stimuli as controls. In all experiments, the participants were instructed to create specific conditions (morning routine, musical composition, positive/negative experience, random sequences) using endogenous control.

I used a wide range of data analysis methods, and statistical tools to explore regularities and changes in spatiotemporal patterns of the brain. In the following chapters, I will gradually unveil the history and background of neuroimaging and other domains involved. The details of the neuroimaging techniques, machine learning methods, connectivity, and graph theory applications are explored in Chapter 3. The statistical tools and temporal regularities analysis methods will be discussed in Chapters 4. After this, I will provide a review of episodic memory and endogenous stimuli in fMRI studies in Chapter 5. In Chapter 6, I will explain the research questions and framework used. In Chapter 7, the flexible analysis pipeline will be introduced. The different experiments conducted and their results - followed by a summary of the results and discussions - will be covered in the following chapters.

2. General Background

2.1. From Phrenology to Brain Networks

In phrenology developed in the 1800s, people once hypothesized that brain functions and personalities could be identified from the external characteristics of the skull (Fig.1). This, of course, was pseudoscience which was proven recently (Jones, Alfaro-Almagro, & Jbabdi, 2018). Nonetheless, this popular science concept attracted countless people to this intriguing domain. This research was the foundation of localization of function - a concept that certain areas of the brain are associated with specific functions.

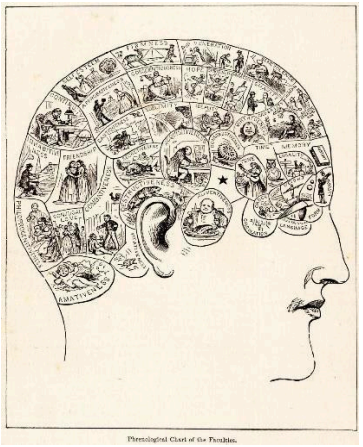

Figure 1: Phrenology chart from 19th century. (De Puy, 1879)

In order to investigate our brain with increasing details and clarity, neuroimaging techniques have evolved from highly uncomfortable pneumoencephalography to MRI and CT scans that are no longer invasive and are much safer over the past century.

In particular, functional magnetic resonance imaging (fMRI) has received significant popularity over the past decades. The initial concept of ”human circulation balance” proposed by Angelo Mosso (Sandrone et al., 2012) was based on a somewhat unproven fact at that time - the brain requires more blood when its activity increases. The device would undergo the rigorous effort of balancing to reach equilibrium and account for many confounding factors such as movement, respiration, et cetera before it’s used to measure the subjects’ blood-flow changes during cognitive activities (Fig.2).

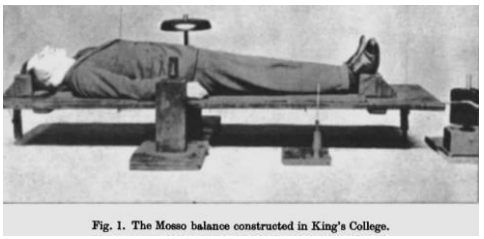

Fig. 1. The Mosso balance constructed in King's College.

Figure 2: Reconstructed Angelo Mosso’s balance device by Lowe 1936 (Lowe, 1936).

Later imaging techniques reflecting the brain’s metabolic demands were a more microscopic version of this concept and have proven Angelo’s concept (Sandrone et al., 2013). Blood-oxygen-level-dependent (BOLD) signal, for example, measures the oxygen consumption of an area (voxel) based on the premise that neurons do not have storage of oxygen and other energy to sustain their function - they require continuous supply from the blood. There are, of course, many other neuroimaging technologies that were developed based on different theories and concepts and have varying time and spatial resolutions (Fig.3)

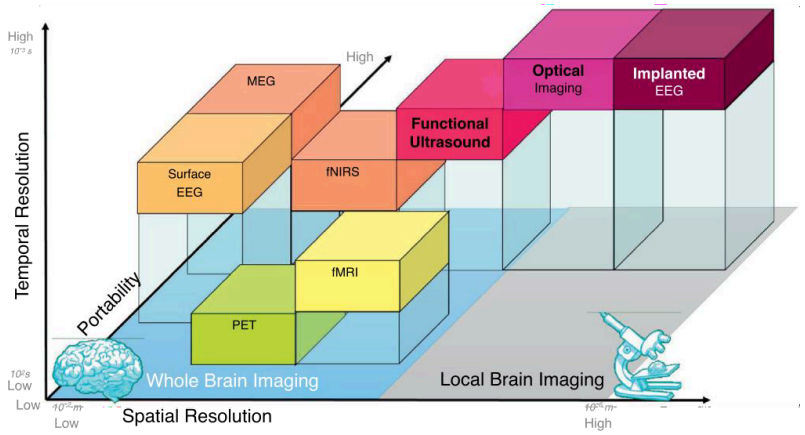

Figure 3: Spatial and Temporal resolution comparison of different neuroimaging methods. (Deffieux et al., 2018)

For example, Positron emission tomography (PET) introduces radiotracers to the brain (Slough et al., 2016) and records its activities in the brain. Functional near-infrared spectroscopy (NIRS) uses light to penetrate tissues and gauge changes in hemoglobin (Chen et al., 2020). Magnetoencephalography (MEG) records the magnetic fields originating from electrical currents in the brain, and Electroencephalogram (EEG) detects the brain's electric signals from the surface using electrodes. There are also efforts to use multimodal methods that harness the power of different imaging techniques like fMRI and fNIRS (Scarapicchia et al., 2017).

We have long observed the phenomenon of multiple brain regions that exhibit similar behaviors during specific tasks but have not been able to extract the concept network until recently (Buckner et al. 2008). Thanks to fMRI and the development of analytical tools like SPM, Greicius and colleagues (2003) were able to identify and extract functionally connected brain regions and develop the concept of default mode network. This evolutionary study has opened the door to many following studies, leading to the discovery of many other large-scale networks in the brain like attention, sensorimotor and visual networks.

The original investigation of the network by Greicius and colleagues was performed using correlation and connectivity. Since then, researchers have examined brain signals using more mathematical and computation concepts like graph theory, community detection, and unsupervised clustering in machine learning. These tools enabled us further to analyze the brain networks at an even finer scale.

2.2. From Neuroscience to Artificial Intelligence

Computational neuroscience, first introduced by Schwartz in the 1980s (Schwartz, 1993), is now one of the most explored branches in neuroscience. It aims to understand the underlying models of the nervous system through the application of mathematical and computational methods. This field fueled the development of neural networks and artificial intelligence which in turn supported the exploration and advancement of the field. While the term "computational neuroscience" was coined in the late 20th century, the foundation of this domain started way earlier.

Scientists have tried to understand our neurons' physiology and underlying mechanism for decades. The discovery of the neural action potential model in 1952 (Hodgkin & Huxley, 1952) was a significant step along the way. In one classic experiment on cats by Hubel and Wiesel in 1959, they accidentally discovered that cats' neurons react to lines swiping across the screen and further experimented with other angles and motion of the lines. This study revealed how the visual system extracted and reconstructed basic features of optical information (Hubel & Wiesel, 1959). Another study by Lettvin and colleagues in 1959 showed that the eye performs rudimentary filtering before the signals are relayed to the brain (Lettvin et al., 1959). These studies and the work of Hodgkin and Huxley laid the foundation of modern-day computational neuroscience. Understanding how neurons and visual pathways work allowed us to establish more accurate models, which were then adopted in artificial intelligence.

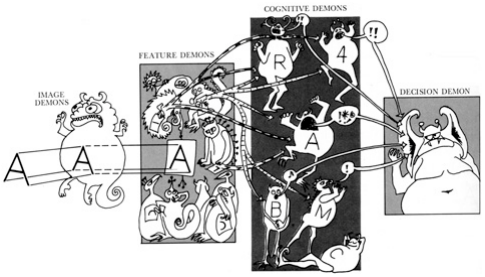

Pandemonium of Object Recognition.

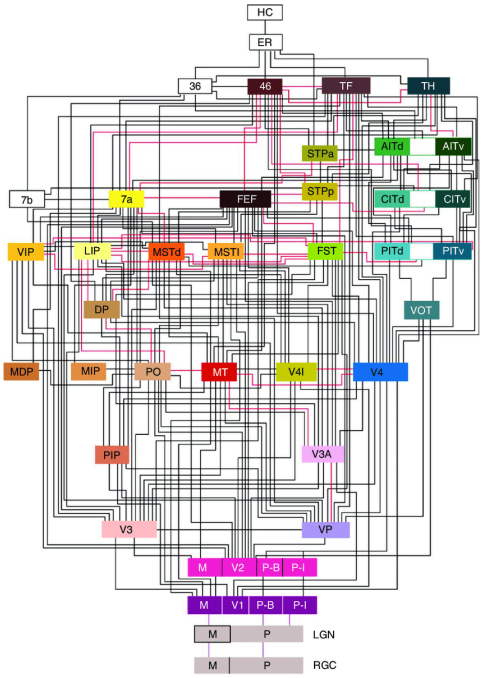

Visual Pathway of Macaque Monkey

Figure 4: Pandemonium representation of the object recognition process and visual system of monkey. (a) This is a representation of what Oliver Selfridge envisioned: the demons in the brain process increasingly complex signals at each level based on inputs. A visual illustration of the architecture in modern neural networks (Sejnowski, 2018). Source: https://commons.wikimedia.org/wiki/File:Pande.jpg (b) Visual anatomical hierarchy of the macaque monkey. Each colored cube is a different cortical visual area. (Felleman & Van Essen, 1991).

In the MIT documentary ”The Thinking Machine” filmed in 1961, Professor Jerome Wiesner from MIT described our understanding of the brain at that time - ”we know so very little about thought processes or about information that makes up thought processes” (Wiesner, 1961). Nonetheless, the series described how the machines could learn - write letters, solve logical problems and play checkers - in their rudimentary form. Since then, artificial intelligence has evolved significantly. While we are still far away from creating artificial intelligence like the one imagined in the 1927 film Metropolis, we have been able to develop powerful chatbots through the deep neural network, which can even pass the Turing test (Arielli & Manovich, 2022).

The development of modern neural networks was mainly contributed by the understanding and advanced modeling of the human visual system. The early Perceptron model could only resolve linear classification problems (Minsky & Papert, 1988). Later in the 1980s, the Hopfield Net (Hopfield, 1982) and the discovery of the back-propagation technique provided the possibility for layered neural networks. These networks need thousands of rounds of computation which was not possible before but is now possible with powerful computers. The pandemonium illustration (Fig.4a) showed how the pattern was thought to be recognized in the visual pathway, the architecture of which led to the primary layered neural network (Fig.5) - which is the foundation of Deep Learning.

Deep Neural Networks and Machine Learning have a wide range of applications - from biology to chemistry, science to industry, and geography to finance. The advanced neural networks that originated from our understanding of human neural mechanisms and processes are now also used to assist our understanding of the brain. As mentioned in the previous section, there is an increasing number of techniques like fMRI, EEG, MEG, PET, and NIRS that can be used to obtain abundant data about our brains. Digging through these big data and extracting patterns thus becomes a natural target of modern Artificial intelligence. Through machine learning methods, neuroscientists have created models that classify patients from healthy individuals, identify complex spatial-temporal patterns in the brain and construct complicated brain models.

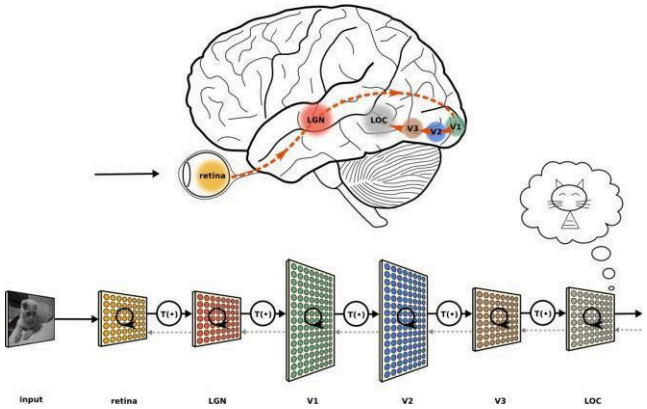

Figure 5: Layered feed-forward neural network and visual pathway. (Deffieux et al., 2018)

Moreover, Deep Neural Networks have enabled computational neuroscientists to construct complicated brain models with millions of parameters that were not feasible previously (Turner et al., 2020).

In short, cognitive neuroscience has been revolutionized over the years by evolving technologies and conceptual developments. The advancement of neuroimaging technologies helped us understand our brain systems and models - leading to the blooming of artificial intelligence (AI). AI, in turn, provided us with powerful tools to enhance our studies in neuroscience.

2.3. From exogenous to endogenous stimuli

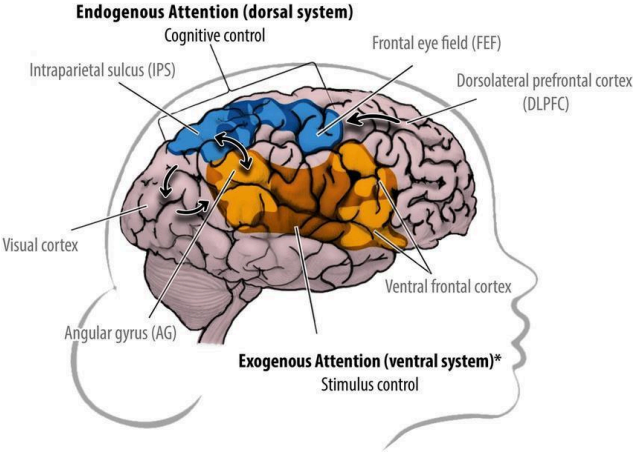

Figure 6: Endogenous and Exogenous systems in attention. (De Boer et al., 2020)

Exogeneity and endogeneity are concepts involved in various domains such as economics, biology, psychology, and geography. The definitions are simple, but the ramifications of these concepts are far more complicated than it seems. Exogeneity or homogeneity refers to an action, object, or stimulus that originates externally or outside the system. Endogeneity, on the other hand, has different definitions depending on the field. In biology, for example, it refers to processes and substances generated from within the living system. In psychology, endogenous stimuli, for example, in the attention domain (Fig.6), refer to the top-down control of attention. In general, the concept of endogenous stimuli refers to the one's generated from within the system - in the neuroscience case, that would be our brain and top-down modulation.

Through the development of neuroimaging technologies, psychologists have explored countless conditions that altered our brains. How these stimuli impact our brain systems and thinking process was scrutinized at the cellular level and led to the discovery of the effect and architecture of many different systems. As indicated above visual stimuli were presented to explore the visual pathway in different creatures like frog (Lettvin et al., 1959) and cat (Hubel & Wiesel, 1959). Studies have also been done on rats - electrophysiological signals were recorded when the rats were placed into different environments (exogenous stimuli) to identify the place and time cells in the brain (Sugar & Moser, 2019). These are the most common types of neuroscience studies - in which external stimuli are presented to the brain, creating a task condition that is then analyzed and compared.

In recent years, however, another form of study is gradually emerging, i.e., how internal modulation processes are made is explored. The most common paradigm used in these studies is a combination of exogenous and endogenous stimuli. For example, in some studies, participants were presented with pictures encoding different emotions. They were given tasks such as telling the gender or whether the emotion presented was positive or negative (Keightley et al., 2003). Another domain of neuroscience research that explored the endogenous implication of the stimuli was neural aesthetics. In a study done in 2012, when artwork was presented to participants, strong brain activations were identified in the default mode network (Vessel et al., 2012). Moreover, studies have examined how different styles of artwork (realistic vs. surrealistic, eastern vs. western art) can elicit different responses in the brain and affect our moral judgments (Pöppel et al., 2013).

These studies examined the potential impact of endogenous stimuli on brain processes and responses in the presence of external stimuli. It has been shown that endogenous processes in the brain can significantly impact how we perceive and construct our world (Kim et al., 2021). However, there is limited insight into how the brain processes if the stimuli are evoked endogenously. This is even more so when combined with episodic memory processes and using fMRI as an analytical tool.

3. Functional Magnetic Resonance Imaging Data Analysis

Functional Magnetic Resonance Imaging (fMRI) is a non-invasive method developed over the past decades. The non-invasive technology equips us with tools to record, analyze and identify different brain areas that are affected or active during various cognitive processes. The technology has undergone significant improvements over the years - increasing spatial and temporal resolutions. With the advancement of computational tools, scientists have developed real-time fMRI technologies (rtfMRI). Aside from technical improvements, there have been significant efforts to the analysis methods since the first introduction of fMRI, aiming to improve its validity, interpretability, and robustness.

3.1. fMRI Foundations

The underlying concept for fMRI dates back to the ”human circulation balance” by Angelo Mosso in the late 19th century (Sandrone et al., 2012). While not fully explored until recently, the concept proposed is still the conceptual basis of modern fMRI technologies (Sandrone et al., 2013). Later in the 1890s, the connection between blood flow and brain activity was established by Roy and Sherrington (see Friedland & Iadecola, 1991). In 1936 Pauling (Pauling & Coryell, 1936) identified that oxyhemoglobin, converted to deoxyhemoglobin, would have its magnetic properties changed - from diamagnetic to paramagnetic. This change means that the hemoglobin would change from not showing magnetic properties - like a piece of wood - to showing magnetic properties temporarily when an external magnetic field is present.

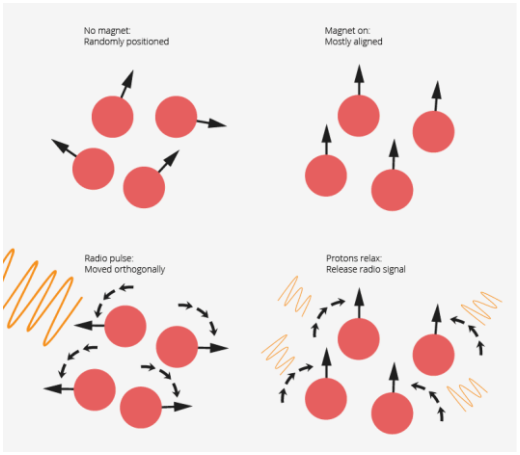

Figure 7: MRI theory example (Farnsworth, 2019). The water protons’ directions are randomized without an external magnetic field. Once the external field is present, the protons will be aligned in a single direction. Pulses of magnetic fields (or radio frequency pulse) cause the water protons to rotate and generate electrical currents, which are then captured and measured. Since the deoxyhemoglobins are paramagnetic, they will distort the magnetic field around them, which enables us to measure the relative level of deoxyhemoglobin and detect metabolism changes in the brain.

Based on this discovery in 1990 Ogawa and Hank developed the method known as functional magnetic resonance imaging (Ogawa et al., 1990). The method based on the detection of magnetic properties of the deoxyhemoglobin provides a sensitive measurement of brain activities and connects the blood flow and energy consumption with the underlying activity patterns. The study showed that the neurons in the hippocampus demonstrate different measurement intensities when provided with different oxygen levels. When the brain region has an increased metabolism level, oxygen consumption increases - which causes blood to carry more oxygen and creates a local over-oxygenation. When applied to external magnetic fields, the paramagnetic deoxyhemoglobin would cause inconsistencies in the surrounding field. The inconsistency would lead to an increase in relaxation time (T_2) and, in turn, cause an increase in image intensity when over-oxygenation happens. Alternatively, when metabolism reduces, this would, in turn, cause reduced relaxation time and hence reduced image intensity (Monti, 2011).

MRI technology provides a static picture of the brain. However, through the continuous measurement of deoxyhemoglobin percentage changes in the brain, it could reflect the dynamic changes in the blood oxygen level in the brain. This signal, termed the blood-oxygen-level-dependent (BOLD) signal, is the foundation of modern fMRI.

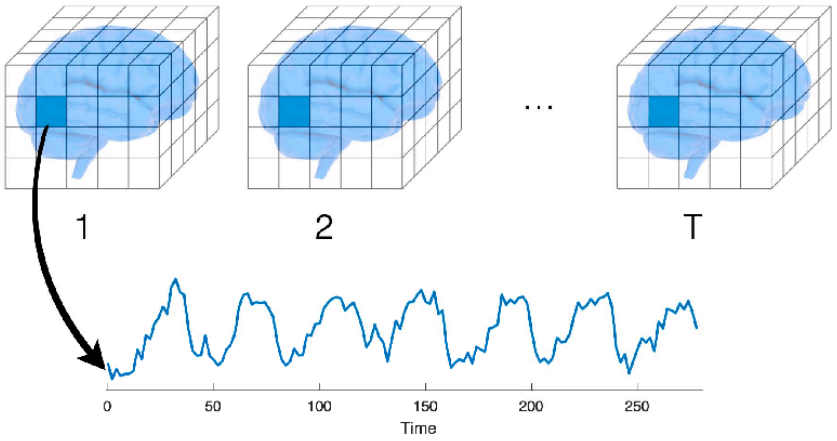

Figure 8: Visual demonstration of fMRI data. The collected data contains a series of 3-dimensional images. Each is a scan of the brain obtained over a small time window. A voxel shown in deep blue here is a pixel of the 3D image.

A typical fMRI scan continuously records the BOLD signal from the brain at predefined time points. As mentioned, fMRI measures the relative deoxyhemoglobin changes in the brain and therefore does not reflect individual neuron activities. The unit of recording, in the concept of fMRI, is called a voxel. A voxel is a unit in the 3-dimensional images generated by the technique, varying in size depending on the strength of the magnetic field (Fig.8). The spatial resolution is usually on the scale of millimeters, which means there are millions of neurons in a single voxel (Kandel et al., 2000). Thus, the basis of fMRI is that the increase in energy consumption corresponds to an increased level of cognitive activities. The method measures the metabolism of the neurons instead of directly monitoring their activity.

3.2. fMRI Limitations

The fMRI technology, while widely used, has its own technical and methodological limitations. It measures as indicated the metabolism rather than neural activities as the BOLD signals collected are based on deoxyhemoglobin content and its relative changes. Furthermore, the measurement does not reflect the absolute changes like those collected from other sources such as cerebral blood flow. This fact means that for brain areas with different baseline states, the recording does not necessarily reflect the actual behavior of the area, but it reflects the baseline signal intensity differences. It also means that since the baseline for instance of patients with specific impairments differs from healthy subjects, they cannot be compared directly.

In addition, the data acquired from the method also has limitations regarding what can be inferred from these data. Logothetis (2008) pointed out that the method's neural-based limitations cannot be resolved through the improvement of engineering. More specifically, the BOLD signal collected from the fMRI technique cannot distinguish between increased energy consumption from the bottom-up and the top- down processes (Fig. 9). Since most brain connectivities or relationships are bidirectional, the pathways of neural connectivity may be affected by both increased activity due to bottom-up signals and top-down controls.

Another limitation of the technology is that it captures the blood oxygen level changes in a specific brain region. However, it has been shown that both excitation and inhibition of the neurons would require an increase in the energy level, and we do not know if oxygen consumption results from excitation or inhibition. However, recent studies using the dynamic causal modeling (DCM) method try to overcome this limitation. Havlicek and colleagues (2015, 2017) demonstrated that through physiological DCM it is possible to dissociate excitation and inhibition neural signals from BOLD signals
- even though the model applied is a significant simplification of the underlying processes.

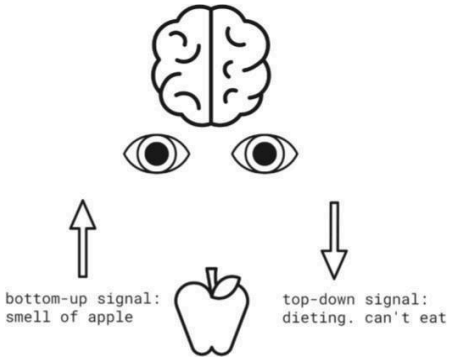

Figure 9: Examples of bottom-up and top-down signals in our daily life. Our brain has more granular bi-directional modulations, such as voluntary control of responses to visual stimuli.

Aside from these technical and conceptual limitations, there are also certain methodological limitations or potential pitfalls associated with functional magnetic resonance imaging or neuroimaging (Turner, 2016). In most studies, the researchers assume a specific cognitive process occurs in unique brain areas (or networks given in most recent studies). Experiments then adopt a paradigm where multiple stimuli are presented. It assumes that the specific brain areas would exhibit different activity patterns for stimuli. If increased activity is observed, the study tends to conclude that the region of the brain is 'activated' for said stimuli, and their hypothesis is confirmed. Given the nature of functional neuroimaging, the issue is that we cannot conclusively determine that a particular brain region is responsible for a particular cognitive function or process. Identifying differences in the brain activation pattern only means that the subjects have been exposed to different stimuli, and specific differences are involved. Further studies using a more accurate cellular level tracing technique are needed to reach conclusive results (e.g., Kandel et al., 2000).

3.3. Univariate and Multivariate methods

As shown in Fig.8, the fMRI dataset usually consists of a series of signals of 3D brain images. Each voxel's intensity value would be collected in a time series. Since a typical image usually consists of 400,000 or more voxels, this poses a challenge for data analysis. Two primary ways of analysis have been explored in the past decades. Univariate-based analysis was the first method to be introduced. After the emergence of machine learning, another branch of methods viewing the fMRI data as features in multivariate space were introduced.

3.3.1. Univariate Analysis

One of the most commonly utilized analysis methods in fMRI is the general linear model (GLM) (Glover, 2011). This method is also referred to as the mass-univariate model-based analysis. The General Linear Model (GLM) is a combination of multiple linear regression models, which can be written as

$$Y = X\beta + \epsilon \tag{1}$$

where $Y = [y_1, ..., y_n]^T$ represents a collection of the bold signals at individual voxels. In other words, one can consider the above equation as a collection of equations like $y_i = x_i\beta + \epsilon_i$, $i \in [1, ..., n]$. In this equation, ϵ is the error vector that is supposed to follow a Gaussian distribution. β is the model parameter that is used to model the actual signal.

The regressor of interest demonstrated in Fig.10 is predicted using the hemodynamic response function (HRF). It should be noted that this introduces yet another issue with fMRI data analysis since the HRF is not homogeneous across individuals and certainly not consistent across healthy and unhealthy subjects (Monti, 2011). Nonetheless, it is still widely used in creating experimental designs in GLM analysis.

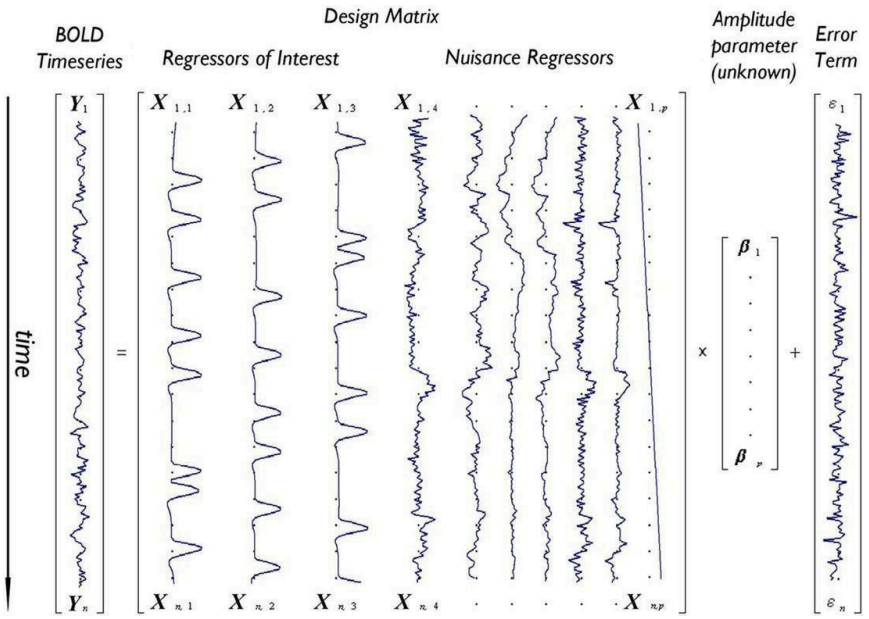

Figure 10: Illustration of General Linear Model (Monti, 2011). A single voxel's time series data is modeled by the design matrix X consisting of task regressors $X_{1,2,3}$ and regressors to account for irrelevant parameters such as motion.

Given the above model, we can estimate the parameters or weights β as $\hat{\beta}$ by minimizing differences between observed signal Y and estimated signal $\hat{Y}$. I.E $\hat{Y} = X\hat{\beta} \rightarrow \epsilon = Y - \hat{Y}$. The estimated parameters $[\beta_1, \ldots \beta_m]$ correspond to the number of regressors in the design matrix. Each parameter or weight β_i quantifies the corresponding regressors' degree of contribution in the original BOLD signal of a given voxel.

Finally, to compare experimental conditions and test for the effect sizes[1], T- or F- statistics are used at an individual level at first-level analysis or individual-level analysis. Through the combination or selection of the coefficients or the contrast vector $C = [c_1, \ldots, c_m]$ we can calculate the effect of experiment factors. For example, the hull hypothesis is usually $H_0 : C^T\hat{\beta} = 0$, meaning that there are no differences between the conditions.

After the first level analysis is completed and contrasts are calculated, a group-level analysis is usually performed (for group studies). At this level, the effect size is tested in the population rather than at the individual level. Depending on the number of factors, different tests are selected. For one effect or two variables, T-tests can be selected. For multiple variables and effects, ANOVA analysis is needed to test the main effects, and then we can look at the effect at a more granular level. The calculated statistics are then used to generate a statistical parametric map (SPM) with the significance level controlled[2].

Despite GLM being the most commonly used approach in the past few decades since the emergence of fMRI, it has various limitations. More specifically, the assumption of GLM is not always met. It assumes that the covariance between surrounding voxels does not contain information about the cognitive process and is often considered noise and reduced with filters or smoothed out. Other limitations of the method include the choice of the hemodynamic response function, auto-correlation of the unexplained components, correlation between regressors specified in the design matrix, and inter- subject comparability (Monti, 2011).

Researchers have made significant efforts to extend the GLM approach or develop alternative analyses to compensate for these limitations and create a more robust analysis. Non-parametric testing for example - using permutation tests instead of statistical mapping[3] - provides alternative testing and is proven to be preferable (Nichols & Holmes, 2001). Multivariate methods are another suite of methods developed over the past decade as an alternative analysis to overcome the limitations of the GLM approach. It investigates the patterns of neural activities without hypothesizing a specific model in the analysis.

[1] The quantified measure of the experimental effect. It positively correlates with the relationship between experimental variables.
[2] Significance level: Appendix
[3] Discussion of non-parametric statistics will be covered in Chapter 4

3.3.2. Multivariate Voxel Pattern Analysis (MVPA)

Multivariate Voxel Pattern Analysis or Multivoxel Pattern Analysis (MVPA) is a method based on the concept of artificial intelligence, more specifically, machine learning. The method adopted the view of the voxels as data points in multi-dimensional space.

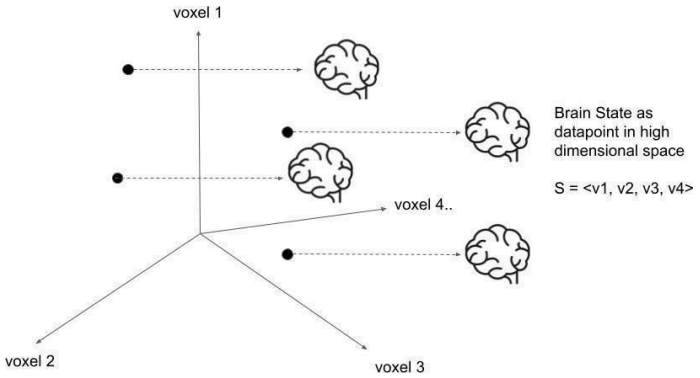

Figure 11: Viewing brain states as data-points in high-dimensional space.

Hence, MVPA examines the overall spatial-temporal neural patterns in the brain instead of focusing on analyzing individual voxels. Imagine you are looking at a GO board. The number of black-and-white pieces represent certain information about the game. However, the distinct patterns become apparent when you look at where the pieces are placed.

There are two primary types of MVPA analysis. One of the commonly used methods is classification analysis. Another branch of analysis is called representational similarity analysis. The classification analysis treats the fMRI analysis as a supervised classification issue. A classifier will be trained to extract the relationship between spatial-temporal patterns of brain activity and experimental conditions. A natural question that comes into play is what features are used for classification. In the context of fMRI experiments, the feature may represent the signals in a group of voxels or voxels of the entire brain. Other abstracted signals can also be represented.

Supervised classification is different from unsupervised classification algorithms in providing a set of labels for the given observations. For example, in the case of distinguishing attention-deficit / hyperactivity disorder (ADHD) patients, fMRI scans from subjects would be labeled as healthy and unhealthy. The machine learning algorithms would then learn the parameters based on the labels to distinguish between the two. The algorithm would calculate a set of weights for each feature, which can be applied to incoming images and calculate a label for them. Once the model is trained, it can then be applied to a set of test data to see if the model can correctly classify healthy and unhealthy subjects. This process involves a human-labeled dataset, hence supervised classification.

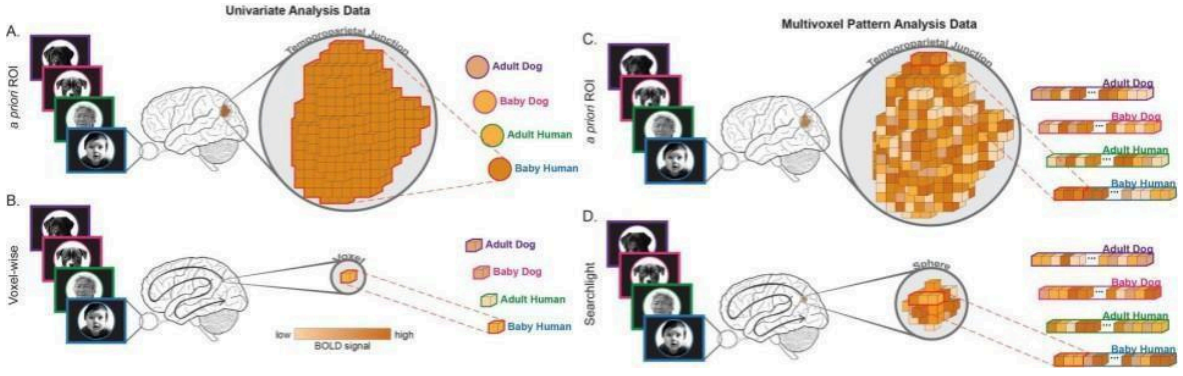

Figure 12: Illustration of MVPA data analysis VS univariate analysis. (Weaverdyck, Lieberman, & Parkinson, 2020). In the left graph A and B, we can see how data from regions of voxels are ag- gregated and analyzed and how data from a single voxel are analyzed. In region analysis (Region of Interest, ROI), the region's signal is aggregated using a certain statistical method - most commonly average across the region. In the right graphs C and D, we can see how data are represented in a typical MVPA analysis at the entire region or searchlight granularity. The pattern of multiple voxels is then extracted into vectors, which are combinations that represent
responses to different stimuli.

Generally, the labeled data would be separated into training and testing datasets. The training dataset would be used to train the algorithm to identify data for different labels, and the resulting

model would be used to predict the label of the data in the test dataset. The predicted label would then be compared with the predefined labels to verify model accuracy. In this way, the algorithm abstracts the spatial- temporal patterns and maps them to the experimental conditions in design.

Among the available classifiers for MVPA, the support vector machine (SVM) is probably the most commonly used method (Weaverdyck et al. 2020). There are different types of SVM in practice. Linear SVM, for example, is a simple version of SVM for two classes. This SVM aims to find a line separating two linearly separable classes, as shown in Fig.13. It should be noted that this form of SVM is innately restricted to two classes. So far, few studies have applied SVM in multi-class settings for MVPA as well (Hausfeld et al. 2014). This form of SVM can be considered an extension to linear SVM because it aims to identify multiple lines to separate multiple classes.

While most fMRI studies use linear SVM for their analysis due to the simplicity of interpretation, there is also a nonlinear version of SVM that can solve non-linearly separable data. This form of SVM, instead of aiming to separate classes using a line, tries to identify a hyperplane for separating data at higher dimensions. The data project at lower dimensions may appear to be non-linearly separable, but at high dimensions, they may still be separable linearly by a plane.

MVPA, given its multivariate perspective, shares a lot of common issues with machine learning, like outliers affecting classification results and dimensionality reduction but it also has its own unique set of limitations. The models adopted in MVPA can sometimes be challenging to interpret - unlike univariate methods, which answer the question of whether a region exhibits different responses to stimuli. MVPA also does not resolve the issue of spatial resolution and cannot distinguish the top-down and bottom-up processes. The MVPA is not a replacement for the univariate method but rather a complementary form of analysis.

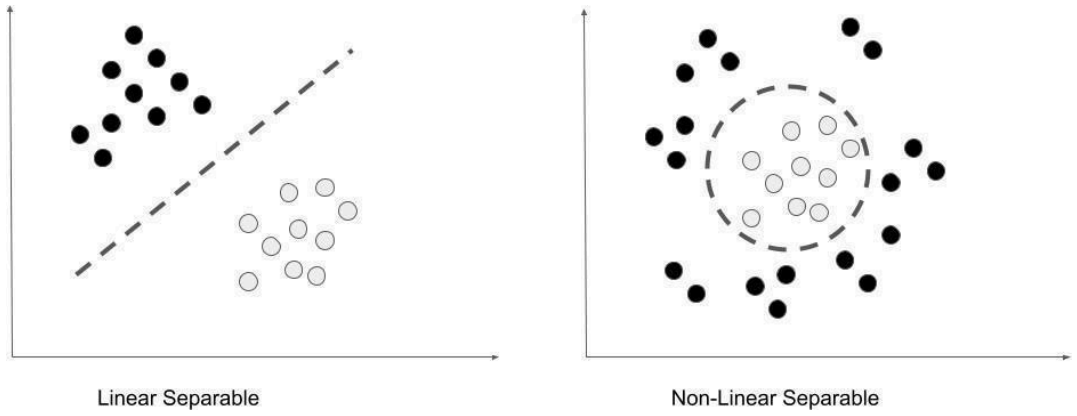

Figure 13: Illustration of sample data for SVM classification. The left class can be separated with a single line, while the right cannot.

3.3.3. Representational Similarity Analysis (RSA)

Representational Similarity Analysis (RSA) was proposed initially by Kriegeskorte and colleagues, 2008) which was based on the multivariate view of fMRI data and is used to extract information - or similarities - between different conditions, tasks, and modalities. The method bridges the analysis of different experiment modalities and provides insight into similarities and dissimilarities between different brain representations.

The RSA method does not directly examine the neural patterns evoked by various stimuli. It looks at the similarity between the patterns for different stimuli instead. For instance, the neural patterns of a subject viewing cat, dog, boar, or car may differ. The similarity of the pattern when viewing each stimulus can then be calculated and compared across subjects. The calculation can be applied to certain brain areas or regions (Pillet, et al. 2020).

RSA usually involves two straightforward steps, as shown in the illustration Fig.14. First-order RSA, or the initial step, extracts the dissimilarity between activation patterns for different stimuli in a particular brain region. In a typical RSA study, the experiment should be designed so that trials under different conditions can be separated and tested for correlations - often, a pairwise calculation is performed (Dimsdale-Zucker & Ranganath, 2018).

While neural response patterns for each stimulus may differ in different subjects, the representational

dissimilarity matrix (RDM) may exhibit specific patterns. In the second order RSA, RDM from different subjects or modalities is compared and tested. As shown in Fig.14, the researcher could create a conceptual model to capture the correlation at the test. For example, animals may have a substantial dissimilarity when compared with inanimate objects like a car. A comparison between behavioral tests could also be tested for the study at this step. Namely, for the behavioral studies of the same experimental stimuli, the correlation between different stimuli could be calculated, and an RDM generated. The RDMS can then be compared to identify commonalities by evaluating dissimilarity between them (Kriegeskorte et al, 2008).

The RSA method allows the detection of relationships between brain regions and across modalities. One natural question to consider in this study is the choice of statistics. What statistical tool can we use to calculate or measure the correlations between different stimuli? Another critical question is how we can test the said correlations. It has been proposed to use the permutation tests for this purpose. For example, the row and columns of the RDM could be recorded randomly and repeated multiple times. The correlation between the permutated RDM can then be calculated by comparing RDM - such as the conceptual RDM. After the calculation, we could get a distribution of the statistics, and then we can see where the original statistics lie in the percentile.

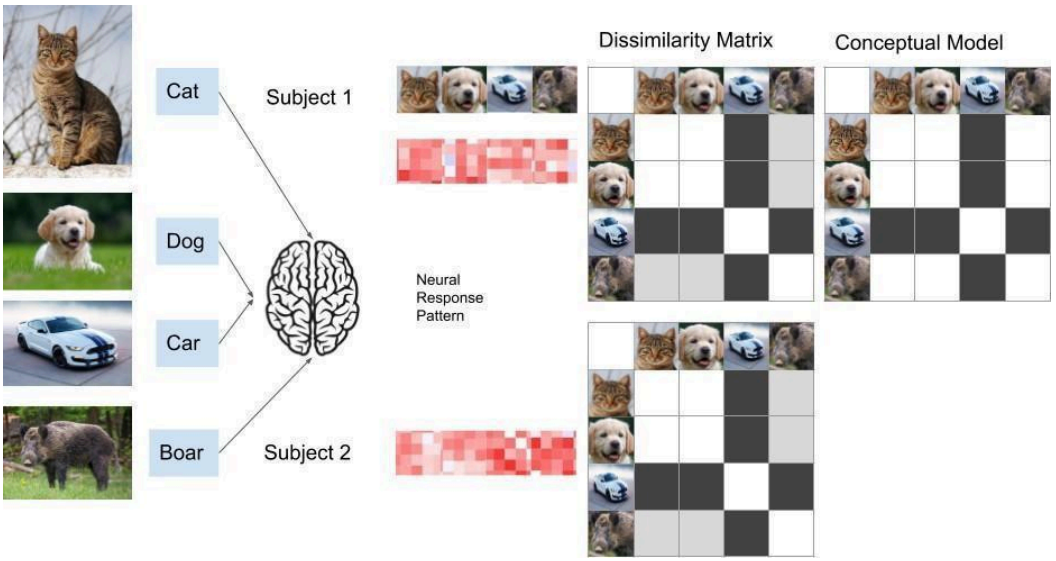

Figure 14: Illustration of steps Representational similarity analysis.

The RSA provides a unique way to examine the neural representations of the brain under different stimuli. It also allows us to explore the relationships across different modalities, experimental paradigms, and species. It is indeed a potent tool and extension of MVPA. However, this method has limitations, the same as MVPA. RSA can tell the neural pattern differences between stimuli, but it cannot uniquely identify the information. In addition, RSA is prone to the limitations of correlational methods. Thus, verification by non-correlation-based representational methods may need to be performed (Diedrichsen & Kriegeskorte, 2017). Outliers may also heavily affect RSA results though rank-based correlation methods alleviate this issue to a certain extent (Nili et al., 2014).

In short, the RSA analysis, while providing an alternative view to the fMRI data and methods that can examine representational neural pattern differences in the brain, have limitations, especially in exploring the connection across different brain regions. Researchers have developed yet another suite of methods, termed connectivity analysis, to explore the networks that underlie the brain's cognitive processes.

3.4. Connectivity Analysis

The brain's neural structures are intrinsically connected, anatomically or co-activating functionally specific neural processes. Connectivity analysis dates back to the emergence of fMRI by Friston and colleagues (e.g., Friston, 1994).

3.4.1. Functional Connectivity Analysis (FCA)

Functional connectivity (FC) is defined as "temporal correlations between spatially remote neurophysiological events" (Friston, 1994). It can be used to conceptualize the relationships or communications between different brain areas during either resting state or task conditions. Functional connectivity extracts internal networks of the base neural pattern when applied to resting state fMRI data. It can also be applied to task-based fMRI to extract intrinsic network - simply by removing the signal evoked by the task (Pillet et al, 2020).

Functional connectivity can describe correlational relationships between brain regions that are not anatomically connected. Two brain regions or areas are considered to be functionally connected if the activities of the two are correlated significantly after applying correlational statistics. In most fMRI studies using FC, the linear correlation coefficients between the BOLD signal time course of two brain regions are calculated to quantify the functional connectivity. This approach enables us to examine the connectivity information across the brain at the subject level, given the hundreds if not thousands of time points for voxels.

FCA can be applied to both task-based experiments and task-free experiments. When applied to task- based experiments, FCA can be used on top of traditional methods like univariate analysis or MVPA to provide information on the degree of interactions between the different brain areas for given experimental conditions (Eickhoff & Müller, 2015).

It is considered resting state fMRI analysis when applied to task-free experiments and has gained significant interest in the past decade. Unlike FCA applied to task-specific experiments with precise experimental paradigms, the resting state FCA does not have information on the timing of stimuli. In other words, researchers do not know the temporal aspect of the underlying cognitive process. In such a study, subjects are often instructed to lie in the fMRI scanner without a specific task or stare at a fixed point without any other instructions. In this scenario, the internal content and timing of the activity are highly individualized - as this task-free state pertains to individual subjects. Hence, FCA becomes a primary tool for exploring functional connectivity between different regions.

In resting state functional connectivity analysis, confounding factors play an essential role in contributing to the noises. Scanner artifacts, motion, and biological and physiological sources "such as cardiac and respiratory cycles" (Eickhoff & Müller, 2015) all make the signal noisy for connectivity analysis. It should also be noted that the so-called resting state differs from individual to individual. Not all individuals can draw a blank and think of literally nothing while lying in a scanner. Hence, direct comparison between subjects is difficult in resting state fMRI even when using FCA.

Common Methods In functional connectivity analysis, there are three commonly used methods in practice; seed-based analysis, network analysis, and independent component analysis (ICA) (Fig.15). In seed-based correlation analysis, a predefined brain region is selected - this is often based on the researcher's experiment design and interest. Once the seed region is selected, the signal from the seed region of interest would then be extracted (BOLD signal in fMRI). The time sources of the seed region would then be correlated with the rest of the data from the whole brain. One of the issues, as mentioned earlier, is that the confounding noises might adversely affect the connectivity identified. Hence, specific preprocessing steps in most studies are usually performed to isolate and remove the noises. Once connectivity is identified at an individual level, the results are tested at the second level (group level) to identify the consistency of correlation patterns across subjects.

In network analysis, a predefined network is often selected and used to extract signals from the brain. These selected regions in the networks are treated as nodes, and the functional connectivity among the nodes would be treated as the edges (Behrens & Sporns, 2012). Many statistical tools

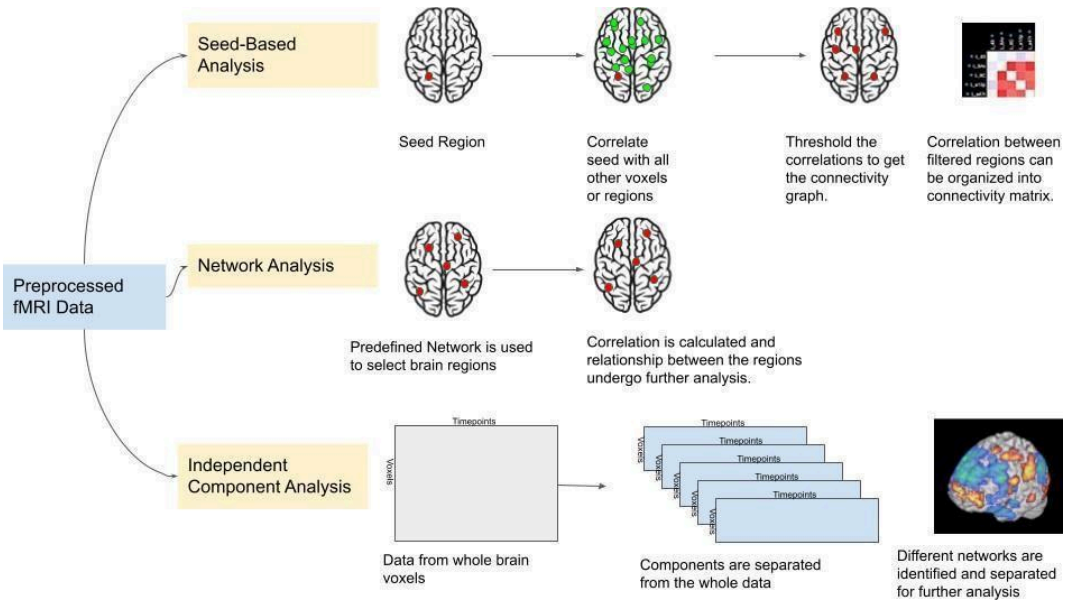

Figure 15: Illustration of different analysis methods for functional connectivity.

can be used to extract the signals from given brain regions. In most studies, simple statistics are used, such as the mean of the data. The extracted data from the predefined nodes are then correlated under different experimental conditions and can also be correlated with behavioral results to explore the relationship (Eickhoff & Müller, 2015). Again, the choice of the network depends on the experimental design and interest which significantly impacts the result.

Independent component analysis (ICA) is a familiar concept used in signal processing. ICA is an entirely data-driven approach in that no prior is required. The approach aims to separate the input signal into independent signals. It assumes that the underlying source signals are independent of each other and have non-gaussian distributions. In the context of fMRI, the input signals are often the whole brain's BOLD signals. ICA would then process the entire dataset and generate individual voxels which make up the source signals. It should be noted that ICA analysis on both resting state data and task- based data has shown significant overlapping results (Eickhoff & Müller, 2015), indicating that the decomposition can be applied to both task-based and task-free experiments.

Limitation Given the nature of functional connectivity, the analysis of brain regions focuses on the correlational relationships between them. Thus, FC inherits some of the common issues with correlation-based analysis. Even if two regions are correlated - meaning a significant relationship, if one changes, the other changes as well – it does not indicate a causal relationship.

More specifically, the correlational relationship could mean that region A changes with region B. It could be due to many different possibilities, such as a change in region A causes a change in region B (or vice versa), a change in region A causes a change in region C, then it causes a change in region B or both regions A and B are caused by region C. It could also be that there is no causal relationship between region A and region B - the correlation is simply a coincidence. One such example is sensory stimuli processing. Stimuli received in early sensory regions are forwarded to parietal sensory areas for perception and the premotor cortex for response. Despite the different systems involved, these stimuli would still cause correlations among the two regions - in other words, we will see these two regions are functionally connected (Eickhoff & Müller, 2015). It should be noted that noise, motion, and even machine parameters could introduce confounding factors into the correlation and need to be accounted for accordingly.

3.4.2. Effective and Structural Connectivity

Effective connectivity (EC) is ”the influence on neural system exerts over another.” This can happen at either the synaptic level or population level (Friston, 1994). In other words, effective connectivity describes the directed impact of one brain region on other regions. This concept of the EC suggests that it is a dynamic process, requiring a relationship model to be specified as a prior. A typical study selects a small set of brain areas, and directed connections are specified. Unlike functional connectivity analysis, where the generated graph based on the correlation matrix is often undirected, effective connectivity studies use a more hypothesis-driven approach (Kriegeskorte & Douglas, 2018). The most commonly used methods for effective connectivity include Granger casuality[4] (GC) analysis and dynamic causal modeling (DCM). While most studies use model-based methods, some branches of studies on effective connectivity have also adopted model-free methods like probabilistic Bayesian networks. These suites of methods, while they do not require prior, share a common issue as fMRI time course data may be lagged (Farahani, Karwowski, & Lighthall, 2019).

Structural connectivity, as the name suggests, refers to the brain’s anatomical structures through the arrangements of fiber tracts (Babaeeghazvini et al., 2021). The connection can be identified using noninvasive neuroimaging techniques such as fMRI and diffusion tensor imaging (DTI).

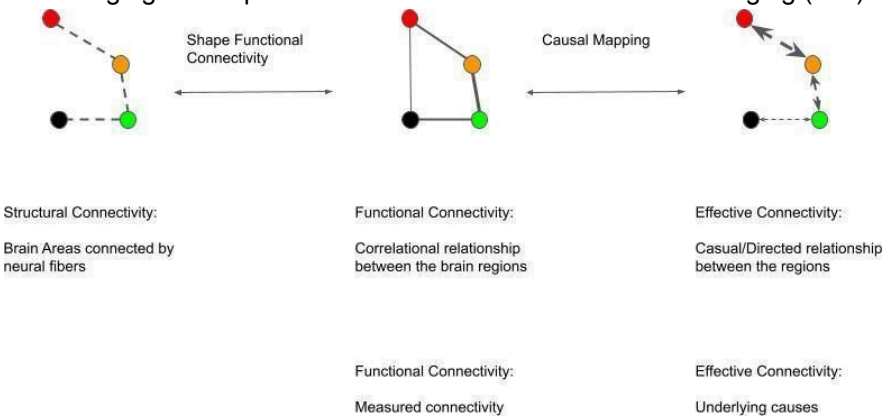

Figure 16: Relationships between functional, structural, and practical connectivity.

The connectivity models of the brain are interrelated. As shown in Fig.16, the structural connectivity is known to shape the functional connectivity of the brain regions even though the degree of impact varies significantly (Honey, Thivierge, & Sporns, 2010). Studies have explored the relationship between structural and functional connectivity by co-registering the diffusion data with fMRI data (Babaeeghazvini et al., 2021). Effective connectivity, which measures the directed relationship between different brain regions, has a tighter relationship with functional connectivity. Since effective connectivity accesses the causal interactions between different brain regions or areas, it surfaces information that is impossible by correlational analysis. In functional connectivity, the two brain regions are analyzed with correlation statistics to identify the relationship, and it only implies correlation as the method dictates but not causality. Effective connectivity fills this gap by providing a more focused, directed analysis based on the hypothesis. However, it should be noted that unlike functional connectivity studies, which can be used on both tasks (model)-free studies and task(model)-based studies, effective connectivity is primarily used on task(model)-based studies due to its prior requirement.

3.4.3. Dynamic Functional Connectivity

The concept of dynamic functional connectivity is proposed in comparison to static functional connectivity. The traditional methods of functional connectivity involve calculating the Pearson correlation statistics between two BOLD signals running through the entire course of the experiment. This calculation does not account for the temporal alterations in the functional connectivity during the experiment. Previous methods mostly assumed that the relationships between different brain areas are the same throughout the recording of resting state fMRI (Friston, 2011). The concept does not hold, of course - it is stating that the relationships between different brain regions are constant regardless of the internal cognitive process during the resting state.

[4] See A.1

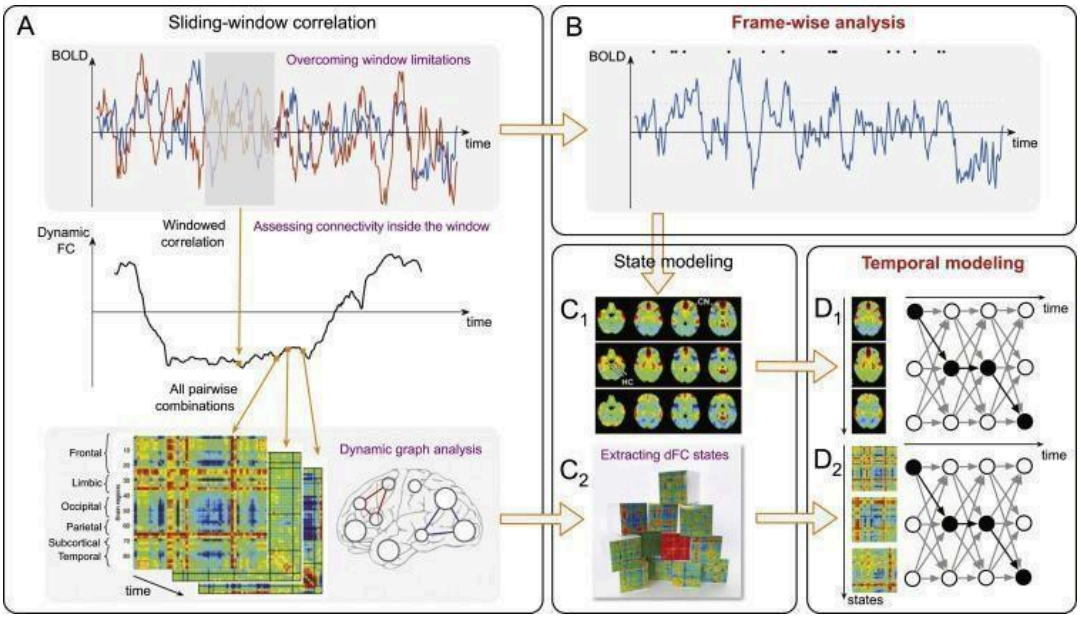

Figure 17: Dynamic functional connectivity analysis methods (Preti, Bolton, & Van De Ville, 2017).

The dynamic functional connectivity analysis provides insight into the temporal dynamics of the brain states, more so in the resting state fMRI, where external stimuli and specific temporal marks are absent. The sliding window approach is the most commonly used method for dynamic functional connectivity analysis. It's a statistical method first developed to analyze data streams (Datar et al., 2002). In DFC, it is most commonly performed by adjusting window sizes over the time course of BOLD signals (Fig.17). The correlation matrix is calculated with the signals for brain regions from the selected window. For example, if the full-time course has 180 time points and the window size is 10, then a total of 170 windows will be created; Hence the dynamic correlation of a single region would consist of 170 values.

The sliding window analysis is the first step in most DFC analysis pipelines. Through the measurement of sequential correlation variations across the brain regions, researchers can perform additional analyses such as clustering analysis to identify temporal functional structures of the brain. Allen et al. (2014), for example, combined sliding window with data created from ICA networks and clustering techniques to identify repeating states in the brain (Fig.17). The sliding window method also has its limitations. The window size, for example, needs to be selected large enough so that proper temporal patterns can be included in the isolated signals.

Other methods in DFC analysis include time-frequency analysis. This method analyzes the relationships and phase lags between two-time series. Wavelet transform is often applied to time series analysis which avoids the issue of selecting a specific time window for analysis. While providing rich information regarding the frequencies and temporal relationships, this approach also poses a challenge for interpretation as the calculations and results increase significantly with the number of subjects and brain regions (Hutchison et al., 2013). The connectivity analysis is also naturally linked with graph theory-based analysis methods, which will be covered below.

3.5. Graph Theory Based Analysis

The introduction of connectivity analysis has opened up an exciting field for neuroscience studies. These studies' emergence of connectivity and complex networks naturally falls into graph theory. While the field of graph theory dates back to the 18th century, its application to neuroscience only emerged in the past decades, primarily due to the advancement of neuroimaging technologies.

Think of the brain as a graph, in which a node is a brain area, and an edge is a connection between the two nodes (Sporns, 2022). The nodes can be voxels, groups of voxels (searchlight), regions of interest, or even neurons. The entire brain can then be translated into a giant graph with nodes and edges that characterize the relationships between the brain areas.

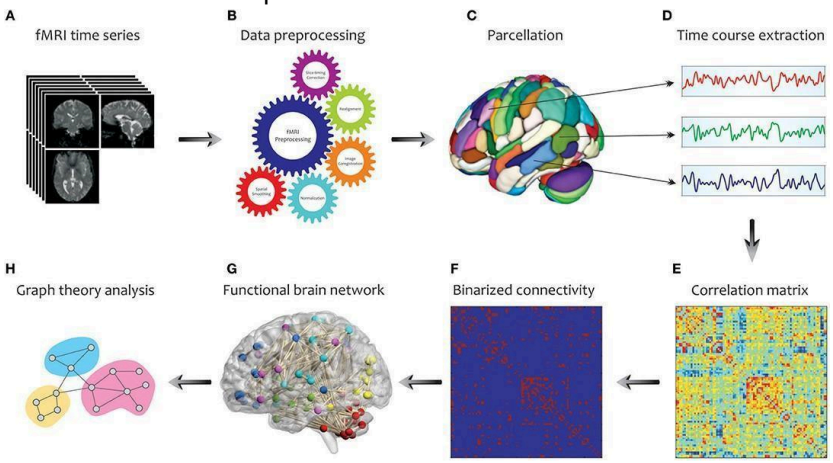

Figure 18: Example analysis pipeline for graph theory based analysis.(Farahani, Karwowski, & Lighthall, 2019).

Fig.18 provides a typical analysis pipeline used in fMRI study in conjunction with graph theory. The fMRI BOLD signals will first undergo preprocessing steps such as motion correction, slice timing correction, normalization, realignment, and smoothing. Other preprocessing pipelines such as fMRIPrep[5] will provide additional preprocessing such as surface preprocessing.

The brain signal, once preprocessed, would then be used to create parcellations of the brain. This step can be performed in many different ways. Anatomical parcellation uses an existing brain region map based on generalized results from a large group of subjects. Searchlight methods create small, focused regions of voxels or neuron groups, and machine learning clustering methods generate clusters of voxels that are closer together. In short, this step aims to identify brain regions that can be used to reduce the amount of calculation and increase interpretability in the following steps. Once extracted, the brain regions' BOLD signals can be used to calculate the correlational relationships between them. As in connectivity analysis, a correlation matrix will be generated based on the pair-wise correlation of all the selected brain regions. Thresholds can then be applied to the matrix to filter out connections that are either weak or insignificant. After this step, we would have a graph converted from the initial brain signals - where nodes are the brain areas selected from parcellation and edges are the connectivities of such areas. From here on out, a wide range of graph analysis methods can be applied to the processed data.

A significant discovery made on neurological networks and other real-world networks by Watts (1998) finds that most of these networks are small-world networks. The concept has long existed in our culture - "it is such a small world" is what people may utter from time to time. In 1967, Milgram formulated this phenomenon into the small-world problem - "Starting with any two people in the world, what is the probability that they will know each other" (Milgram, 1967). The experiment performed by Milgram inspired the concept of six degrees in popular culture. In mathematical terms, the small world networks have a short average path length between nodes and a relatively high clustering coefficient (See Appendix.A.2).

[5] Package details available at https://fmriprep.org

The human brain is expected to have a small world structure as shown in Liang and colleagues (2016). Since the human brain is one of the most energy-demanding biological structures in the brain, the cost needs to be optimized through evolutionary means. The energy required by metabolism for interactions between anatomically close brain regions is smaller than those that are not. The remote brain region interacts at a high cost simply due to the distance the signals need to travel and the potential intermediates between them. Chen and colleagues 2013) and Vértes and colleagues (2012) have shown that the brain areas are much more likely to interrelate with surrounding areas to reduce overall energy consumption. In the meantime, these areas can also maintain a small number of distant relationships to facilitate information exchange.

Common Methods Complex brain networks, while small-world in nature, can be explored with various methods and at different scales. On the granular level, the local attributes of the nodes and edges can be explored. Hubs, for example, refer to the nodes with a very high relative number of edges (or high appearance on shortest paths between other nodes). Neural hubs at the granular level play a central role in the brain neural networks in that they often appear in multiple small networks and serve as the center of the connection between them. In short, the granular analysis focuses on the properties of nodes and edges in a graph, describing the attributes of the network from a bottom-up perspective. This type of analysis often involves the calculation of simple statistics such as node centrality and local efficiency (Medaglia, 2017).

On a higher level, common graph algorithms are applied to explore the module and community structures of the brain. Communities (modules) are defined as ”divisions of network nodes into densely connected subgroups (Newman & Girvan, 2004)”. A common algorithm for community detection is the Louvain algorithm. The algorithm uses an iterative method to optimize the modularity (See Appendix.A.3) of the subgroups and identifies the brain regions within the same community.

Community detection in fMRI studies often involves first-level (subject-level) and second-level (group-level) analysis. Since each person’s brain structure is unique, the community structure detected within the subject often cannot be generalized to others. Hence, several algorithms were developed to explore the community properties across subjects. One type of method, termed ”virtual-typical-subject (VTS)” (Taya et al., 2016) is to create averaged connection matrices of the participants. In the VTS method, the connectivity matrix of each subject is averaged across the group and then thresholded (Meunier et al., 2009). The community structure of the brain is then detected using the Louvain algorithm on the averaged connectivity graph. Another type of method, termed ”group analysis (GA)”(Taya et al., 2016), attempts to maximize the modularity of the communities across all subjects. At each iteration, the community structure with the maximum modularity calculated across all subjects is chosen and provided for the next steps.

In addition to exploring community structures, many other algorithms can be adopted to explore brain networks in graph theory. Many of these algorithms have not been fully explored in the context of fMRI studies or neuroimaging in general and present possibilities in future studies.

Limitations Network structure, as shown above, has individual differences and may be less interpretable on cross-subject analysis. In addition, humans’ functional and biological network structure tends to change throughout one’s lifetime. Hence generalization of the results should be time-bound. Given the heuristic nature of graph analysis, establishing consensus from the meta-analysis also poses a challenge (Farahani, Karwowski, & Lighthall, 2019). Another major challenge in graph theory analysis is the construction of graphs. The nodes are defined across various studies, and there has yet to be a consensus on what type of brain representation is the optimal choice for graph theory-based studies. Nonetheless, graph theory provides a robust set of tools and perspectives of analysis for researchers to explore and explain brain networks in accordance with cognitive processes. Significant efforts have been made to apply the analysis to various neurological diseases to understand the function and structural changes in patients from the network perspective in the past decades, and they are likely to grow over time.

3.6. Machine Learning and Deep Neural Networks

This section will review machine learning and deep learning methods in brevity. Historical remarks have been covered in the previous section so I will focus on the methods here. For a complete and systematic review of the methods, I refer to the article by Rashid and colleagues (2020).

Machine Learning has become the most popular analysis approach in many fields in the past decades - largely thanks to the improved understanding of neural mechanisms and hardware advancements. Machine learning refers to developing machines that can learn and adapt based on real experiences without explicit programming (Sejnowski, 2018). It is a subset of Artificial Intelligence methods - which encompasses any form of technology that enables computers to obtain human-like intelligence. In the meantime, deep learning and neural networks are a subgroup of machine learning methods.

While the boom of machine learning originated from our understanding of neural pathways and brain structure, its application has, in turn, aided researchers in understanding the neural patterns underlying cognitive processes. For example, the method of Multivoxel Pattern Analysis (MVPA) is rooted deep in machine learning. In the domain of fMRI, the neural signals that serve as the basis of machine learning are the BOLD signal time course recorded on voxels in the brain. The experimental paradigm includes task-based and task-free (resting state) fMRI studies. In machine learning, the methods are applied to both domains.

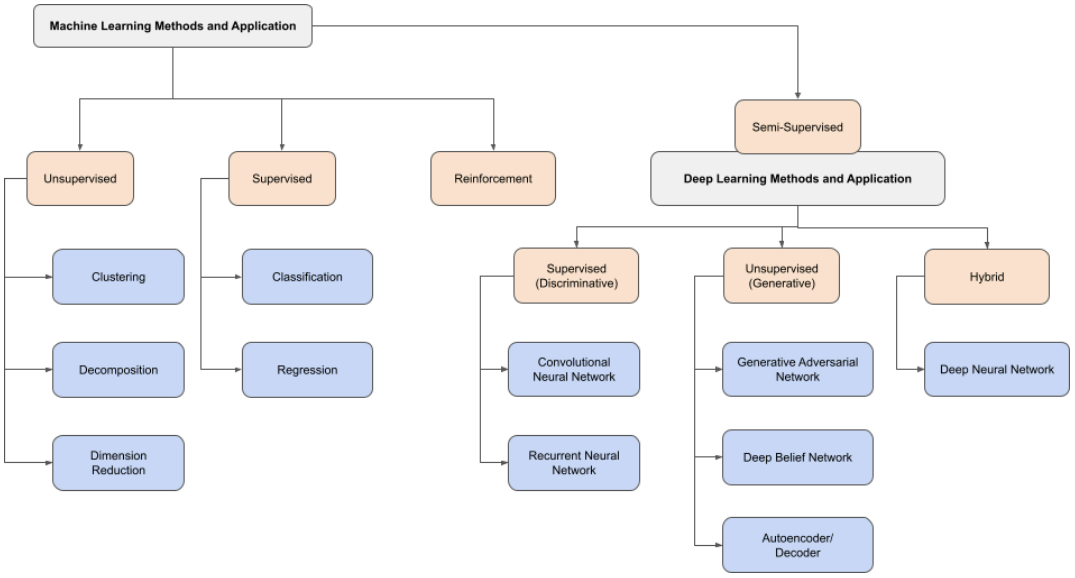

Figure 19: Illustration of standard machine learning and deep learning categories and methods. This is a non-exhaustive list. Many machine learning and deep learning methods have been developed over the past decades, but not all of them have been explored extensively in the domain of neuroimaging studies. These algorithms have been widely used in other domains, such as computer vision and natural language processing. Many methods like CNN, RNN, DNN, DBN, classification, and clustering have been integrated with neuroimaging studies and yielded promising
results.

Three types of methods are most common in machine learning studies. Supervised methods imply that experts or other algorithms label the data supplied to the machine learning algorithms. On the other hand, unsupervised methods use unlabeled data and aim to deduce information from the data. Reinforcement learning, however, differs from the two in that it uses less supervised data and trains the agent to perform a certain action with higher probability through reinforcement (O'Sullivan et al., 2020). I will only cover the top methods adopted in fMRI studies here. For a detailed investigation of artificial intelligence, I refer to the following books and articles: Sejnowski (2018), Rashid, Singh, and Goyal (2020).

Classification is probably the most commonly used method in fMRI studies in the past 20 to 30 years. In classification studies, the general assumption is that the predicted variables are discrete. A classifier takes in the features of a given sample and generates a prediction of the corresponding class for it.

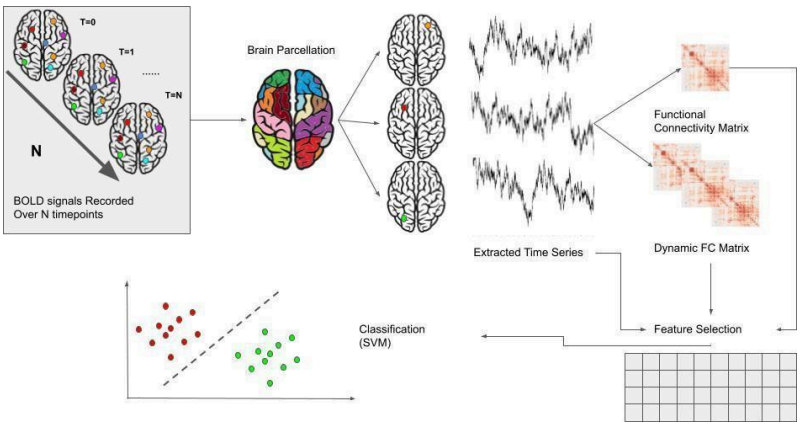

Figure 20: Illustration of typical fMRI classification pipeline.

In typical fMRI studies, the features could be the BOLD signals of voxels collected like in MVPA analysis. Other ways of defining features for further machine learning study include selecting regions of interest, calculating connectivity matrices, et cetera. The network of brain regions selected can also be based on unsupervised machine learning algorithms such as clustering. An essential step in the process of supervised learning is feature reduction. This step, again, can be performed using machine learning methods. The high dimensionality of any data set can prove problematic for analysis methods (Chapter 4 will cover this topic in detail). Standard feature reduction methods include simply using an ROI mask, calculating abstraction layers like (dynamic) functional connectivity, and decomposition methods like Principal Component Analysis (PCA) and independent Component Analysis (ICA). After the feature reduction, standard classifiers are selected, such as Support Vector Machine (SVM), Linear Discriminant Analysis (LDA), and less common classifiers such as nonlinear SVMs (Pereira, 2009).

The results of classification would also need to be tested and evaluated. The testing often involves a technique termed ”cross-validation.” One simple form of this method is “leave-one-out cross-validation.” In this method, one sample is singled out from the sample set; the classifier is then trained on the remaining samples and used to predict the label of the singled-out sample. This step would be repeated for all the samples, and the accuracy of classification on all samples can be established (Pereira, 2009). There are also forms like ”leave-M-out” and k-fold cross-validation used in fMRI studies as well (Poldrack, Huckins, & Varoquaux, 2020). As for testing the significance of the result, standard methods like the chi-square test and binomial test have been applied as permutation tests (Details discussed in Chapter 4).

Clustering and Decomposition are the common methods used in standard machine learning-based studies (O’Sullivan et al., 2020). This step can be integrated with the fMRI analysis pipeline in different stages. In the classification pipeline shown in Fig.20, an unsupervised method can be injected into steps like brain parcellation, signal extraction, and feature selection. In addition, the clustering technique can be applied directly without integrating with the classification pipeline to identify the brain’s neural patterns’ different clustered states. One such example is dynamic functional connectivity, where the connectivity matrix is calculated over time, yielding a sequence of the matrices. Allen and colleagues (2014), for example, used clustering techniques to identify repeating patterns in the temporal functional structure by putting correlation matrices of short time intervals together.

Standard clustering techniques used in fMRI studies include k-means, ward, spectral and hierarchical clustering[6]. Thirion and colleagues (2014) showed that based on the number of clusters researchers aim to generate, different clustering algorithms need to be chosen. The ward’s clustering is preferred for the more significant number of brain parcellations (>= 500), while for smaller numbers, K means. The number of parcellations specified for clustering should be around 200-500 for optimal categorization results.

[6] See clustering methods Appendix.A.4

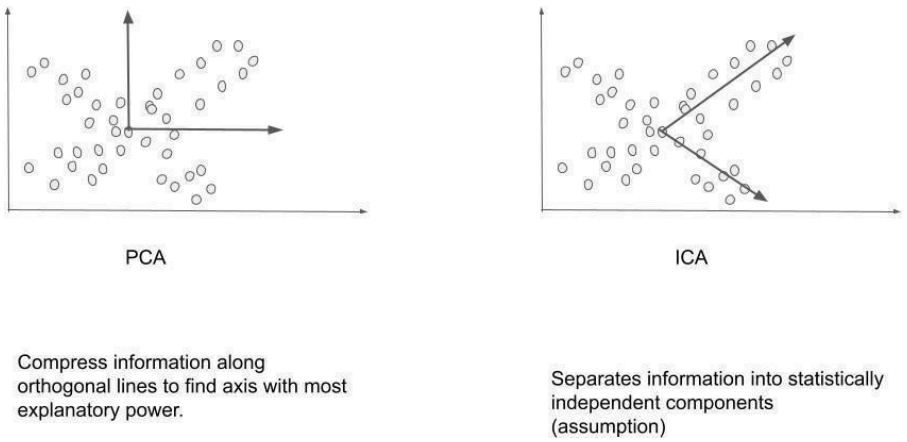

Figure 21: Principal component analysis (PCA) vs. Independent component analysis (ICA).

The decomposition methods include well-known methods like principal component analysis (PCA) and independent analysis (ICA) (Abraham et al., 2017). PCA extracts the information of multi-dimensional data to orthogonal axes, where the one axis that explains the most data is called the principal component. ICA, on the other hand, aims to extract the data into separated sub-components based on the assumption that these components are statistically independent and are non-Gaussian signals[7]. As mentioned, these decomposition methods are often integrated into the analysis pipeline of neuroimaging studies, serving as a predicate to isolate signals and components or identify principal components for exploring the statistical relationships between different brain areas (McKeown, Hansen, & Sejnowski, 2003).

Deep Neural Network (DNN) related methods can be categorized as supervised, unsupervised, and hybrid. As reviewed in chapter 2, deep neural networks originated from understanding our brain networks. It has been shown that DNN can achieve the human-level result in selected tasks (Turner, Miletić, & Forstmann, 2020) and even pass the Turing test (Johnson, 2022) - a historical method used to determine whether the machine can exhibit intelligence equal to humans. Initial methods inspired by visual pathways were feed-forward networks where information flow unidirectional along the network. The following methods like recurrent neural network (RNN) and long-short term memory (LSTM) address the issue by allowing the backflow of information. These types of methods are inspired by the memory system of humans - though in a much-simplified manner.

This section will focus on one common methodology used in research and industry. The auto-encoder neural network model is an unsupervised method to identify efficient encoding of the given unlabeled dataset (Sejnowski, 2018). The auto-encoder neural network consists of an encoder that takes the given data and compresses it through multiple layers of a neural net and a decoder that takes the compressed representation of the data to reconstruct the original data. In a typical fMRI pipeline, the input data compression is often used for dimensionality reduction, and the resulting compressed encoding is used for further analysis.

Fig.22 illustrates common analysis pipelines used in fMRI studies with an autoencoder. In the encoder model of the autoencoder, the number of ”neurons” decreases at each layer, forcing the algorithm to choose the essential features that can be used to represent the original data. The result is often a compressed form of original data (embedding), reducing dimensionality. For the decoder part of the model, the embedding is used to unveil information at each layer with an increasing number of neurons and eventually generate reconstructed data at its output layer.

[7] See details on PCA and ICA at Appendix.A.5

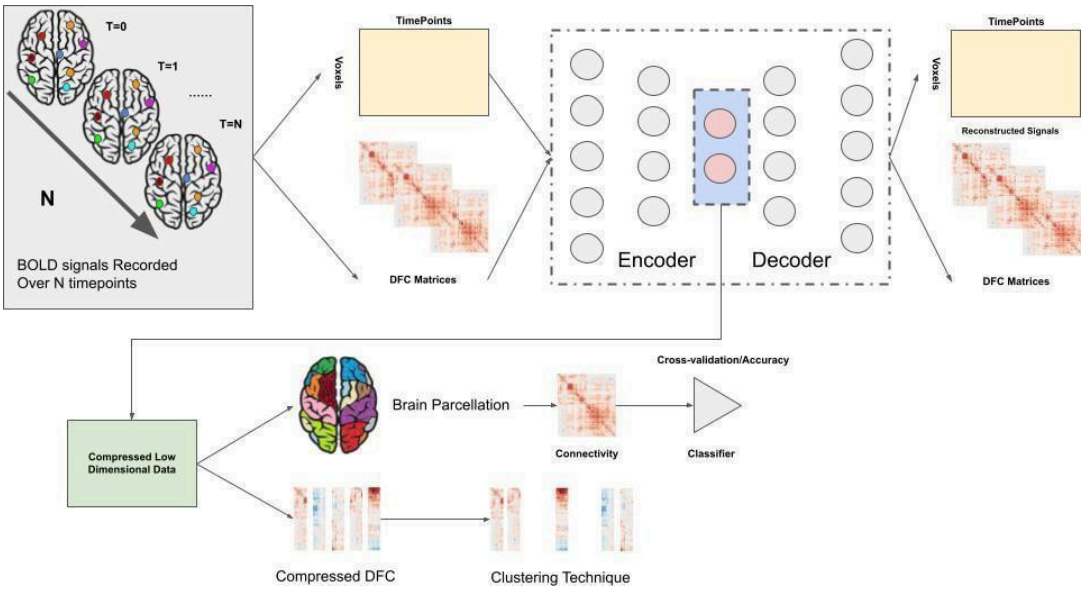

Figure 22: Example pipelines of autoencoder neural networks in fMRI analysis.

In the context of fMRI studies, the input data to autoencoders is mostly BOLD signals. The four-dimensional data of BOLD signals are often flattened into two-dimensional data, which consists of the number of voxels at the corresponding time points. This two-dimensional representation of data is then used as the unlabeled original data. Other studies have also used inputs such as functional connectivity matrices or dynamic functional connectivity matrices. The adoption of connectivity matrices would chain the Deep Neural Network pipeline with previously shown systems such as Fig.18 and Fig.20. The autoencoder would then be trained to encode and decode based on the connectivity matrices. The generated embedding, again, provides a much-simplified version of the matrices that can then be used to perform common analysis pipelines such as classification and clustering. In a most recent study by Spencer and Goodfellow (2022), they have shown that the clustering results based on the autoencoder model are significantly more accurate than the traditional dynamic functional connectivity analysis pipeline shown in Fig.17.

Despite its popularity in the past decade, deep learning and neural networks also have their share of issues. Historically, the intermediate representations are not accessible - hence the black-box model. However, this limitation is no longer valid, given the advancement of computational infrastructures and methodologies. Nonetheless, interpreting a complex model involving thousands or even millions of parameters is still a complex task and sometimes goes beyond the grasp of most neuroscientists. In addition, the structure of neural networks used in the experiments largely depends on the researchers and is most often tailored toward the specific paradigm. This introduces complexity in the generalization of results across studies.

Another major concern with deep neural networks is that the different layers of neural networks create an abstraction that is sometimes not directly transferable to biological and anatomical interpretations. Some even argue that deep neural networks are too simple to capture biological realities (Turner, Miletić, & Forstmann, 2020). Take autoencoder, for example, the embedding generated has significantly reduced dimensions - the biological meanings of these embeddings are difficult to formulate in terms of anatomical language. Despite these limitations, deep learning and deep neural networks still present a powerful tool for the analysis of neuroimaging data and have been widely adopted (Kriegeskorte, 2015; Sejnowski, 2018; Turner, Miletić, & Forstmann, 2020).

4. Statistical Tools In Neuroimaging

4.1. Similarity Measures in fMRI

All the fMRI analysis described in Chapter 3 explores the underlying spatial-temporal neural patterns of the brain's cognitive processes. One foundational question involved in these discussions is how to measure the brain's similarities and dissimilarities. Or, simply put, given two representations of the brain, whether direct neural signals or abstracted patterns such as correlation matrices, how can we tell if the two states under comparison are similar or dissimilar? Among the neural imaging studies, Pearson correlation is the most commonly used method, followed by other suites of measures. This section will discuss the reliability and applications of different similarity measures.

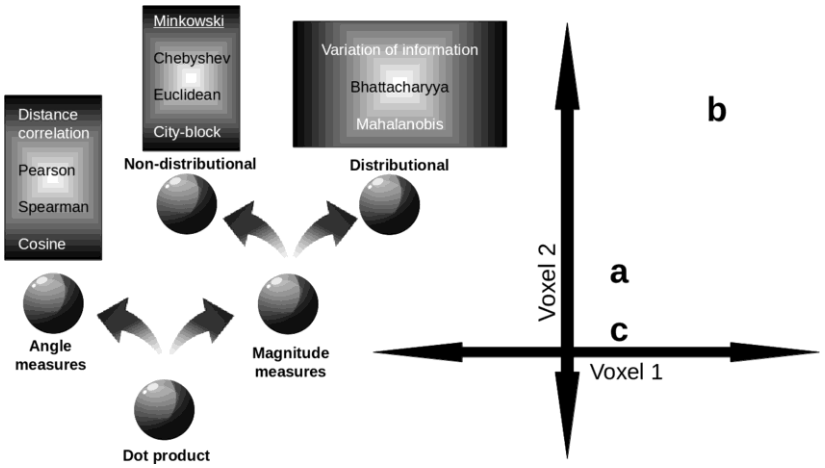

Figure 23: Illustration of different families of neural similarity measures. (Bobadilla-Suarez et al., 2020).

The two most essential methods are angle-based and magnitude-based measurements (Fig.23). Pearson correlation and cosine correlation are probably the most common angle-based measures. Euclidean distance, in the meantime, is the most commonly used magnitude-based measure - primarily due to its simplicity and commonality.

Pearson Correlation Coefficient between two variables is defined as ρ:

$$\rho_{X,Y} = \frac{cov(X,y)}{\sigma_X \sigma_Y} \quad (2)$$

where the Pearson distance can be simply defined from the coefficient as $d_{X,Y} = 1 - \rho_{X,Y}$. Here the cov(X, Y) indicates the covariance of X, Y while $\sigma_X \sigma_Y$ are the standard deviations of X and Y, respectively.

Euclidean Distance (ED) for two high dimensional data $X = x_1, ..., x_N$, $Y = y_1, ..., y_N$, is simply defined as:

$$d_{X,Y} = \sqrt{\sum_{i=0}^{N} (X_i - Y_i)^2} \quad (3)$$

This means calculating the pairwise differences between the corresponding values on the same dimension and summing them up.

In most studies in the past few decades, Pearson correlation were chosen as the similarity statistic that captures the similarity profile between different brain states (Kriegeskorte et al., 2008; Bobadilla-Suarez et al., 2020). This view, of course, is not always the case. The different ways researchers represent the brain states and the types of measures, as well as datasets, all contribute to the different statistical properties of the neural signal. In addition, the different types of information represented through the signal, task differences, ways of abstraction used for the signals all may lead to different optimal similarity measures (Braunlich & Love, 2019; Ahlheim & Love, 2018).

Take Fig.23 for example. On the right graph, point a and point c are closer together from a Euclidean perspective. However, when evaluated using angle-based measures such as Pearson correlation or cosine correlation, points a and b will be closer than points a and c. In interpretation, this means that a is similar to c in the Euclidean distance and b in the Pearson correlation. It is easy to see how the choice of similar measures would affect the result of similarities and even our interpretation of the results.

As shown in Fig.23, one crucial family of measurements is the distributional measure. In the multivariate domain, Mahalanobis distance has been adopted and proven to be preferable to Euclidean distance, primarily because of its consideration for correlation between the variables and noise (Kriegeskorte, Goebel, & Bandettini, 2006). Mahalanobis Distance (MD) is defined as follows: Given a distribution D, two high dimensional point $X = (x_1, \dots, x_N)$, $Y = (y_i, \dots, y_N)$, the mahalanobis distance between X and Y is defined as (Mahalanobis, 1936)):

$$d_M(X, Y, D) = \sqrt{(X - Y)^T S_{-1}(X - Y)} \quad (4)$$

The distance between two points in Mahalanobis distance can be thought of as the distances of two points in a new coordinate space created based on the data; the distances indicate deviations from the standard. When applied to fMRI data, the researchers have developed variations of Mahalanobis distance to account for the data properties of BOLD signal - high dimensional, noisy, and needs estimation for the correlation matrix. For example, the covariance matrix of the distribution sometimes cannot be properly calculated but can be estimated using Ledoit-Wolf shrinkage (Ledoit & Wolf, 2004). MD, as it establishes an interpretation of the distances in standard space, is most commonly used for outlier detection. However, due to its multivariate nature, studies have also used it as a similarity measure when combined with different covariance estimation methods. The Mahalanobis distance was shown to perform better than most statistical measures - including Minkowski, Euclidean, and cosine - when evaluated on neural similarity by Bobadilla-Suarez and colleagues (2020).

It should be noted that most of these measurements provide measurements on vector data. In practice, fMRI signals are extracted as specific time series, aggregated signals. A natural question extending from this is whether we can examine the data in its raw form. In the realm of fMRI, this directly evaluates the similarities between matrices that represent the brain signals over time.

Non-parametric Measures Another important group of methods that have been used in the evaluation of similarities is non-parametric statistics. Non-parametric measures usually do not assume the data distribution under examination or have an open-ended distribution model. As such, non-parametric tests are often used when underlying data violates the distribution assumption - which happens more often than not in fMRI data and neuroimaging studies (McKeown & Sejnowski, 1998; Mahmoudi et al., 2012; Monti, 2011). Given the amount of noise in the fMRI signals, rank conversion-based non- parametric statistics is also useful in extracting the underlying neural patterns (Dewalle et al., 2007; Galdi et al., 2019). Some of the common methods will be discussed.

Kendall Tau Distance calculates the distances between pairwise differences between two lists consisting of ranking. The values of the input would be converted to ranks first. Defined as below:

$$K_d(\tau_1, \tau_2) = \sum_{i,j \in N, i<j} \overline{K_{i,j}}(\tau_1, \tau_2) \quad (5)$$

where $\overline{K_{i,j}}(\tau_1, \tau_2)$ equals to 0 if i, j has the same rank and 1 otherwise. Note that the Kendall-tau distance, while using rank, differs from the Kendall-tau correlation coefficient. The correlation coefficient is defined as $K_{corr} = 1 - 4K_d/(n(n-1))$. Similar to other measures, the distances often differ from the coefficient calculated.

Kolmogorov-Smirnov Distance compares the given samples' probability distribution. In gist, it measures the distance between the actual distribution and the reference distribution, or between the actual distribution between two samples (Puzicha, Hofmann, & Buhmann, 1997). The KS Distance is based on empirical distribution function (EDF) and is shown to be one of the most powerful non-parametric tests (Conover, 1999)

Crame'r–von Mises Distance is yet another measure based on EDF and a powerful non-parametric test statistic as well. Suppose a vector consisting of value $x_1, \ldots, x_N$ CMD is defined as:

$$D = \frac{1}{12N} + \sum_{i=1}^{N} \left[\frac{2i-1}{2N} - F(x_i)\right]^2 \quad (6)$$

where F is the theoretical distribution function. The CDM methods can be applied to two samples as well. The two samples do not need to be of the same length. The statistic tests whether the two samples come from the same distribution.

Spearman Rank Distance The Spearman rank correlation coefficient is calculated the same as that of the Pearson correlation coefficient - except the values of the variables are being replaced by ranks. The distance measure is then calculated based on the coefficient

$$corr_s = \rho_{R(X),R(Y)} = \frac{cov\,(R(X),R(Y))}{\sigma_{R(X)}\sigma_{R(Y)}},\ d_s = \frac{corr_s - 1}{2} \quad (7)$$

where $R(X)$, $R(Y)$ is the ranked variable. In this way, the Spearman rank distance similarity measure d_s is defined between 0 and 1 - a value of 1 means that the two variables are strongly positively correlated, while a value of 0 means that the two variables are strongly negatively correlated (not similar).

Chi-square Distance measures the similarity between two variables, most commonly used to explore similarities between histograms. There are different forms of this distance measure. One of them is defined as below:

$$\chi(X,Y) = \sum_{i=1}^{N} \frac{(x_i - y_i)^2}{x_i + y_i} \quad (8)$$

In the context of histograms, the N corresponds to the number of bins, and each value x_i, y_i corresponds to the number of items in the bin. This method is most commonly used in computation imaging (Rényi et al., 1961).

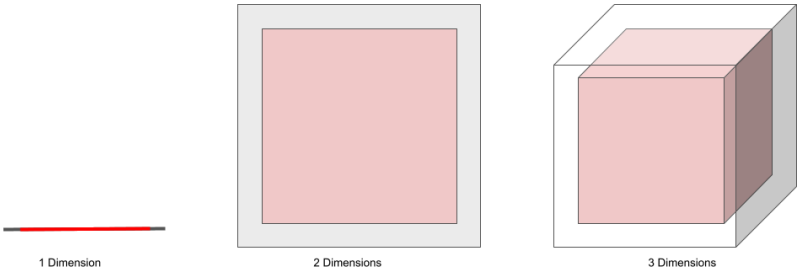

Figure 24: Confined space in different dimensions. Illustrates the distribution of data in different dimensions.

High Dimensional Measure The fMRI data often contains a vast amount of information and is of high dimensions. In high dimensional space, the common measures are often not as applicable as in low dimensional space. This phenomenon is called the "curse of dimensionality" (Aggarwal, Hinneburg, & Keim, 2001). Simply put, as the dimension of the data increases, the data becomes more and more sparse in the space and has an increased possibility of separation. This poses a major challenge for effective distance measures.

The point distribution disperses significantly, as shown Fig.24. In one dimension, the red line takes 80% of the space, and roughly 80% of the randomly generated points would fall on that. In two dimensions, the theoretical distribution of randomly generated points in confined space reduces to 64% for a confined space defined by a cube of 0.8 by 0.8. In three-dimensional space, the percentage further decreases to 51.2%. And the higher the dimension, the lower the concentration. In 10 dimensional space, the concentration further reduces to 10.7% and almost 1% in 20 dimensions. This means the higher the dimension, the more likely the data will be sprinkled across the surface of the high- dimensional space. This also indicates the standard distance metrics, such as Euclidean distance, would be prone to concentrated metrics at higher dimensions - meaning that the distances between two randomly selected points in high dimensional space are likely to be closer together and hence the difficulty to distinguish between each other (Aggarwal, Hinneburg, & Keim, 2001).

A two-step distance measurement was proposed to overcome the high dimensionality issue. Termed shared nearest neighbor similarity. This measure is based on the number of shared observations between two given observations. Suppose a data set S, where $|S| = N$, let $NN(X) \subseteq S$ be the list of nearest neighbors of X. Then the shared nearest neighbor similarity can be defined as follows:

$$SNN(X, Y) = |NN(X) \cap NN(Y)| \quad (9)$$

There are alternatives to the SNN measure, for example, to have it normalized by the number of elements within. The first level distance metrics can be chosen at will, often using Manhattan distance (L1) or Euclidean distance (L2). In the application in fMRI, the nearest neighbors are often first calculated using K-nearest neighbor, then overlaps between voxels are calculated (Kauppi et al., 2017).

4.2. Non-parametric Tests

These tests are different from the similarity measures. The non-parametric tests family includes standard methods like the Mann-Whitney test, Kolmogorov-Smirnov test, and Cramer-von Mises test. It also includes a whole suite of tests termed permutation tests.

Permutation Tests Traditionally, statistical parametric methods are used to identify significant neural patterns. This parametric framework includes methods like t-tests, F-tests, ANOVA, correlation, linear regression, and many others. It assumes that the data being explored are normally distributed. This assumption, however, is not always the case. The non-parametric test introduced by Holmes et al. (Nichols & Holmes, 2001) provided an alternative where the restriction on the assumption is much less stringent.

The permutation test concept is rather straightforward. Assuming two samples X_A, X_B collected, which could be the averaged BOLD signal of one region of interest (ROI) under resting and task conditions, respectively. Say each sample set contains N observations. We first calculate the test statistic T_{orig} of the original sample. Then we exchange labels of observations within the sample. Suppose there are 3 observations in X_A, X_B respectively, the total number of permutations would be $(6\ 3) = 20$. The rank of the original statistic would then be calculated and tested against all the test statistic values of the permutations. A percentile would then be calculated based on the rank $p = \frac{r_{orig}}{N_{perm}}$, where N_{perm} is the total number of permutations. The testing procedure can be formalized into the algorithms shown in Algorithm.1.

This is the basic form of the permutation test. As shown, one of the critical assumptions in the non-parametric permutation test is the exchangeability of labels. This weak distributional assumption (Nichols & Holmes, 2001) is required to enable us to perform permutation. The essence of this assumption is that, under the null hypothesis where the samples are coming from the same distribution, the labels of the observations can be interchangeable. Take the fMRI example, the BOLD signal of averaged ROI under resting and task conditions would be from the same distribution under the null hypothesis. This would mean that we can assign a label of either resting or task to any observations from the sample set.

This basic form of testing is commonly used in fMRI studies and has shown to be more reliable than parametric tests (Eklund, Nichols, & Knutsson, 2015). While the permutations of labels can provide better performance on testing, it should also be noted that due to the number of total possible permutations, calculating test statistics for all the permutations is often not possible in fMRI studies. This is mostly due to the computational infrastructure and budget constraints. In practice, a fixed set of permutations or random permutations are often selected - often on the scale of thousands - which is a subset of all possible permutations. The percentile or significance is then calculated based on this subset of statistics (Wang, Li, & Gu, 2017; Wang et al., 2017).

Algorithm 1 Basic Permutation Test Algorithm

Require: $T \in \Re$ ▷ T(x) is the function for calculating test statistic for given observations.
Require: $X = \{x_1, ..., x_N\}, Y = \{y_1, ..., y_N\}$ ▷ Observations
Require: $T_{stats} = []$ ▷ Empty list to hold all test statistics
Ensure: $N > 0, M > 0, H_0 : X_{dist} = Y_{dist}$ ▷ Labels are exchangeable under Null hypothesis
  $t_0 = T(X, Y)$ ▷ Test statistic for original data
  $P =$ All permutations of X, Y, $|P| = N_p$
  for i in N_p **do**
    $t_i = T(X_i, Y_i)$
    T_{stats}.add(t_i)
  end for
  $r = \sum_{i=1}^{N_p} [t_i \geq t_0]$
  $p = r/N_p$
  if $p < \alpha$ **then**
    reject H_0
  else if $p \geq \alpha$ **then**
    H_0 is not rejected. X, Y are from the same distribution.
  end if

Test Statistics Aside from the permutation test, simpler test statistics have also been applied in fMRI studies. Tests like the Mann-Whitney U test, Wilcoxon signed rank test, Kruskal-Wallis test, and spearman rank correlation test have all been adopted (Nakao et al., 2011; Dewalle et al., 2007; Galdi et al., 2019). I will give one example here. For details of the methods used, see Chapter 7 for analysis methods.

Mann–Whitney U test has quite a few assumptions: all observations from sample groups are independent; responses are at least ordinal; under the null hypothesis, both populations have identified distribution (Mann & Whitney, 1947). Assuming two-sample

$X = \{x_1, ..., x_N\}$, $Y = \{y_1, ..., y_M\}$, the Mann-Whitney statistics can be defined as follows:

$$U = \sum_{i=1}^{N} \sum_{j=1}^{M} S(X_i, Y_j) \quad (10)$$

where $S(x, y) = 1$ if x > y, 0 if x < y and 1/2 if x = y.

The non-parametric tests, while having less stringent distribution assumptions than parametric tests, also have their share of issues. One issue is that the computation is sometimes more demanding than parametric tests, resulting in the need for estimated significance - as is the case of permutation testing. If the data meets the assumption, parametric testing may be more efficient.

4.3. Time Series analysis

Functional magnetic resonance imaging (fMRI) collects blood-oxygen-level-dependent (BOLD) signals from the brain over a predefined period of time. The signals collected are therefore time series data in nature. In the traditional analysis method of the General Linear Model (GLM), the time series from individual voxels are treated as independent time series to estimate the parameters of a linear regression model. This is often not the case in reality (Monti, 2011). In other methods like multi-voxel pattern analysis (MVPA), and functional connectivity analysis (FCA), the time series of individual voxels are treated as correlated, and their relationships are extracted from the data.

Further, in deep learning methods, the time series data are used either directly as features or as the basis for additional features. The resulting data, such as dynamic functional connectivity (DFC) analysis, is often time series data as well. It has previously been shown that the BOLD signals are not independent of one another. Moreover, they are not independent within themselves - often auto-correlated, meaning the data correlates with itself in different time intervals. Hence, significant effort has been made in the domain of time series analysis in fMRI data and I will cover the methods used for identifying patterns and regularities from time series in the next few sections.

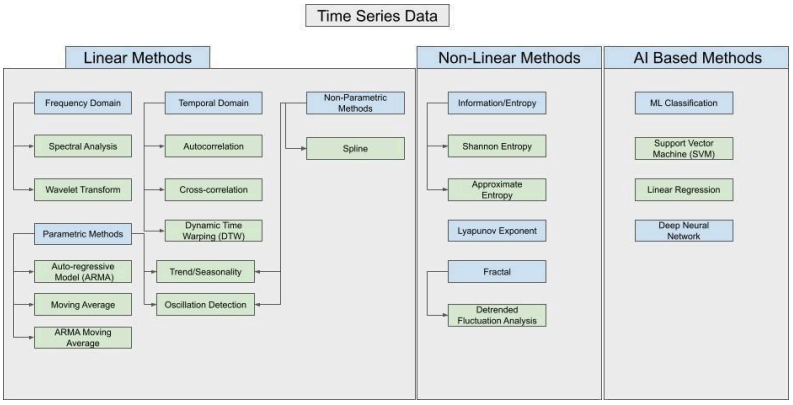

Figure 25: Illustration of different families of time series analysis methods. The suite of linear (Fulcher, Little, & Jones, 2013) and non-linear methods (Henriques et al., 2020) are both well-explored and applied in time series analysis.

Time series data, as the name indicates, is recorded data taken over a period of time. The analysis of time series data expands across many domains and researchers have developed a significant amount of methods to identify, extract and test the underlying structure model of the data. A whole suite of methods has also been proposed to forecast the signals of the time series data. In the domain of fMRI, the BOLD signal is the most straightforward time series data, while the dynamic functional connectivity changes are an example of derived time series data. As shown in Fig.25, there is a wide array of methods available for time series analysis. Here I will discuss only the relevant methods in the thesis[8].

Dynamic Time Warping (DTW) is an algorithm used for evaluating the similarity between time series. The method was initially proposed for text and speech analysis (Sakoe & Chiba, 1978) and has been applied to domains such as walking gesture analysis afterward. DTW has also been used in fMRI domains and has been shown that it can correct for non-stationary signal changes that are introduced by the switching of brain states (Sakoe & Chiba, 1978). In short, the DTW algorithms produce the best match between the time series - creating a discrete matching between the data points of one-time series to another (Sakoe & Chiba, 1978). The matching should abide by the following rules: all indexes must be matched between two series; the first (last) index must match the first(last) index; mapping of indices from one base series to another must be increasing (vice versa).

[8] Machine learning related methods shared the same principle as used with fMRI and are covered in Chapter 3

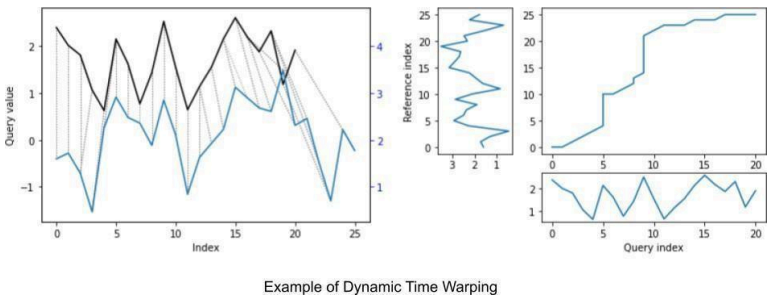

Figure 26: DTW method is applied to time series of different lengths.

Fig.26 shows an example DTW result between two time series of different length. The figure on the left illustrates the matching between the series while the figure on the right visualizes the matching in terms of steps. DTW in fMRI has been applied to BOLD signal series as well as functional connectivity analysis pipelines. This method is often used as a step in pre- or post-processing. It should be noted that the DTW method does not consider the scaling of temporal segments within the series - this issue has been addressed by other methods like correlation optimized warping (COW).

Wavelet Transform as the name suggests, decomposes a time series into a selected set of wavelets. This is different from the very commonly used Fourier Transform which decomposes time series into a combination of sines and cosine signals. Wavelet is a wave-like oscillation where its amplitude starts at zero, goes up or down then back to zero over and over again - just like a wave. There are two major types of wavelet transform used in practice: discrete wavelet transform (DWT) and continuous wavelet transform (CWT).

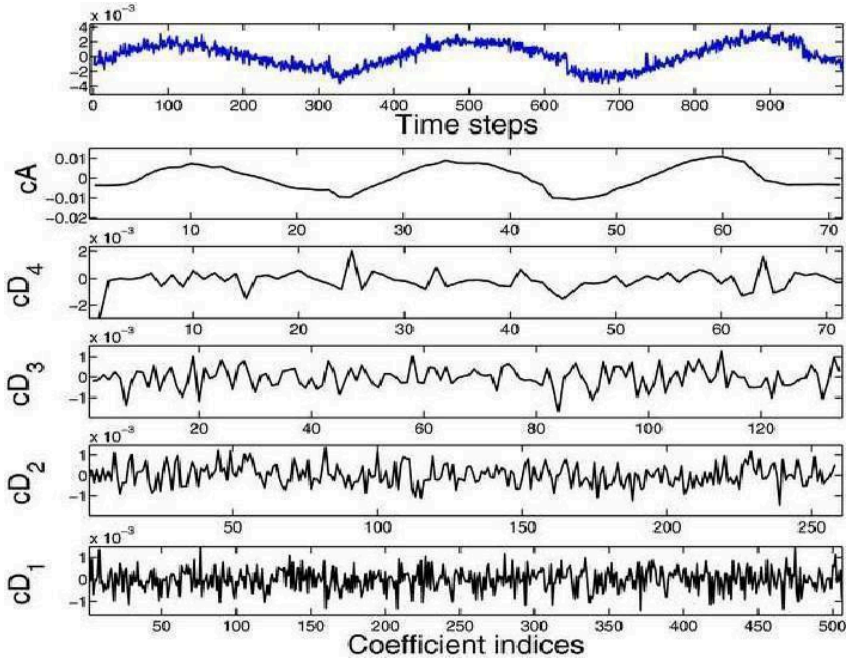

Figure 27: Example of Discrete wavelet transform (Tilani & Najamuddin, 2014). Note how the original signal is decomposed into daughter wavelets of different sub-frequency.

In a typical wavelet transform, a main finite oscillating wave is selected, known as the mother wavelet. This mother wavelet is then stretched (scaled) and shifted (translated) to create different daughter wavelets to match every component of the given time series. In CWT, all the possible modifications of the mother wavelet are tested against the signal. In DWT, however, only a selected, finite set of wavelets with specific scale and position are used to correlate with the original signal.

In the domain of fMRI, both CWT and DWT have been explored and adopted in analysis pipelines. DWT has been used for the ”decorrelation” of nonstationary time series in fMRI data. The decorrelation is especially useful for auto-correlated data - which is often the case for BOLD signals. Moreover, wavelet transform reduces (compresses) the original signal and reduces the signal-to-noise ratio which helps provide better data for subsequent analysis. In gist, the DWT method decomposes the fMRI signal into different frequencies and allows detailed analysis for sub-frequency bands while retaining

the temporal properties of the signal (Nikolaou et al., 2016). It should be noted that wavelet transform can also be used as a step to extract features for further analysis in machine learning methods (both CWT and DWT). For example, Al-Hiyali et al. (2021) introduced an analysis pipeline where CWT is used to convert BOLD signals extracted from brain regions into scalograms. The resulting data are split and fed into machine learning models for feature extraction, followed by standard classification methods like SVM and KNN.

4.4. Non-parametric Oscillation Detection: PnP Method

Oscillatory components are a common occurrence in various domains, ranging from business cycles like Kondratieff Wave to geology and even astronomy. It's also commonly found in organic systems like human heart circulation and the periodic firing of neurons in the brain. Hence, the detection and examination of the oscillatory components in signals is an important aspect of neuroimaging studies. Among these methods, non-parametric methods, given their weak assumption of the data, are of particular interest in application to neuroimaging signals.

Pöppel (1970) proposed a non-parametric method to identify oscillatory components from complex signals like those recorded in EEG or fMRI, which was not affected by stationarity, trend, and presence of noise within the signal. The fMRI signal is usually limited in duration (I.E time points or length) which means it contains only a limited number of periods, especially in the low-frequency domain. Hence, standard methods which require a large number of occurrences of periods within the series may not apply (Li, Pöppel, & Bao, 2018). The algorithm representation of the method is shown below.

Algorithm 2 Poppel-non-parametric (PnP) Oscillation Extraction

Require: $X = \{x_1, ..., x_N\}, \alpha = 0.05$ ▷ Time Series Data
Require: $Res = []$ ▷ Identified periods
Ensure: $N > 10$ ▷ Number of data should not be too low
$K_{max} = N/2 - 1$ ▷ Get max of supported period. Larger than N/2 means there is less than one period and cannot be tested.
for k in $1, 2, ..., K_{max}$ **do**
$T_{stats} = []$ ▷ Empty list to hold all test statistics
for j in $1, 2, ..., N/k$ **do**
$window_j = X[x_j\ x_{j+k}]$
$tau_j = KendallTau(window_j, [1, 2, ..., k])$
T_{stats}.add(tau_j)
end for
$\chi_{state}, \chi_p = \chi^2(T_{stats})$
if $chi_p < \alpha$ **then**
Res.add(k)
else if $p \geq \alpha$ **then**
continue ▷ k is not period
end if
end for

The initial non-parametric is a rather straightforward concept based on the Kendall-tau correlation metric introduced earlier. Suppose a time series $X = \{x_1, ..., x_N\}$ with N elements is given. An interval of k which is roughly half of the period under test is then chosen. A rank function would then be used to convert the signals within a given window of size k to rank. As the window shifts over time, a series of windows consisting of k values from the time series can be obtained. The Kendall-tau correlation can then be obtained between the sequential windows and natural number sequence[1-k] to get a series of correlation coefficients - a total of N-k+1 coefficients would be calculated. For the given time series of correlation coefficients, a chi-square test can be adopted to test its distribution. Assuming a null hypothesis where the data is random, then the transformed correlation coefficients should follow a Gaussian distribution. For large N compared to selected period k, χ^2 test can be used to verify if the distribution is normal and accept to reject the theory (Li, Pöppel, & Bao, 2018).

In a following study by Miescke and Pöppel (1982), a modified version of the method was proposed to include a smoothing factor and modified counting to improve performance. The original method was in mathematical terms. Here I propose an algorithm based on the method with slight optimization for calculation:

Algorithm 3 Poppel-non-parametric Modified (PnP-M) Oscillation Extraction

Require: $p \in \Re, p_1 \leq p \geq p_2, p_2 - p_1 \leq p_1$ ▷ p_1 and p_2 are the lower and upper bound of suspected period p.
Require: $S = [p_1, p_1 + 1, ..., p_2]$
Require: $X = \{x_0, ..., x_N\}, \alpha = 0.05$ ▷ Time Series Data
Require: $sign(x) = 1(-1, 0)$ if $x > (<, =)0$
Require: $Result = []$ ▷ Identified periods
Ensure: $N = |X| > 10$ ▷ Number of data should not be too low
  for n in $3, 4, ..., p_1 - 1$ **do**
    $r_{base} = [1, 2, ..., n]$
    $T_{stats} = []$ ▷ Empty list to hold all test statistics for case n
    for i in $0, 1, ..., N - n$ **do** ▷ Step.0 Smooth
      $T_i(\{x_i, x_{i+1}, ..., x_{i+n-1}) = \sum_{k<j} sign(x_k - x_j) sign(k - j) = \sum_{k<j} sign(x_j - x_k)$
      T_{stats}.add(T_i)
    end for
    $t_{pairs} = [t_1, t_2], \frac{n(1-n)}{2} < t_2 \leq t_1 < \frac{n(n-1)}{2}$
    for t_{pair} in t_{pairs} **do**
      $M_1 = [], M_2 = [], A = [S][S][2]$ ▷ A is a matrix holding computed value
      for s in S **do**
        for i in [0, 1, ..., s-1] **do**
          $A[s][j][t_1] = 0, A[s][j][t_2] = 0$
          for k in [i, i+s, i+2s, ..., i+ms] **do** ▷ Max cycle index below N
            if $T_k >= t1$ **then** ▷ Count number of peaks greater than t1 or t2
              $A[s][j][t_1] = A[s][j][t_1] + 1$
              $A[s][j][t_2] = A[s][j][t_2] + 1$
            end if
          end for
        end for
      end for
      for s in S **do**
        if $max(A[s][:][1]) = max(A[:][:][1]$ **then**
          M_1.add(s)
        end if
        if $min(A[s][:][2]) = min(A[:][:][2]$ **then**
          M_2.add(s)
        end if
      end for
      if $|M_1 \cap M_2| == 1$ **then**
        return $M_1 \cap M_2$
      end if
    end for
  end for

The method provided a way for period detection based on the signal and showed that the method works better when the size of the selected window is larger (greater than 5). For details of the mathematical notation of the method, I refer to the article by Miescke and Pöppel (1982).

5. Episodic Memory: A window to our cognitive process

The memory system may not be the most critical component of our brain functions - as in without which we can not survive - but it is certainly one of the components that affect our life deeply. In the movie Astu, directed by Sumitra Bhave and Sunil Suktankar, a scholar, Dr.Shastri, was struggling with the process of Alzheimer's Disease (Dundoo, 2015). A disease that damages the hippocampus area of the brain and causes progressive memory deficiencies among patients. In the movie, Dr.Shastri forgot his own home and how to get back, returning to a child-like state - curious and innocent. The reality of the disease, however, can be much harsher. As the illness progresses, subjects lose semantic memory, then episodic memory than implicit memory even. The movie is a reminder of how important the memory system is in our daily life - without which, we may not even be who we are.

Our memory is the process where the information is encoded, stored, and later retrieved (Kandel et al., 2000). Episodic memory, part of long-term memory, is particularly important and meaningful in the system. It's the memory of personal experiences and autobiographical memory. As we age and tell others of our life story, passing on the experiences as our ancestors did, episodic memory is what we draw upon. It's highly integrated with our daily life and can even be drawn upon as an endogenous source of information or stimuli. In this chapter, I will review the critical component of our long-term memory system, how episodic memory is categorized, how it's analyzed, and how studies have explored its endogenous application.

5.1. Long Term Memory in Humans

5.1.1. Implicit and Explicit Memory

Our memory system consists of short-term and long-term memory. The short-term memory is selectively converted into long-term memory - meaning that not everything we experience is encoded and stored (Kandel et al., 2000). The famous subject, H.M., demonstrated the role and importance of the hippocampus in our memory system and showed direct proof that even within long-term memory, there are different subtypes. More specifically, H.M. and many other patients with medial temporal lobe lesions were still able to form certain types of long-term memories (Squire, 2009). For example, H.M. was able to improve on drawing stars despite the fact that every time the task was presented, H.M. always thought this was a new task. This type of unconscious memory formation is known as implicit memory.

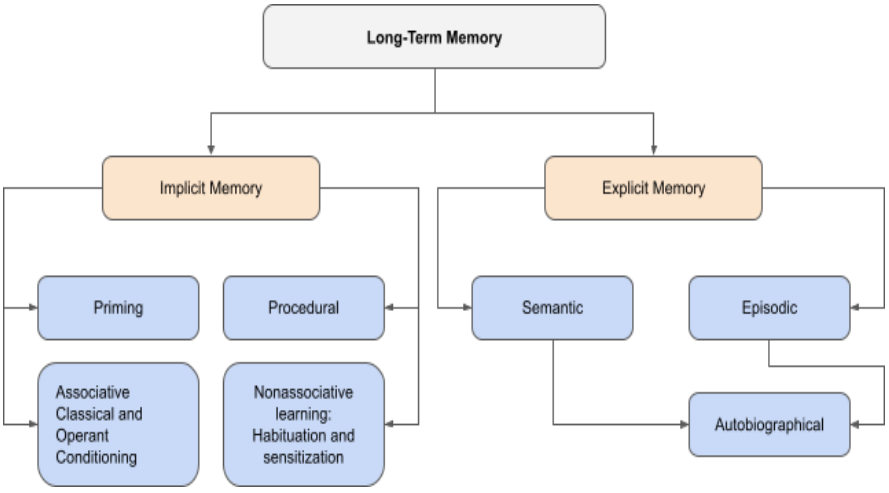

Figure 28: Illustration of the human long-term memory system. Implicit and Explicit memory affects almost everything we do - from habits and activities to recollection, learning, and language. It is the de facto center of social and personal life.

Implicit memory is also sometimes referred to as non-declarative or procedural memory. As the name suggests, it's often part of an unconscious and automatic process - concerning perceptual, motor, and procedures (Bauer & Dugan, 2020). Take golfing or bike riding, for example. These particular sports activities involve complicated motor control and perceptual and behavioral patterns that are specifically tuned for the situation. When engaging in these activities, people often do not consciously recollect the skills required to perform a golf shot or ride a bike - these skills are imprinted in us in an

implicit way. This also contributes to the phenomenon where one may not have touched a bike in years, but when presented with a bicycle, the person just ”knows” how to ride such a vehicle.

As with long-term memory, there are also sub-types of memories within the implicit domain, as seen in Fig.28. Priming is the form of memory that depicts the case where the pre-conditioned stimuli would affect the retrieval of associated items - often used for improving amnesic patients (Bauer & Dugan, 2020). Procedural or motor skills acquired are much more common in practice, such as the example with golfing and bike riding. The non-associative learning, as explained by Schacter in principles of neuroscience (Kandel et al., 2000), is formed when people are repeatedly exposed to a specific type of stimuli. This type of memory can result in either heightened or reduced sensitivity to stimuli presented based on whether the stimuli elicit negative or positive experiences. Other forms include associative learning, which comprises classical and operand conditioning. The former creates a connection between two previously unlinked stimuli while the latter associates a behavior with a specific event (Rovee-Collier, Hayne, & Colombo, 2001).

The implicit memory, while not part of our conscious retrieval of memory, affects us in very significant ways. It has been mentioned that through the unconscious manifestation of the memories, our social behaviors and even personalities are affected (Scalabrini, Esposito, & Mucci, 2021). Indeed, imagine when you were presented with a delicious plate, was your decision to ingest the food a conscious choice or the result of conditioning? When young people have a few minutes of spare time and decide to turn on their phone and TikTok and browse short, captivating videos, is it a conscious choice or merely a procedural memory encoded through hundreds or even thousands of times of repetition? At any rate, the impact of implicit memory and the human memory system is still an ongoing field and receiving much attention from researchers (Massot-Tarrús, White, & Mirsattari, 2019; Stuss & Alexander, 2000; Bauer & Dugan, 2020).

5.1.2. Explicit: Episodic and Semantic Memory

Another type of memory, which involves the deliberate recollection of previous experiences and factual information or knowledge, is known as explicit memory. While implicit memory is tied to encoding conditions, explicit memory is more flexible and involves major reconstruction efforts during the recollection phase (Rovee-Collier, Hayne, & Colombo, 2001). Explicit memory does not simply have a single, unified storage location in the brain - instead. It’s scattered across various brain regions and can be recollected and reconstructed as we consciously pull the information up. A common decomposition of the explicit memory involves four processing processes though there could be more to be uncovered (Kandel et al., 2000; Bauer & Dugan, 2020).

The explicit memory process involves the encoding, storage, consolidation, and retrieval phase. Encoding, as the name suggests, is the process during which the new information acquired from different sensory channels is analyzed, reorganized, and linked with existing information in the brain. This is usually a top-down driven, endogenously modulated process that often requires the modulation of attention as well. Think about the techniques taught by social gurus on how to remember people you have met during networking events - identifying specific characteristics of the person, like facial features, locations, and so on. Then associate that information with the person’s name repeatedly and try to recollect it a few times. This technique is essentially teaching a way for enhanced encoding through intentional focus and processing - later, when that person appears in front of you, you can easily recollect the situation when you were met and, hopefully, the other person’s name as well. This coincides with the study finding that testing during encoding enhances the encoding performance of new information (Einstein, Mullet, & Harrison, 2012).

After the information is encoded, the next natural step is the storage of information. It refers to the neural process during which the memory is stored (maintained) over a longer period of time. Unlike working memory, which has a small amount of storage space, long-term memory appears to have unlimited capacity. Consolidation is the process in which the not-so-stable stored memory is enhanced and stabilized in our brain.

The last part of the memory process is retrieval or recollection. Simply put, it’s the process during which the stored information is pulled up and surfaced. Since the memory is usually encoded and distributed, retrieval is a constructive process and is error-prone. Even in individuals who claim to have highly superior memories, the accuracy is fallible (Patihis et al., 2013). The retrieval process can be facilitated with the same encoding cues if present. For example, imagine you walk to a place - maybe a hotel - that you were in years ago. It would be easier for you to recall the good times you have had there versus performing such recalls from the other locations. Similar to implicit memory, explicit memory can also be subdivided. In 1972, Tulving proposed the concept that explicit memory

can be further split into two groups: episodic and semantic (Tulving, 1972). Episodic memory, which is termed this way as the recollection of the memory comes in episodes, is what consists of our life's memories. The encoding, storage, and retrieval of information related to personal experiences make up episodic memory. Our memory of the parks we went to as a child, the players hitting the ball back and forth during a tennis tournament, and the beautiful musical pieces orchestrated by composers are examples of episodic memories in our life. It's the common form of memory when the term "memory" is referred to in popular media.

Semantic memory refers to the general information and knowledge that is separate from personal experiences. The general facts, concepts, and language knowledge, like words and their meanings, are all part of this form of memory. It is often not associated with the specific context in which the information was attained and is also stored in a distributed manner. Studies have shown the lesion in one region may damage a particular type of knowledge (memory) but not the others (Kandel et al., 2000).

Our memory system is a delicate piece of a complex system in which all may come into play. Take golf, for example. Our semantic memory might encode the concept of golfing, the knowledge of golf rules, and the knowledge of golf clubs. Our implicit memory might encode how to swing different types of clubs. Our brain would pull up both implicit and explicit memories to decide the next plausible steps in the game - maybe call upon our previous experiences in a similar (episodic) situation to determine the next best club to use. In short, the long-term memory system is a critical component of our life.

5.1.3. Autobiographical Memory

In addition to episodic and semantic memory, there is one hybrid form of explicit memory, termed autobiographical memory (AM). AM is a form of explicit memory where the episodic and semantic components intersect. The personal experiences are combined with semantic knowledge of the world at the recollection stage to form the autobiographical memory.

Conway and Pleydell-Pearce (2000) proposed the concept of the Self-Memory System (SMS) as a model for the formation of autobiographical memory. SMS consists of an 'autobiographical knowledge base' and a 'working self'. The autobiographical knowledge base, as shown in Fig.29, contains three components. "Lifetime periods," which are the periods of one's life categorized by themes. "General events" refers to the single occurrence of events or collection of events that are often grouped together
- meaning events are interrelated within a group, and often recollection of one event would trigger another. Finally, "event-specific knowledge (ESK)" is the detailed knowledge about specific individual events, often encompassing visual imagery and other sensory modalities.

As shown in Fig.29, the three components are in a layered hierarchy where the lifetime periods serve as the cue for general events. The general events would then elicit retrieval of ESK. In the figure, the ESK component is illustrated as a huge pool of features. Selected feature sets (circle regions) are activated by the cues or stimuli presented as general events. The working self, in the meantime, refers to the collection of active personal objectives or self-images. The objective and self-image combine to define the current self and dictate the cognitive process under which the memory is recollected. The working self serves as the control center of cues that are eventually used to elicit ESK hence forming autobiographical memory (Conway & Pleydell-Pearce, 2000).

There are other theories of autobiographical memory model as well, such as the autonoetic consciousness described by Tulving (2002), or the very recent perceptual and conceptual remember (Sheldon, Fenerci, & Gurguryan, 2019). Regardless, the concept of self is a critical piece of autobiographical memory. As described, one's ability to perform mental time travel, project oneself to the past and recollect previous situations, even perceptual cues such as visual, tactile, or even auditory, are all integral parts of autobiographical memory. In the example of golfing described previously, one's ability to recollect previous game situations and use that to direct the decisions in the current game is one form of application of autobiographical memory.

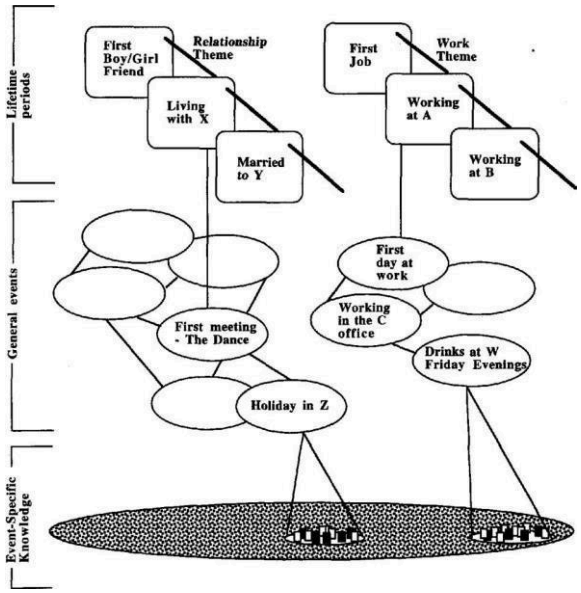

Figure 29: Illustration of autobiographical memory knowledge base (Conway and Pleydell-Pearce (2000).

It has been shown that for humans previous positive A.M.s are more likely to contain vivid sensory information and details (ESK) (D'Argembeau, Comblain, & Van der Linden, 2003). People with high self-esteem also recollect positive memories more frequently than people with low self-esteem (D'argembeau & Van der Linden, 2008). It's also shown that positive memories may be consolidated and stored for longer periods of time compared with negative memories. Given our tendency to avoid recollecting negative experiences, it's not surprising that negative AMs dissipates (Walker, Vogl, & Thompson, 1997). It should be noted that this is not always the case. In certain situations negative AMs are frequently revisited, whether consciously like patients with clinical depression (Kuyken & Howell, 2006) or non-voluntary flashbacks like PTSD patients (Ehlers, Maercker, & Boos, 2000). Nonetheless, it's apparent that both positive and negative emotions have a strong influence on our memory.

As mentioned, in autobiographical memory, the ability of back projecting oneself also introduces the question of the frame of temporal reference and perception. It has been shown that in episodic memory and AM that the time is compressed after being encoded (Jeunehomme & D'Argembeau, 2019). Since explicit episodic memory and AM is a constructive process, there should exist a certain form of temporal anchors within the encoding that serves as the point of reference upon which we reconstruct the compressed memory.

All of these questions and fields in AM and in broader episodic memory have received great attention over the years. Instead of classic methods like a diary and probing cues (Tulving, 2002), major efforts have been made using neuroimaging techniques over the past decades to explore episodic memory.

5.2. Episodic Memory fMRI Analysis

Episodic memory involves many different systems in our brain, and each type also have different underlying neural mechanisms. The study of episodic memory using fMRI has unveiled our complex brain networks at work. From Default Mode networks to other large-scale brain networks, many different methods have been applied to fMRI studies to identify brain patterns.

5.2.1. fMRI Paradigms and Analysis Methods

Historically, two major approaches have been involved in the study of episodic memories in neuroimaging studies. One approach, termed laboratory condition, involves instructing the participants to learn and retrieve materials from controlled experimental settings. For example, showing visual images like pictures, objects, and faces and then asking subjects to retrieve the information later (McDermott, Szpunar, & Christ, 2009). This method provides more control over the experiment but also assumes the neural underpinnings of the experimental condition are similar to that of real-life situations. For example, a classic paradigm like paired-associate learning (PAL) is used to evaluate subjects' episodic memory capabilities. Another approach involved is not to use lab-based conditions but instead use real-life events of the subjects. This approach involves the autobiographical facet of episodic memory and requires the subjects to recall personal memories with various cues.

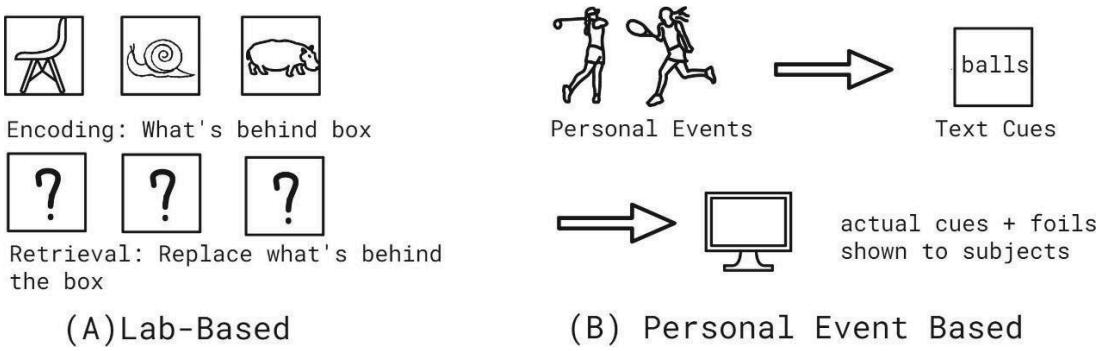

Figure 30: Examples of common Episodic Memory experimental paradigms. These do not include all paradigms used nor represent the whole experimental design.

While these two types of methods are commonly adopted, fMRI studies show that these two types of conditions evoke significantly different neural patterns. This suggests a clear separation of underlying systems in the two conditions (Chen et al., 2017). The different neural machinery involved in episodic memories is further explored with the help of modern neuroimaging techniques, such as fMRI and other methods like EEG, MEG, and fNIRS (Yu et al., 2021).

Both lab-based and personal-event-based episodic memory studies have been integrated with fMRI. For lab-based studies, the primary approach is to introduce subjects to new information and later record the subjects' brain images during memory retrieval (Wammes et al., 2021). These studies surface the correlational relationship between different memory tasks and brain states and regions - often highlighting specific areas of the brain and related voxels. The lab-based studies have surfaced roles or brain regions in human memory systems (Smith & Mizumori, 2006; Trimble & Cavanna, 2008).

The personal-event-based episodic memory fMRI studies have also gained some attention over the past decades. These studies involve the voluntary retrieval of autobiographical memories (AM) based on specific cues given, such as restaurants you have been to, words like a particular food, and specific questions about college life (Cabeza & St Jacques, 2007). Autobiographical memories are associated with personal experiences from one's past. In most popular culture, this is what is referred to as memory. Autobiographical memory often retains strong emotional characteristics and visual imagery in our brain. While sometimes it has been associated with mental conditions such as post-traumatic stress disorder (PTSD), it provides a unique window into our conscious mind.

Another form of personal-related episodic memory experimental paradigm has emerged in recent years. Based on personal-event-based episodic memories, these studies not only explore the particular memory with cues but also explore the possibility of using episodic memory as a factor in experiments (Avram et al., 2013). Since emotions are a vital component in autobiographical memories, these studies used endogenous conditions that were purely generated based on subjects instead of using the classic lab-based learning and recollect paradigm. Vedder et al. (2015), for example, instructed subjects to recollect positive and negative, pleasant and unpleasant environments in the study. Aside from this, other studies have explored eliciting emotions from musical pieces (Juslin et al., 2010). These studies rely on recollection across different modalities and involve multiple systems at work.

The memory system, especially episodic and autobiographical memories, involves many different components of the brain. It encompasses processes such as the reconstruction of memory, recollection of emotions, or remote memories (Bird & Burgess, 2008). Such involvement opens up the application of AM in examining various clinical conditions and introduces the complexity of analysis in fMRI. Unlike other more straightforward cases, the complex brain patterns are no longer individual brain region activation but rather orchestrated co-evolving networks that exhibit unique spatial-temporal characteristics. The studies of autobiographical memory and its commonalities with other internally focused tasks in terms of brain pattern have correlated it with the default mode network (DMN) in the brain. In particular, DMN was thought to be associated with the manifestation of the internal, spontaneous thought that occurs daily (Andrews-Hanna, 2012) as well as the memory retrieval, reconstruction, and perception of others (Buckner, Andrews-Hanna, & Schacter, 2008).

The default mode network (DMN) proposed in the early 2000s (Fox et al., 2005) was a concept that's correlated significantly with internal stimulation. It was initially based on the non-task activity states in the brain (Fox et al., 2005). It was thought to be only present in task-negative conditions, but later studies have shown that the DMN can still be identified in the internal task conditions (Ekhtiari et al., 2016; Spreng, 2012). This discovery provided an essential tool for looking into the underlying mechanisms of episodic memory.

5.2.2. Connectivity and Time Series Analysis of Episodic Memory

The default mode network was identified using meta-analysis performed over various studies and functional connectivity combined with functional magnetic resonance imaging (fMRI) technologies. This complex network is then subdivided into different smaller networks and hubs. Specific brain regions like the posterior cingulate cortex (PCC), medial prefrontal cortex (mPFC), and angular gyrus have been identified as functional hubs. Other areas like hippocampus (HF+), para-hippocampus (PHC), retrosplenial cortex (RSC), and posterior inferior parietal lobe (pIPL) were also identified as autobiographical memory-related networks (Andrews-Hanna, Smallwood, & Spreng, 2014).

The study by Andrews-Hanna and Spreng used methods like functional connectivity combined with resting-state fMRI to uncover the different components of the default mode network and the dynamic nature of the process (Fig.31). The resting state functional connectivity data is then analyzed using k-means and spectral clustering tools to identify further connected large-scale brain systems present (Petrican et al., 2020). Given the definition of functional connectivity, it is natural to use the method to explore the interactions and relationships between different components of the brain and a given network.

While functional connectivity surfaces the spatial and temporal patterns, it still overlooks some temporal features of the signal. Hence, dynamic functional connectivity was also used in episodic memory studies. Most commonly using a sliding window of various sizes across the entire period, resting state functional connectivity data was extracted from the overall brain signal. The features of the patterns within the window are then combined with techniques like clustering to identify other temporal structures of the networks (Allen et al., 2014).

Another suite of methods involved in episodic memory study analysis was those adopting a multivariate perspective. As shown in chapter 3, the adaptation of MVPA, Graph theory, and Deep Learning techniques all provide unique and powerful tools for memory encoding, retrieval, and reconstruction systems. While predominantly used in EEG and MEG studies, time series analysis of fMRI data has also been adopted using a multivariate perspective. This is used in conjunction with other methods to increase neurological patterns' detection (Jeong, Chung, & Kim, 2015). In this study, the analysis will be built upon these established and verified methods

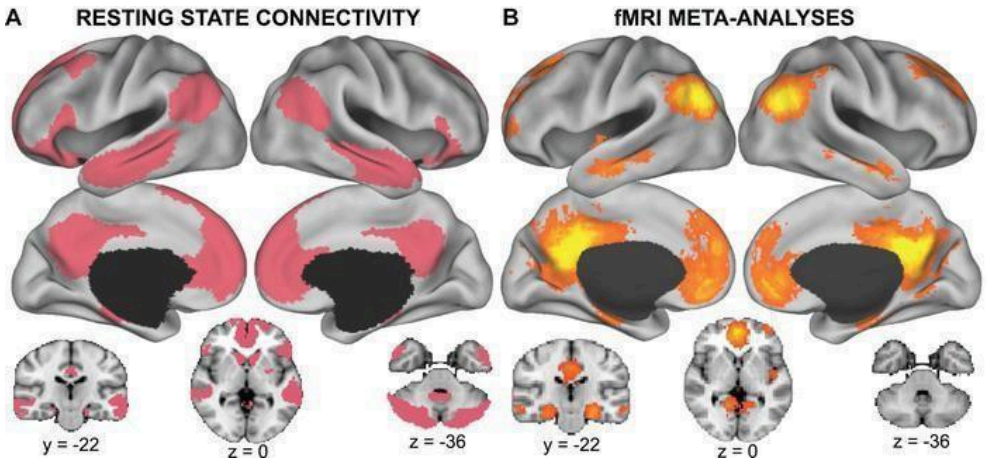

Figure 31: Default Mode Network obtained through functional connectivity data (A) and NeuroSynce software (Andrews-Hanna, Smallwood, & Spreng, 2014).

to aid our investigation of the endogenous stimuli paradigm used in episodic memory studies.

5.2.3. Brain Networks In Episodic Memory

Previous studies have identified many brain regions and networks active during episodic memory episodes. This includes autobiographical memory also. Hassabis and Maguire (2007) showed that the default mode network (DMN) and related regions play a critical role in the episodic memory process. These regions are activated during the retrieval process and in various other functions.

Rugg and Vilberg (2013) examined the brain networks that are commonly activated during the various stages of episodic memory sessions. In particular, they have identified stimuli-agnostic regions - the ones that are active regardless of the actual memory content of the episodic or autobiographical memory session. More specifically, they have identified a general recollection network that consists of the hippocampus, parahippocampal, retrosplenial/posterior cingulate and lateral parietal cortices, and medial prefrontal cortex. These regions are the proven components of the default mode network - the functional hub and medial temporal sub-system (Andrews-Hanna, Smallwood, & Spreng, 2014). These regions are stimuli agnostic - meaning that these regions are activated regardless of the episodic memory content.

A similar core network was identified in autobiographical memory studies through static functional connectivity analysis (Inman et al., 2018). The core network consisting of the hippocampus, medial and ventrolateral PFC, posterior cingulate, and temporoparietal junction were identified. As shown in other studies, these regions are active during various memory retrieval tasks regardless of the actual content of retrieval.

The episodic memory process involves many different sub-cognitive processes and, as a result, activates different brain regions based on the actual memory task involved. It has also been shown that the brain network activated varies between the early and late stages of the autobiographical memory retrieval process. The core network is most notable in the early phases. Other regions are more active in later phases, including those involved in sensory information retrieval (visual cortex), mental imagery for sensory information (precuneus and inferior parietal cortex), and goal-directed control processes.

Other brain regions and networks have also been identified for different types of endogenous stimuli. It has been shown that emotional episodic memories involve the interaction of several brain regions, including the amygdala, hippocampus, and prefrontal cortical regions, in the encoding and retrieval process (Dolcos et al., 2017). In addition, it has been suggested that the effect of emotional information on the memory of faces may be mediated by the interaction between affective systems (such as the amygdala, medial orbitofrontal cortex, and insula) and memory systems (such as the hippocampus and fusiform face area). These findings demonstrate emotion's importance in shaping how we remember and retrieve information.

When it comes to music-relevant sessions, the studies have also shown distinct regions and networks that are active. Previous research (Reybrouck, Vuust, & Brattico, 2018) has shown functional connectivity between brain networks involved in aesthetic judgment, evaluative decision-making, and reward processing. However, the connection between music and the default mode network (DMN) remains a topic of debate, both during active listening and at rest. Episodic

musical memory has been linked to increased cerebral blood flow in the middle and superior frontal gyrus and precuneus. In contrast, semantic musical memory has been associated with increased blood flow in the medial and orbitofrontal cortex, left angular gyrus, and left anterior middle temporal cortex. These findings suggest that these two types of musical memory have distinct neural representations and overlap partially with verbal semantic and episodic memory systems.

Brain regions have also been identified for randomization processes in humans. In the study by Jahanshahi et al. (2000), a network consisting of the dorsolateral prefrontal cortex (DLPFC), anterior cingulate, bilateral superior parietal cortex, right inferior frontal cortex, and bilateral cerebellar regions were identified. These results have shown that episodic memory and endogenous processes activate many different regions in the brain throughout its life course.

5.3. Endogenous stimuli in Episodic Memory

Endogenous stimuli are generated internally, as opposed to exogenous stimuli, which come from the external environment. In the context of autobiographical memory, endogenous stimuli are often related to thoughts, feelings, and emotions generated within the individual and can trigger memories of past events or experiences.

Endogenous stimuli in this study refer to the internal, self-controlled stimuli applied to our experimental paradigms. There have not been many studies in this specific domain. Most studies exploring episodic memories aimed to investigate their underlying system. These studies employ techniques including learn and retrieval paradigm to identify brain regions and networks at play during episodic memory episodes. The internalization of the stimuli often takes the form of providing specific cues to subjects. In the case of autobiographical memory, it involves asking the subjects to create cues to these events and recall specific conditions or events that had happened before based on the cues. However, these studies do not explore the experimental paradigm where subjects use conscious control of the internal stimuli.

Studies on endogenous stimuli in autobiographical memory have focused on how these internal stimuli can influence the retrieval of memories. For example, research has shown that emotions play a significant role in retrieving autobiographical memories, with certain emotions more likely to elicit specific memories. For instance, negative emotions such as sadness or anxiety may be more likely to elicit memories of negative experiences. In contrast, positive emotions may be more likely to elicit memories of positive experiences. In the study by Vedder and colleagues (2015), episodic memory was employed to explore the positive and negative aesthetics and emotional impact on subjects' perception of the environment. These studies try to use episodic memory or internal stimuli to identify significant or robust brain pattern dissimilarities in different experimental conditions.

Other research has focused on cognitive processes, such as attention and interpretation, in retrieving autobiographical memories. For example, some studies have shown that attention to specific details or aspects of memory can increase the likelihood of that memory being retrieved. In contrast, other research has shown that how we interpret or make sense of our experiences can also influence the retrieval of autobiographical memories. For example, mindfulness and meditation involve self-awareness, self-regulation, and self-transcendence (Vago & Silbersweig, 2012), which is the manifestation of endogenously invoked experiences. Other studies exploring internal stimuli focus on topics like dreams and insomnia. These studies differ from the previous ones in that they are trying to explore the conscious application of endogenous stimuli in the cognitive process in addition to memory retrieval paradigms.

Despite these efforts, there has not been a systematic review of the robustness and feasibility of using internal stimuli in episodic memory sessions or combining them with cognitive paradigms in general as a source of experimental stimuli.

As mentioned, the endogenous stimuli referred to in this study are controlled through subjects. This manifests in providing minimal cues to subjects during an episodic memory session. Previous studies show a significant brain pattern difference between lab-based conditions and personal-event-related memory retrieval (Chen et al., 2017) during memory processing. This indicated logical neural differences in recollection of remote memories (life events) and rather recent memories (lab conditions). In endogenous stimuli-based experiments, the subjects were instructed with only basic cues when the recording happened. After the experiment, the subjects recorded or reported the complex stimuli. Through the application of endogenous stimuli as an experiment condition, we are hoping to be able to identify more complex neural patterns or brain activity.

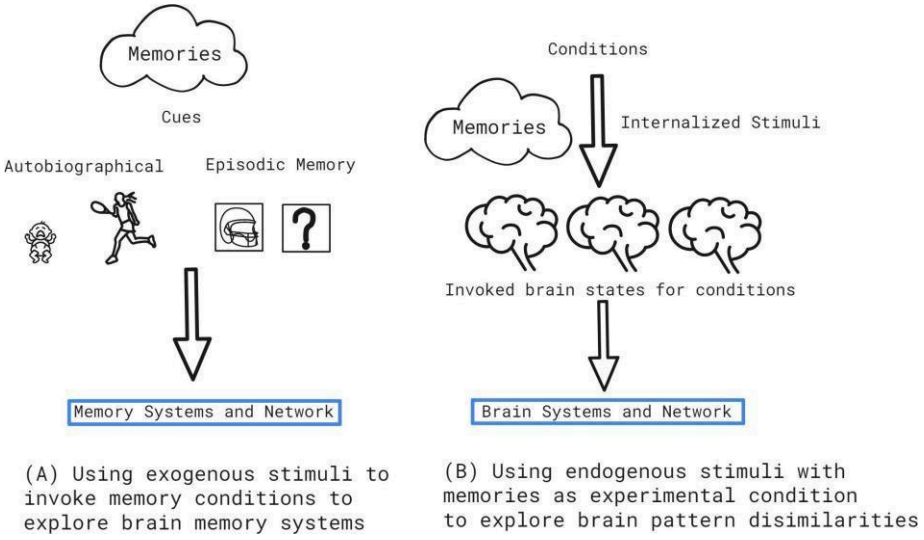

Figure 32: (A) In common episodic memory and autobiographical memory studies, stimuli-induced memory sessions were used to identify brain pattern differences concerning different aspects of the memory process. (B) In endogenous stimuli experiments, subjects are instructed to use internalized stimuli/cues for different experimental conditions. Like the one with beautiful vs non-beautiful environments (Vedder et al., 2015). This application provides insight into brain pattern dissimilarities in conditions with respect to the internal processing of the subjects.

Instead of investigating the brain networks at the memory system processing level, we hope to use this paradigm to study complex brain activities ranging from neural aesthetics to temporal control and perception. In this study, an analysis consisting of vetted existing methods will be used to explore and verify the possibility of using endogenous stimuli as a paradigm. Methods including functional dynamic connectivity, artificial intelligence, deep learning tools, and statistical and temporal analysis methods provide us with the power to explore the data and find what is hidden behind the patterns in the brain.

6. Research Questions and Framework

6.1. Research Questions

As shown in the previous chapters, fMRI is a commonly used method in neuroscience and has a wide range of analytical tools available for analysis and interpretation. In recent studies (Keightley et al., 2003; Vessel, Starr, & Rubin, 2012; Pöppel et al., 2013), an increasing trend in using endogenous stimuli in conjunction with fMRI techniques has been observed (Fig. 33). However, its implication and application still have not been fully investigated in the fMRI domain.

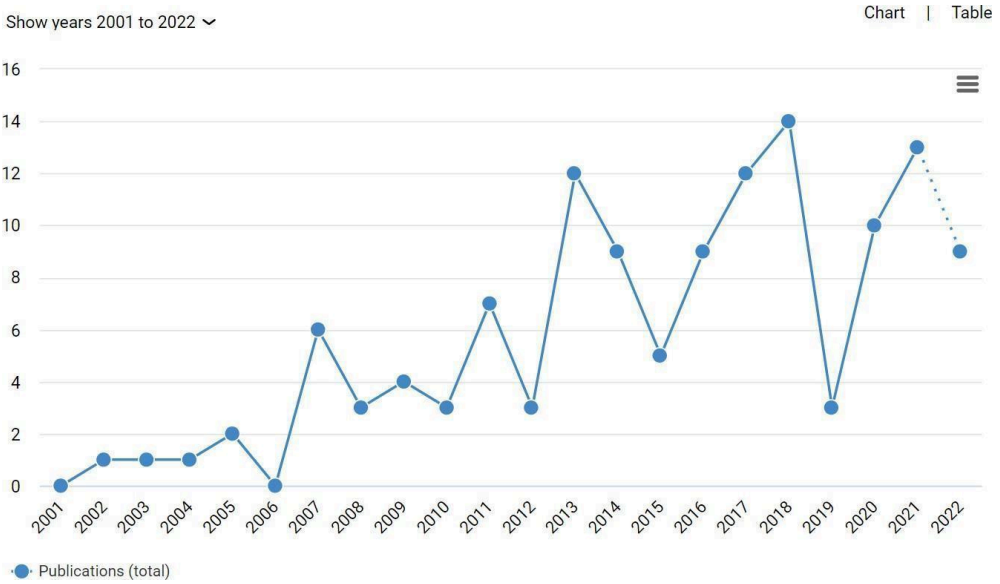

Figure 33: The number of publications. (Deffieux et al., 2018)

This study explores the feasibility of using endogenous stimuli in fMRI studies as a reliable paradigm. Through comparative analysis, I aim to explore whether endogenous stimuli can create robust and significant differences in different experiment trials. The result of our methodology would further prove its validity.

6.1.1. Endogenous Experimental Paradigm

Endogenous stimuli have been discussed and studied for a long time, like the works of Freud (Knockaert, Geerardyn, & Van de Vijver, 2002). Popular science has examined the impact of endogenous stimuli in the form of willpower, meditation, and dreams (Hobson, Pace-Schott, & Stickgold, 2000). It needs to be made clear that, in the concept of thesis, the endogenous stimuli refer to not only the visual images and inner speech that are generated internally but also the higher-level top-down modulations involved in different human activities. It is the internal manifestation of stimuli that is being elicited by the functioning self under experimental instructions. Was the subject reliably recollecting the morning routines? Was the subject reliably retrieving knowledge of music and replaying the piece in his or her mind? Be it the working self or the autonoetic consciousness model; subjects were expected to experience the past time as episodes and project them to the present. There is no doubt that self-modulation plays an essential role in explicit memory retrieval, but to what extent we can trust it as a robust supply of stimuli is to be explored.

In the past decades, we have seen increasing studies incorporating certain aspects of endogenous stimuli. Some common themes among these studies were to understand internal control and attention modulations in humans (Abrams & Dobkin, 1994; Casagrande, M., & Mereu, S., 2009; Lutz et al., 2008; Dugué et al., 2020). Most studies were designed around attention modulation and compared

the behavioral results or certain brain region activation patterns. Some recent studies have tried to expand the scope and incorporate endogenous stimuli more meaningfully in the domain of neuroaesthetics and moral judgments. In a study led by Avram and colleagues (2013), fMRI studies were conducted to compare internal activation in aesthetic and moral judgments for subjects - the study was based upon the endogenous interpretation of art and ethics. In other studies, subjects were asked to recall pleasant/unpleasant, beautiful/non-beautiful environments in episodic memory, and their neural activities were compared using fMRI (Vedder et al., 2015).

Overall, the study of endogenous stimuli in episodic memory highlights the importance of internal factors in retrieving memories and helps shed light on the processes involved in memory retrieval.

Episodic Memories is a natural aspect when thinking about endogenous stimuli, and there are indeed studies (Vedder et al., 2015; Suckling et al., 2008) that try to combine both into the experimental paradigm. In autobiographical memory, where one's personal history is retrieved (Robinson, 1976), there is the possibility of extensive application for endogenous stimuli modulation. For instance, major accidents may create stronger memories when recalled (Wang, 2010) and possibly result in post- traumatic stress disorder (PTSD) (Thome et al., 2020).

These studies and others (Pöppel et al., 2013) unveiled the possibility of using endogenous stimuli as experimental conditions in neuroscience studies. However, the validity of the endogenous stimuli is yet to be answered. In previous studies, the focus was on attention modulation, visual imagery, and aesthetic judgment for endogenous stimuli; this also left the question of endogenous stimuli application in other channels. In particular, it has been previously mentioned that humans can generate random numbers (Persaud, 2005), but are there underlying structures yet to be unveiled?

6.1.2. Question and Hypothesis

The question is whether the endogenous stimuli-based experimental paradigms could be used to elicit reliable spatiotemporal differences when applied to autobiographical memory sessions, episodic memory sessions, or as a top-down internal modulation process in experiments that involves both endogenous and exogenous stimuli. In other words, can the endogenous stimuli paradigm be used as a reliable input source in experiments involving various conditions?

The question can then be decomposed into sub-questions centered around exploring the paradigm's feasibility or reliability. 1. Can endogenous stimuli reliably modulate long episodic memory sequences? 2. Can endogenous stimuli (strong emotions) elicit consistent differences in short episodic memory sequences? 3. Can endogenous stimuli/processes reliably elicit differences in memory sequences and modify retrieved information? 4. Can endogenous stimuli/processes reliably induce differences in content generation under different scenarios?

These questions progress the exploration of the reliability of endogenous stimuli/processes from pre-defined retrieval to open-ended retrieval, to retrieval of memory and internal modification, then to retrieval of memory and content generation based on the internal modification. The thesis will examine the validity of the endogenous stimuli/processes' paradigm from the inward scenario to modification and outward scenarios.

The question to follow is, how can reliability be defined? As with any study, the center of the analysis is focused on the comparisons. Therefore, whether consistent spatiotemporal differences in brain regions can be identified through comparisons can be used as an indicator to identify reliability properties and demonstrate the feasibility of the paradigm.

The hypothesis, therefore, is that endogenous stimuli can be reliably used as a source of stimuli for experimental conditions in all the scenarios - from retrieval and modification to generation of cognitive processes.

6.2. Experiment Framework

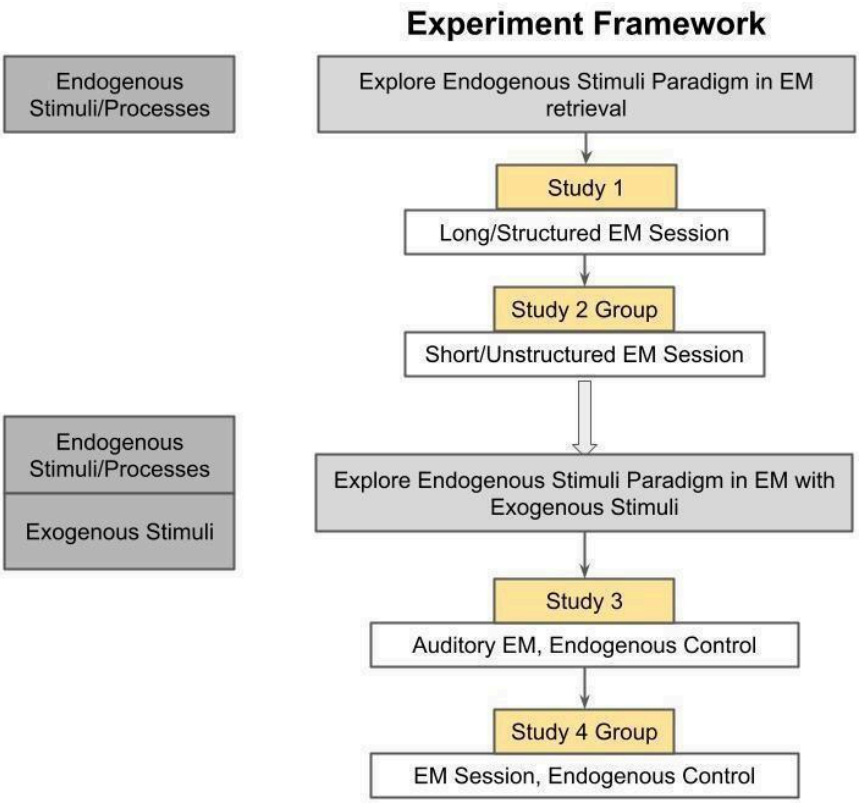

Figure 34: Experiment Framework

6.2.1. Framework

The breakdown of the research question leads to the experimental framework constructed to answer the questions. As mentioned, this study aims to examine the validity of the application of endogenous stimuli experimental paradigm in different episodic memory (EM) scenarios and EM experiments with exogenous stimuli involving content modification and generation (Fig. 34). The validity will be examined through comparative measures - identifying consistent spatiotemporal regularities by comparing different experimental conditions. The experiments will start with single case studies followed by group studies.

I begin with episodic and autobiographical memory using endogenous stimuli. To establish the feasibility of the method, I first explore whether this approach can elicit differences in multiple sensory channels when combined with episodic memory in single-case scenarios. A single case study was conducted with a long sequence of episodic memory retrieval scenarios. The subject was given no external stimuli during the session, in which she was told to recollect morning sequences of activities. Timing control was an inherent component of the study. Hence, I want to examine the temporal structure of the memory episodes to see whether it is consistent. The hypothesis is that endogenous stimuli can be reliably used in a long structured episodic memory session.

Then, I want to answer whether strong emotional cues as endogenous stimuli can elicit robust differences among several subjects in episodic memory sessions. Many studies have shown that positive and negative emotions impact one's autobiographical memory. A group study consisting of short-duration episodic memory sessions was conducted. This study examined a group of highly successful people in leadership positions. They were instructed to recollect strong (intense) positive and negative experiences that had happened before, either to themselves or others (Due to the sensitivity and privacy of the issue, detailed contents were not asked to be reported). Would the analysis identify coherent spatial-temporal structures? Could strong emotional cues be used reliably in short-duration episodic memory tasks?

The next question is whether endogenous stimuli can reliably induce differences in memory retrieval. A single case study was conducted in which the subject was instructed to recollect musical pieces that the subject had conducted before in different tempos. The single case study involved the endogenous

stimuli of both auditory and temporal processes with varying duration. The hypothesis is that the endogenous process can elicit consistent temporal regularity differences at varying tempos - meaning that the paradigm of endogenous modulation can be reliably used.

Finally, I would like to expand the investigation to semantic memory studies, where exogenous and endogenous stimuli are combined with memory retrieval and content generation tasks. A group study was conducted in which the experiment includes semantic memory (numbers or words) and calls upon endogenous processes in randomized content generation. Subjects were instructed to produce random items (numbers or words) at different tempos in a randomized manner. The analysis would aim to identify potentially common structures. In addition, the study should answer the question of whether endogenous stimuli/processes reliably induce differences in content generation.

6.2.2. Analysis Methods

The analyses are based on comparative measures to explore and further examine the reliability of endogenous stimuli experimental paradigms. This form of analysis is commonly adopted. For instance, most fMRI studies conduct experiments in different conditions and compare the different neural activities (Vedder et al., 2015; Avram et al., 2013; Silveira et al., 2015) between these conditions. The fact that different conditions can elicit significant differences in the brain would indicate that applying the experimental paradigm has a certain level of validity and re-usability.

As reviewed in Chapter 5, the explicit memory process (semantic and episodic) in humans engages a wide range of brain regions and networks. To examine the consistent spatiotemporal regularities induced through comparison, suites of different brain networks were selected based on the experiments conducted.

The commonly activated networks, like the Default Mode Network (DMN), were selected to be examined in all the studies. This network includes functional hubs like the angular gyrus, the precuneus cortex, and the posterior cingulate gyrus. Memory hubs of the DMN were also included, such as the parahippocampal gyrus and the hippocampus.

After selecting the brain networks, a pipeline was employed, combining machine learning and a wide range of statistical tools to examine the comparative differences from many directions. Proven methods used in previous studies have been integrated into the pipeline. The methods range from functional connectivity analysis and whole-brain dynamic functional connectivity analysis to temporal analysis methods like the PnP method. These proven methods were combined to create an analysis pipeline that aims to extract more artifacts for comparison among conditions and studies to investigate further and prove the experimental paradigm’s validity. It should be noted that there does not exist a single golden analysis standard for all experiments. Therefore, the pipeline presented resembles that of an arsenal where a wide range of tools can be picked to tackle the analyses.

7. Analysis Methods

7.1. fMRI Analysis Pipeline

fMRI data analysis usually involves two significant steps: pre-processing and post-processing. Pre-processing steps will be described in detail in each study. Here I will give an overview of the post-processing steps and explain each step afterwards.

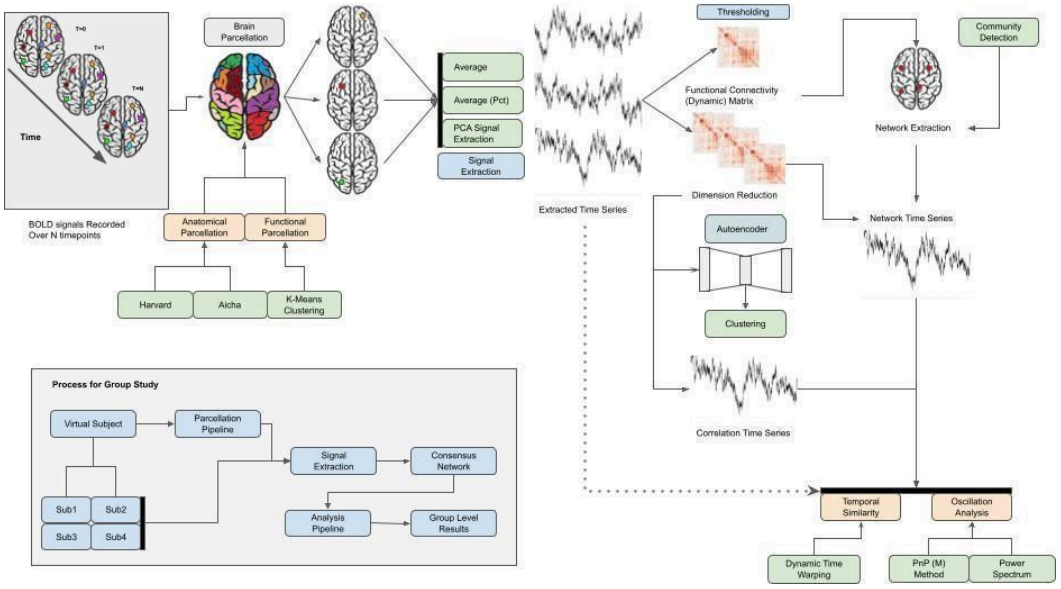

Figure 35: Overview of the analysis pipeline involved in the studies. The illustration covered the overall pipeline, except for standard pipelines like GLM and RSA.

The proposed post-processing analysis pipeline is shown in Fig.35. This post-processing pipeline is based on the general processing pipeline for functional connectivity and graph theory analysis. After acquiring the pre-processed fMRI BOLD signals, the first step is identifying brain regions for further analysis. The identified brain regions would create a parcellation of the brain and be used for further analysis. While many studies explore this brain parcellation problem, none of the methods is the golden standard in fMRI studies. Hence, I will employ different parcellation methods to identify relevant brain regions for subsequent pipelines - including standard methods like clustering and dictionary learning and complex methods like graph theory (see Chapter.7.1.1).

After identifying the brain parcellations, a brain map containing regions of interest (ROIs) can be obtained to reduce the amount of data considered. For example, through the anatomical parcellations, regions known to be active during the initial autobiographical memory stage, such as the ventrolateral prefrontal cortex and anterior hippocampus (Inman et al., 2018), can be extracted. After acquiring these regions, the idea is to extract signals from them and use the reduced signal to compare the relationships between different brain regions. In most fMRI studies, this step simply uses the averaged, standardized (usually z-score) BOLD signals from each ROI (Friston, 2011). A natural question is the reliability and expressiveness of the averaged signals compared with original, uncompressed signals. Hence, alternative methods are also explored - including PCA-based principal signal extraction and autoencoder-based signal reduction. Another simple yet effective method is to use the percentage change of the BOLD signals instead of using them directly (see Chapter.7.1.2).

After acquiring the compressed signals, the step is to calculate the (dynamic) functional connectivity matrices (see Chapter.7.1.3). This step uses the standard practices in fMRI studies - calculating the Pearson correlation between ROIs and thresholding the resulting matrices to identify connectivities (Eickhoff & Müller, 2015). However, the analysis that follows identifying the matrices differs from standard analysis pipelines.

After identifying the static functional connectivities, community detection methods like Louvain methods will be used to identify brain networks that are functionally close (see Chapter.7.1.4). With the network identified, I can compare the similarities and dissimilarities between different stages (or time points) of the network throughout the experiment recordings. The dynamic (dis)similarities would provide the temporal changes within the networks, and I can apply different temporal analysis pipelines. Another analysis using dynamic functional connectivity will also provide temporal changes in the brain. This method was proven effective in a recent study by Spencer and Goodfellow (2022). The primary logic is to use auto-encoders for reducing the dimensions of the dynamic functional connectivity matrices and then use the reduced representation for clustering.

In this study, the distances between different low-dimensional representations are also calculated to create a temporal sequence that can be used to capture the temporal properties. As reviewed in 4.1, many different similarity/dissimilarity metrics can be applied. Not all metrics perform well under high dimensional space. Hence, through the reduction steps introduced in the previous pipeline, I can obtain a more feasible problem space for calculation. All time series signals will then be sent into the temporal analysis pipelines, and detailed temporal analysis methods will differ based on the details of the experiment design. This study examines two aspects of temporal dynamics: temporal similarity and oscillations. Dynamic time warping (introduced in 4.3) will be used for temporal similarity. For exploring the oscillations, a Python package was implemented based on non-parametric regularity detection methods proposed by Pöppel, 1970.

As indicated, two single-case studies and two group studies were conducted. As shown in Fig.35, additional steps need to be performed on group studies. A virtual subject (VS) was created to identify reliable brain parcellations for groups based on the averaged pre-processed BOLD signals. The brain parcellations would then be applied to the VS to identify ROIs for further steps. The signals from individual subjects would be extracted based on the brain regions to identify first-level statistics. The cross-subject (second-level) analysis would then be conducted to identify standard networks and significant temporal patterns across the group. Non-parametric testing methods, as introduced in Chapter 4, will be applied to identify significant results.

I have combined proven fMRI analysis pipelines with novel methods, such as autoencoder-based ROI signal reduction, network temporal dissimilarities, and temporal pattern analysis using non-parametric methods (see Chapter.7.1.5). These methods are chosen from a plethora of methods developed over the past century and are put together to help identify, extract, and understand the spatiotemporal patterns within the brain during endogenous stimuli-based studies.

7.1.1. Brain Parcellation

Over the years, many methods have been developed and explored to provide parcellations for the brain. One of the primary reasons why this method is so important is that it reduces the neural imaging data to a manageable size and enables it to examine changes in identifiable brain areas. As mentioned previously, there has yet to be a golden standard on one method that should be chosen to produce brain parcellations (Thirion et al., 2014). Given this, two primary suites of methods (anatomical and functional parcellation) used in parcellation were adopted in the pipeline to provide comprehensive insight into different parcellation results.

Anatomical Parcellation Anatomical parcellations of the brain are usually based on T1-weighted images. The T1-weighted images provide visualizations of the patterns of the cortical and subcortical areas. These visualizations may be used to generate labels for specific locations in the brain and form an anatomical atlas (Moghimi et al., 2021). Despite lacking a golden method there are several commonly used atlases in practice, and one study has aimed to create a common standard based on these atlases (Lawrence et al., 2021). In my analyses two atlases were selected. The most commonly used template across studies - The Harvard-Oxford cortical (HOC) atlas is chosen along with the AICHA (Atlas of Intrinsic Connectivity of homotopic areas) atlas, which provides a fine-grained parcellation of the brain up to 384 regions.

The FSL Harvard-Oxford cortical (HOC) atlas was chosen as it is one of the most frequently used anatomical parcellations in fMRI studies and is also used as the default brain atlas for the standard tool Conn Toolbox (Whitfield-Gabrieli, 2012). The atlas contains 132 regions, including cortical and subcortical areas. The FSL HOC atlas was created from a balanced sample pool of 16 females and 21 males, with subjects' ages ranging from 15 to 80 years old. The atlas is normalized to MNI 152 space to stay aligned with the standard representations.

AICHA atlas provides detailed parcellations of the brain. Joliot et al (2015) published the initial atlas AICHA V1 and posted the improved version in 2021. The V2 version projected the AICHA to MNI 152 space as defined by spm12. This atlas includes a total of 192 matching regions in the brain, resulting in an atlas of 384 areas (Joliot et al., 2015). This atlas was generated based on the resting state network and k-means clustering of the functional connectivity. Homotopic regions were then calculated and labeled to generate the final atlas. The atlas provides the center ROI coordinates and can be used to identify fine-grain mappings between anatomical parcellations and other parcellation methods described below.

Functional Parcellation Functional parcellation methods include k-means clustering, ICA parcellation, and Ward clustering. The number of clusters selected was 350 for K-means, 20 for ICA, and 500 for Ward. The ICA parcellation results are further decomposed into 40 images between positive and negative ROI images. However, our studies' analysis of the Ward parcellation and ICA methods yields too many small, trivial clusters that are difficult to analyze and interpret. Hence, I have selected K- Means clustering as the functional parcellation method.

7.1.2. Signal Extraction

After acquiring the brain parcellations, I can identify brain regions of interest (ROI) to reduce the dimensions of the brain signals. Common methods include averaging the signals within an ROI and calculating the percentage changes (Rana et al., 2016). Alternative methods like counting the activated voxels have also been proposed but are unreliable (Poldrack, 2007). Here I propose to include three signal extraction steps, average-based, percentage-based, and PCA-based, in neuroimaging studies as references to each other.

Average Signals This method is the most commonly adopted method in fMRI experiments due to its simplicity and relative accuracy. Suppose we have a brain region R with V voxels inside it. Each voxel is recorded over time T and has a corresponding value x at each time point. The average representation of the brain region R is calculated as follows:

$$R = \left\{ val_t = \frac{\sum_{n=1}^{V} X_{tn}}{V} | t = 1,\dots,T \right\} \quad (11)$$

The averaged signal is usually normalized using z-score before being analyzed with PCA, ICA, or functional connectivity analysis.

Percentage Change Most common fMRI studies, while they do not directly look at the BOLD signal raw values, use these values nonetheless. For example, calculating the average signal value of a given brain region, then standardizing the value (convert to z-score) and using the value to calculate the correlations between different regions. However, the raw BOLD signal in fMRI recordings varies from machine to machine and reflects magnetic strength. Therefore, directly interpreting the voxel value does not entail much meaning (Logothetis, 2008). A common practice also used in other domains, like finance and geology, is calculating the signal percentage change. This value is calculated as the following:

$$pct_{Ti} = \frac{(v_{Ti+1} - v_{Ti})}{v_{Ti}} \quad (12)$$

A study done by Rana et al. (2016) has demonstrated that high correlations can be identified by comparing the percentage change of the BOLD signal in selected ROIs. The connectivity matrix

calculated using the standardized BOLD signal is much noisier than the one calculated using the percentage change shown in Fig.36a and Fig.36b.

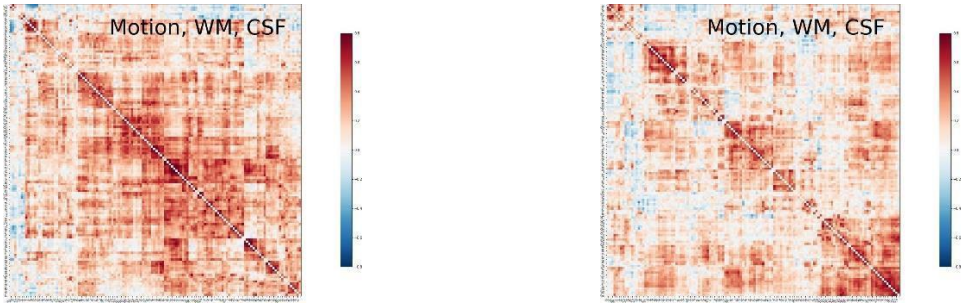

(a) Correlation Matrix of Raw Signal (zscore)

(b) Correlation Matrix of Percentage Change (zscore)

Figure 36: Different correlation values calculated using the percentage change and raw value. The regions are regrouped to show regions that activate together.

PCA-Based signal extraction PCA (principal component analysis) based signal reduction is the processing of extracting the principal signals from a given region. The PCA method will decompose the original signal into an array of signals that can be used to explain it. The first component decomposed usually can explain around 60-70% of the original signal, hence termed the principal component[9]. The benefit of this approach is that the signals are no longer extracted using the average method, hence providing more meaningful results. The principal signal of an ROI would also provide a better abstraction in that a significant amount of signal properties are preserved in the principal component.

7.1.3. Functional Connectivity Analysis

The functional connectivity analysis (FCA) concept details have been described in 3.4. As shown in Fig.35, the FCA involves two types in my analyses. The static FCA in which a connectivity matrix will be calculated over the entire time course of the BOLD signal between different ROIs. The method used is simply Pearson correlation, as with most fMRI studies. The connectivity matrix will then be fed into the graph-theory-based analysis pipeline to identify sub-networks for subsequent steps in the pipeline.

Another analysis step is the dynamic functional connectivity (dFC) analysis. It has been shown that the accuracy of sliding window technique was most prominantly influcned by the window length (Shakil, Lee, & Keilholz, 2016). In a recent study by Spencer and Goodfellow (2022), however, it is shown that when integrated with autoencoder to reduce dimensions of calculated dynamic functional connectivity matrix, the clustering results are much more accurate in terms of reflecting the underlying states. I employed dFC analysis to identify and compare different brain states resulting from clustering autoencoder-based low-dimensional brain connectivity representations as part of the deep clustering technique.

7.1.4. Graph Theory and Network

The application of graph theory aims to identify the community structures within the functionally connected brain regions. Sub-networks or community structures within the functional brain networks are relevant to cognitive functions and can reflect neural mechanisms at a smaller scale than within whole brain networks (Crossley et al., 2013).

Graph Construction An undirected graph {G = (E, V)} is constructed from the Functional Connectivity Matrix calculated from previous steps.

$$V = \text{Individual ROI}$$

$$E = 1 \text{ if the correlation between two ROIs exceeds a threshold. 0 otherwise} \quad (13)$$

[9] Details of PCA see Appendix.A.5

Graph Theory Methods The method adopted in this study is Louvain algorithms, which is highly efficient and robust even for large-scale graphs. The method is based on the concept of modularity[10], which is between [-1, 1] and measures the density of edges within and between communities. I employed graph-theory-based methods to separate communities in the graph in several steps. First, the FC matrices are thresholded to remove unwanted correlations. An undirected graph is then constructed based on the remaining correlations. The third step is simply applying the community detection algorithms to extract communities from the FC matrices. These communities are the functional brain networks that are highly correlated during the session. Further analysis can then be applied, for example, to narrow down the network in consideration by identifying overlaps with pre-defined brain networks. The community detection algorithm used here is the Louvain-Algorithm - a robust and scalable algorithm based on greedy modularity maximization.

Greedy modularity maximization The concept of greedy modularity is relatively simple. The greedy dictates at the selection step would be ”greedy” in that it should aim for the largest possible value. This algorithm will aim to merge communities that maximize modularity. The pseudo-code is as follows:

Algorithm 4 Greedy Modularity Maximization (GMM)

```
Require: G, E, V                          ▷ Graph G, Edge set E, Vertices V
  for v in V do
      Set Each node v to be a different community
  end for
  while possible to increase modularity do
      Join two communities that cause max modularity increase
  end while
```

Louvain modularity optimization The Louvain algorithm aims to optimize the modularity - if properly optimized, this results in the best grouping of vertices. The exhaustive calculation, however, is not practical on more extensive networks due to its complexity. The Louvain algorithm, similar to GMM, is a heuristic method. In gist, the smaller communities are identified by optimizing local modularity, and this process is repeated by collapsing small communities into a single node. The pseudo-code is as follows:

Algorithm 5 Louvain Modularity Optimization (LMO)

```
Require: G, E, V                          ▷ Graph G, Edge set E, Vertices V
  for v in V do
      Set Each node v to be a different community
  end for
  while possible to increase modularity Or modularity < threshold do
      while possible to increase modularity do
          for v in V do
              Try to move an isolated node to the community
              Calculate modularity gain
          end for
      end while
      G' = New network where a node is communities found in the previous step
  end while
```

The communities extracted from these methods will be isolated and used to identify temporal structures within the network. More specifically, the overall functional connectivity can be used to identify smaller communities within the brain as the unit of analysis. The temporal signals of each community, identified from previous signal extraction methods, will be collected to represent the temporal dynamics of the networks. A series of temporal pattern analysis and comparison methods can be used for further investigations.

7.1.5. Temporal Pattern Comparison

Temporal Dissimilarity As functional brain networks have been identified at this stage, time series data can be extracted from each network. To extrapolate the differences between the networks over time, I defined a neighboring brain state distance that aims to capture the temporal dynamics of multiple

[10] See Appendix.A.3

brain regions. More specifically, a single cross-sectional slice of the network is extracted at each time point, representing the brain network state. The different distance metrics can then be used for each sequential time point to evaluate the distances between neighboring functional brain network states.

For example, after acquiring the community from the brain network, each community C can be represented as a matrix consisting of different regions over time T. The dissimilarity between sequential time slices or baseline (mean) can be calculated.

$$C = \{R_i | i \in N\}, R_i = \{r_i(t) | t \in T\} \quad (14)$$

Where the dissimilarity between two the time points within the community can be defined as $Dist\ (C(t_l), C(t_k))$, as reviewed in 4.1.

It should be noted that no single optimal distance measure can be concretely selected in fMRI studies. The commonly used Euclidean distance in high-dimensional spaces is not as applicable as in low- dimensional spaces. Based on existing studies reviewed in Chapter 4, I choose three distance measures to extract dissimilarity representations between neighboring brain states. The methods selected include angle measure (cosine distance), distributional measure (Mahalanobis distance), and non-distributional measure (Euclidean distance). As shown previously, each distance metric would examine the relationships from a different perspective. Since the perspectives differ in each measure, a result agreed in all measures means it is significant and highly robust. However, a visible result in a single measure does not mean it is insignificant - it simply means the other perspective does not apply.

As shown in Fig.35, the last step in the pipeline is time series analysis to extract and compare temporal patterns from the different time series data. The extrapolated temporal sequences neighboring brain states and the raw time series extracted from each brain network can then be used to compare differences between different scenarios or conditions in the following pipelines.

Temporal Pattern Analysis As reviewed in 4.3, many families of time series data range from linear and non-linear to AI-based methods. In endogenous stimuli-based paradigms, the temporal structures are not known a priori and, in some instances, are unethical to obtain. Hence, it is an empirical task that statistical methods are employed to explore such temporal regularities. I used time series analysis methods to compare directly or indirectly different conditions within the experiment. The goals of these suites of methods are twofold: identifying temporally similar sequences and comparing regularity compositions of the signals.

The temporal similarity is tested using the Dynamic Time Warping (DTW) method (see 4.3). As for temporal regularities I adopted linear methods to identify the regularity components of the signals. One method used is the wavelet analysis (wavelet transform). This is because the neural signals are often spikes or saw-tooth oscillations (Kandel et al., 2000; Logothetis, 2008). The decomposition provides insight into the temporal structures of the brain patterns and allows us to explore the potential change points in the sequence. Another branch of the method is the
Non-parametric oscillation detection or PnP method (Pöppel, 1970; Li, Pöppel, & Bao, 2018). This method identifies oscillatory components from the time series with small samples and removes the implication caused by the trend of the data. Moreover, the non-parametric data does not assume data distribution and can be applied to most scenarios. The PnP method was used to detect and compare periods of similarities between signals from selected brain communities and BOLD signals, revealing the spatiotemporal regularities in the brain.

7.1.6. Deep Clustering Analysis

Deep Learning based whole-brain state analysis was performed based on the results of dynamic functional connectivity (dFC) graphs. The DFC matrices are calculated through a sliding window for the different selected atlas - anatomical and functional. The window size (25s) was chosen due to the limitation of experimental data. Since most studies do not have a long recording period, a lower threshold was selected to accommodate all studies. The overall pipeline of deep learning analysis is shown in Fig.37.

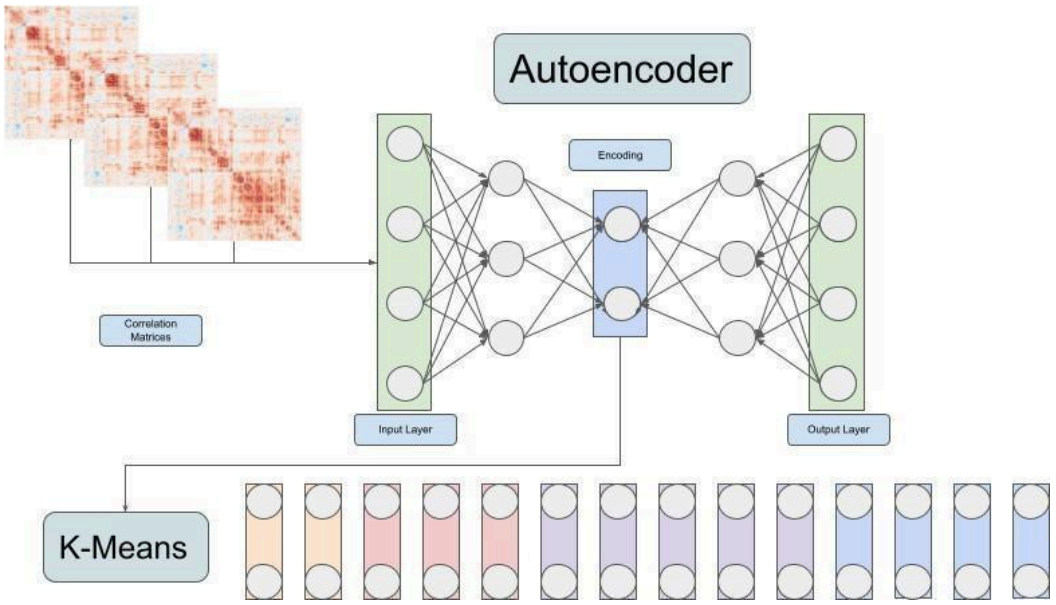

Figure 37: Deep learning autoencoder analysis pipeline.

An autoencoder is trained for each experiment and atlases used. The resulting models are then trained to generate encoding for each slice extracted using DFC. This creates an encoding with reduced dimensions. The encodings of each slice are then clustered into different groups using the k-means clustering method - common selections of clusters range from four to six (Allen et al., 2014). Through this method, a holistic view of the brain-state changes over time can be created and its transitions at a whole-brain level can be explored. This is a complementary analysis to explore the whole-brain-wide patterns and dynamic changes and serves as the last step of the analytical pipeline.

8. Single Case Study: Blind Lady Experiment

The single case study of a blind lady involves temporal control and autobiographical memory retrieval. Endogenous stimuli (ES) include visual, tactile, and temporal perception, which are used to construct the episode for mental travel. In this study, I would like to examine the spatiotemporal regularities among the ES trials and compare that with each other and the resting state. Through comparison, I can understand whether ES can elicit consistent states.

8.1. Subject and Experiment

8.1.1. Subject

The subject in this study is a 78-year-old female, a.k.a blind lady (BL). BL lost sight in her mid-twenties and has been living with assistance since then. No health concerns or neural-degenerative diseases were identified during the experiment. BL reportedly could formulate clear mental pictures of her frequently interacting with physical environments. BL had an established morning routine that can be recollected which is required as a prior for this experiment. The Ethics Committee of the Medical Faculty of the University of Munich has approved the behavioral and fMRI experiment protocols.

8.1.2. Experimental Paradigm

BL was instructed to provide a verbal description of the morning routine first. After the description, BL was asked to retrieve the morning routine in detail without any reporting. The experimenter dictated the beginning of the retrieval process, while BL indicated the completion of the process. The completion time was 7 minutes and 40 seconds in all three trials. After the initial experiment, fMRI data were acquired in four sessions. Starting with a resting state session followed by three morning-routine sessions, each lasting 7 minutes 40 seconds.

8.1.3. Data Acquisition

The fMRI data were collected using ascending order on a 3T MRI Phillips scanner in the University Hospital of LMU, Munich. During the experiment, four separate trials were conducted. The initial run was resting-state, in which BL was instructed not to focus on any topics. During the subsequent three runs, BL was instructed to recollect the details of her morning routine. A less than one-minute pause was provided between each run. The beginning of the run was provided to BL via a speaker.

The T1-weighted structural image was acquired with magnetization-prepared rapid gradient-echo sequence (MPRAGE) with the following arrangement: repetition time (TR) = 8.2 ms, echo time (TE) = 3.76 ms, flip angle (FA) = 8°, number of slices = 220, matrix = 256 x 256, slice spacing and slice thickness = 1 mm, in axial orientation. T2*-weighed functional images were acquired after the T1 session with an echo-planar image (EPI) sequence with the following arrangement: repetition time (TR) = 2500 ms, echo time (TE) = 30 ms, flip angle (FA) = 90°, number of slices = 48, number of volumes = 180, matrix = 144 x 144, slice spacing and slice thickness = 3 mm, ascending sequential acquisition in axial orientation.

8.1.4. Data Reprocessing

The T1 and T2-weighted images collected were converted into Brain Imaging Data Structure (BIDS) format using the dcm2bids python package[11].The preprocessing of the converted BIDS data was performed using the fMRIPrep package, which is a NiPreps (NeuroImaging PREProcessing toolS) application (www.nipreps.org) for the preprocessing of task-based and resting-state functional MRI (fMRI). The preprocessing steps include motion correction, slice timing correction, realignment, unwrapping, skull stripping, segmentation, spatial normalization to MNI 152 space, and smoothing (https://fmriprep.org/en/stable/workflows.html). All slices are realigned in time to the middle of each TR. Motion-corrected images have their motion confounds (three rotations, three translations) exported.

[11] https://github.com/UNFmontreal/Dcm2Bids/

8.1.5. Pre-defined Brain Network

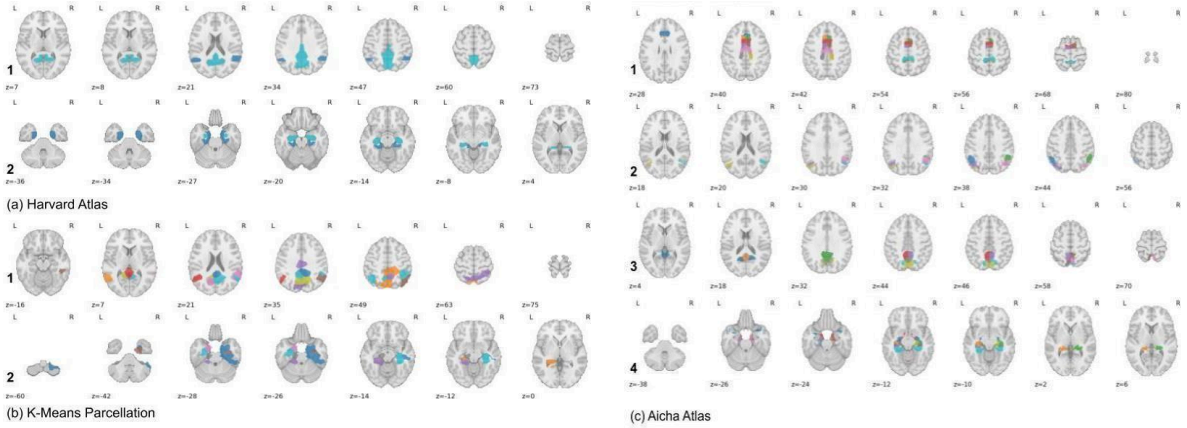

Figure 38: (a) DMN Network in Harvard Atlas. a.1 is the functional hub (PCC, angular gyrus, pre- cuneus). a.2 the memory hub (parahippocampal and hippocampus). (b) DMN Network in K-Means parcellation. The regions are selected based on overlap with Harvard regions - b.1(2) is based on a.1(2). (c) DMN Networks in Aicha Atlas.
c.1 Posterior cingulate cortex (PCC). c.2 precuneus. c.3 angular gyrus. c.4 Memory hub including parahippocampal and hippocampus.

In this single case study of the Blind Lady, I want to explore temporal regularities in selected brain regions known to be engaged in episodic and autobiographical memories. As a result, Default Mode Network (DMN) areas were included as pre-defined brain regions. As reviewed in Chapter 5, DMN and other brain regions are involved at different stages of the autobiographical memory sessions.

Given such, DMN regions concerning memory and functional hub were selected based on different atlases. Matching selection in functional parcellation was also generated for analysis. Note that different atlas and parcellations have slightly different ROIs, as shown in Fig. 38. The K-Means parcellation is functional parcellation based on whole-brain voxels; hence the shape of each ROI would differ from that of an anatomical parcellation. The Aicha atlas provides much more granular parcellations than Harvard. Therefore, the DMN is further divided into smaller networks for better granularity.

8.2. Results

The analysis followed the steps outlined in the pipeline, and the results are aggregated. The static functional connectivity-based network extraction results are combined with the pre-defined brain networks to identify regions that should be focused on in the analysis. Following the reduction of brain networks, the differences between the task conditions and resting state were compared from different perspectives. The PnP method was used to extract temporal regularities and identify discrepancies. The network-based PnP method was used to compare the spatial-temporal regulations in individual sub-networks. Finally, I compared the whole-brain state transitions between different conditions combining deep learning and dynamic functional connectivity analysis.

8.2.1. Functional Connectivity and Networks

Based on the analysis pipeline for single case studies, the signals were extracted from each ROI defined in the atlases, and whole-brian functional connectivity matrices were calculated. Pearson correlation was used to define the correlation between each ROI identified from the atlases. For each atlas, the signals were extracted from each ROI using three different methods: average signals of each ROI, percentage change of averaged signal for each ROI, and principal components extracted from each ROI's raw signal using the principal component analysis (PCA) method.

Due to the computation limitations, the whole-brain voxel-wise functional connectivity is not selected for this analysis. A single image in this study consists of 144*144*48 1 Million voxels, and roughly 300,000 are mapped to the brain. The 300k voxels would lead to a correlation matrix of 45 billion pairs (halved) for calculation and analysis. Since the ROI-based FC analysis has been used in most studies, I adopted this method. This approach is applied in analyzing all experiments described here.

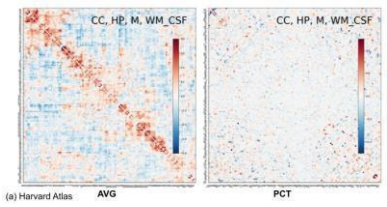

(a) Harvard Atlas FC matrix

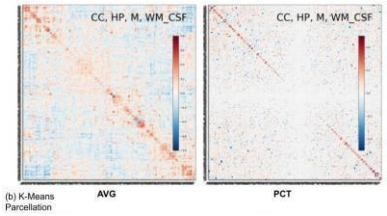

(b) K-Means Atlas FC matrix

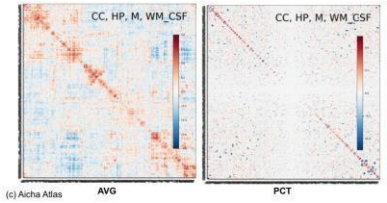

(c) Aicha Atlas FC Matrix

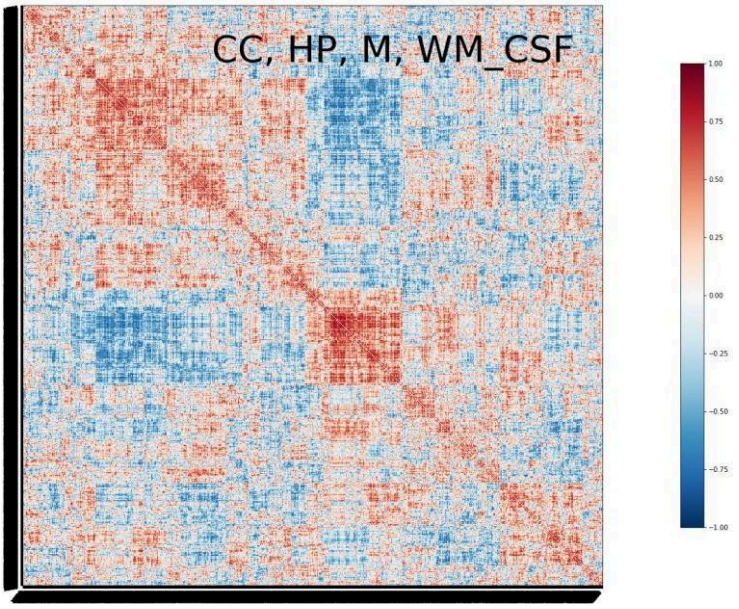

(d) whole-brain voxel-wise functional connectivity matrix

Figure 39: Functional connectivity matrices with confounds removed, including component correction, high-pass filter, motion, white matter, and cerebrospinal fluid. (a) Functional connectivity (FC) matrices for Harvard atlas averaged signals and percentage signals. (b) FC matrices for K-Means atlas averaged signals and percentage signals. (c) FC matrices for Aicha atlas averaged signals and percentage signals. (d) Whole-brain voxel-wise
functional connectivity matrix.

As shown in Fig.39 (a)(b)(c), correlation matrices for each atlas were calculated. Aicha atlas consisted of 384 ROIs, Harvard atlas had 132, and K-Means parcellation had 350 ROIs. The resulting FC matrices were then analyzed using community detection methods based on graph theory. An undirected graph was constructed from the FC matrix using methods described in Chapter.7.1.4. The communities' sizes identified from the FC matrices vary based on the actual threshold applied, as shown in Fig.40a. Averaged signal provides the largest variances in community sizes across different

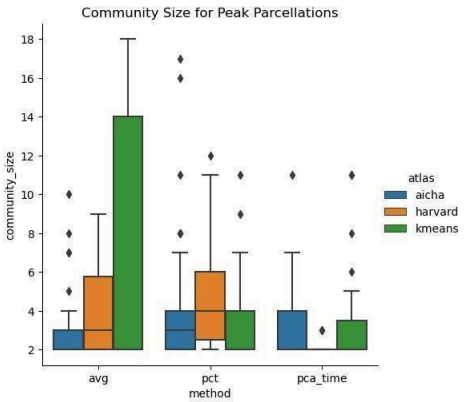

(a) Size (number of regions) of the communities identified through functional connectivity matrices.

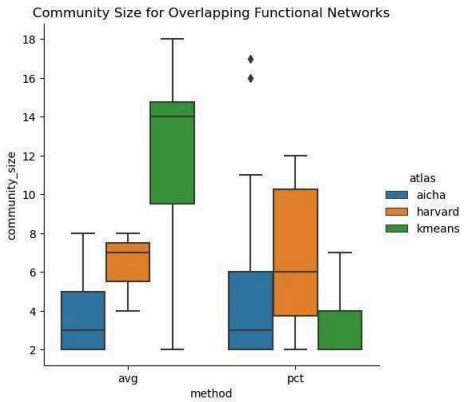

(b) Size (number of regions) of the communities selected based on existing studies.

Figure 40: Distributions of community sizes in brain networks. (More detailed explanations in the legend)

atlases. Percentage-based signal resulted in similar community size distribution between Aicha atlas and K-Means parcellation - a good signal as in Aicha and K-Means have similar ROI numbers. The PCA-based signal extraction, however, did not provide sufficient results for the Harvard atlas. This

indicates that the method is unsuitable, although the Harvard atlas is the most commonly used template. In addition to the predefined brain networks, additional functional networks identified based on the functional connectivity matrices are selected. The overlap metric is defined as the total number of brain regions in a functional network that also appears in the pre-defined brain networks. Only functional networks with overlaps are selected for further analysis. In this way, I can incorporate spatial brain patterns derived from the experiments in conjunction with existing studies. As shown in Fig.40b, the Size of the communities - defined in the number of brain regions included in the community - is smaller than that of ones generated based on pre-defined networks. The results mean that graph-theory-based community detection can provide more reliable networks in fMRI analyses.

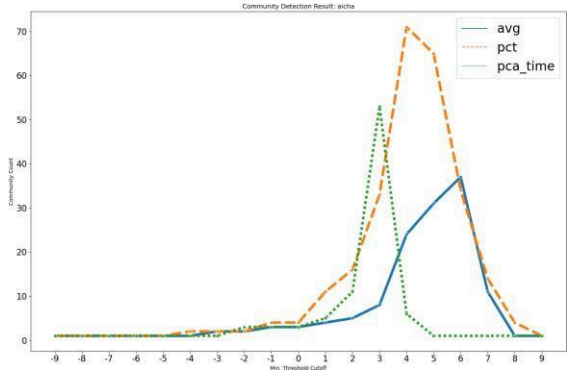

(a) Community count for aicha atlas

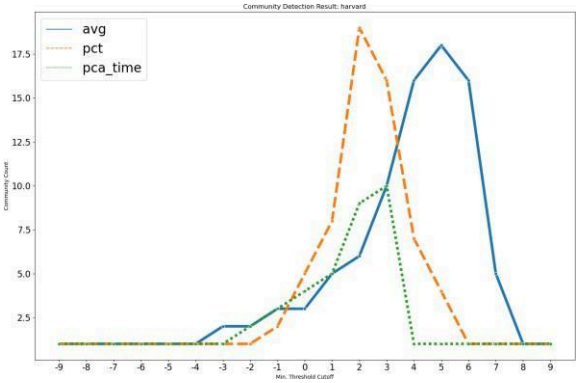

(b) Community count for harvard atlas

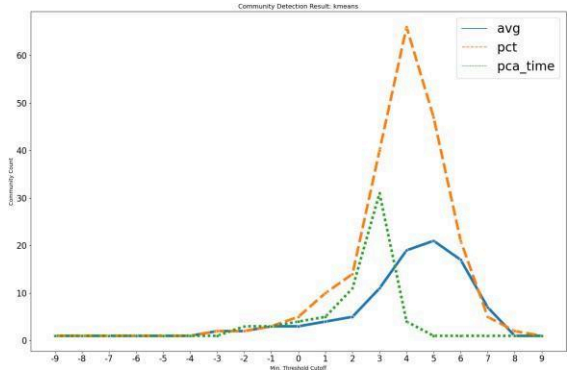

(c) Community count for k-means atlas

Figure 41: Total number of separated community distribution by threshold. The x-axis is the correlation value threshold used. A value of 5, for example, means that all values below 0.5 in the original FC matrix were removed from the calculation

Similar patterns can also be observed in Fig.41. The average signal aggregation method tends to have better community separation performance when the threshold is higher - meaning the correlations are stronger. This indicates that the communities identified in the average method (and percentage) are more strongly correlated than those identified by the PCA method and percentage-based methods in most scenarios. Given these observations, the method that yields most networks at high correlation levels should be selected in each study. In the case of the BL experiment, an average-based aggregation will be used.

8.2.2. Spatiotemporal Regularity

The multi-step temporal analysis results demonstrated that consistent spatiotemporal regularities could be identified in different brain regions. As shown in Chapter.7.1.5, the temporal signals extracted from each brain network are further processed to identify dissimilarities between neighboring brain states. I used three types of measures: angle-based distances, distributional and non-distributional distances. The resulting temporal sequences are then analyzed using PnP methods introduced in Chapter.4.4 to identify potential temporal patterns.

PnP Regularity Analysis Results of PnP analysis using the Brunner-Munzel test demonstrated consistent and significant spatiotemporal regularities extracted from the different brain networks. Fig.42 shows the half-period distributions identified from PnP methods with p=0.001. The angle, distributional measure (Mahalanobis distance), and non-distributional (Euclidean distance) demonstrate slight differences. It should be noted that when a result is agreed in different distance measures, it means that it is sufficiently different. Default Mode Network (DMN) functional hub and

memory subnetwork show consistent temporal regularity differences with respect to resting states. Additional functional networks are also shown to exhibit significant differences, as shown in the detailed comparisons in Fig.43. Network 6 in Fig.43(a) consists of angular gyrus, supramarginal gyrus, and inferior frontal gyrus. Brain regions in this network are involved in language processing and spatial recognition. As subject BL was instructed to recall the morning routine and provide the detailed routine in words before the study, the subject was likely to adopt a recollection method based on language. Network 7 consists of the bilateral lateral occipital cortex, PCC, and precuneus. The functional network highlights regions involved in object recognition and episodic memory retrieval. Significant differences in half-period distribution were identified between these networks' resting state and task conditions. In addition, as shown in Fig.43(b) and (c), the functional Hub of DMN also demonstrated significant differences in both K-Means parcellation and Aicha atlas. More specifically, in the Aicha atlas, where more granular networks are used, robust differences are observed in the precuneus ($p < 0.0001$, ****) and angular gyrus ($p < 0.0001$, ****). The latter is visible in distributional measures and angle measures. The activation overlaps with the result identified through the Harvard atlas.

It can be observed from the result that a consistent temporal regularity was created in the morning routine (task) conditions compared with resting state in functional hubs and memory hubs of DMN with high significance, as well as functional networks involving sensory, object recognition, and spatial recognition.

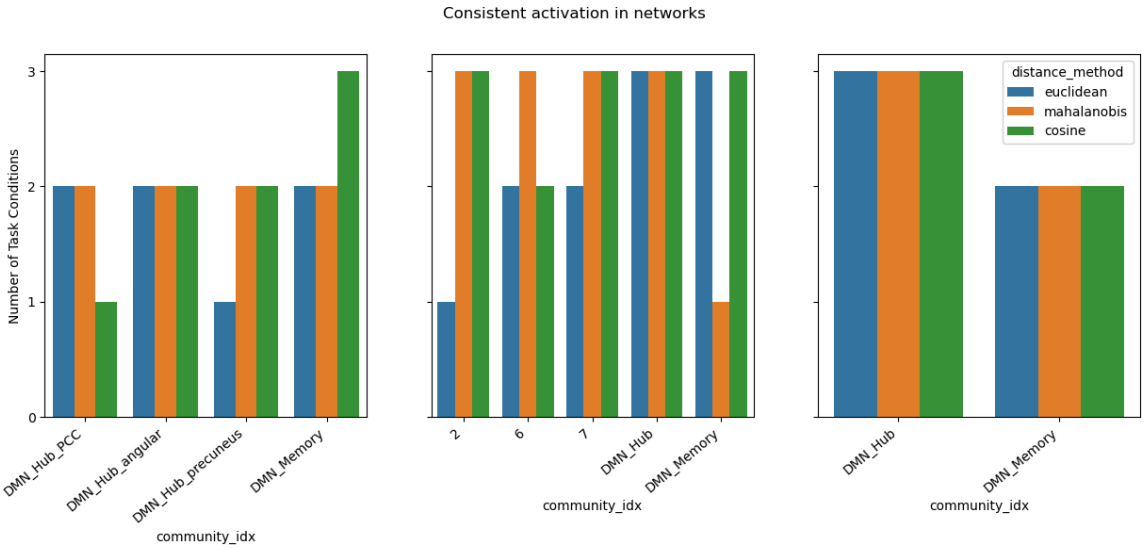

Figure 42: Consistent and significant half-period differences in brain networks by distance type. The Y-axis indicates the number of task conditions' PnP distributions that differ from the resting state. A total of 3 task runs are recorded; a value of 3 means that the PnP distribution is consistently different from the resting state in all three task conditions.

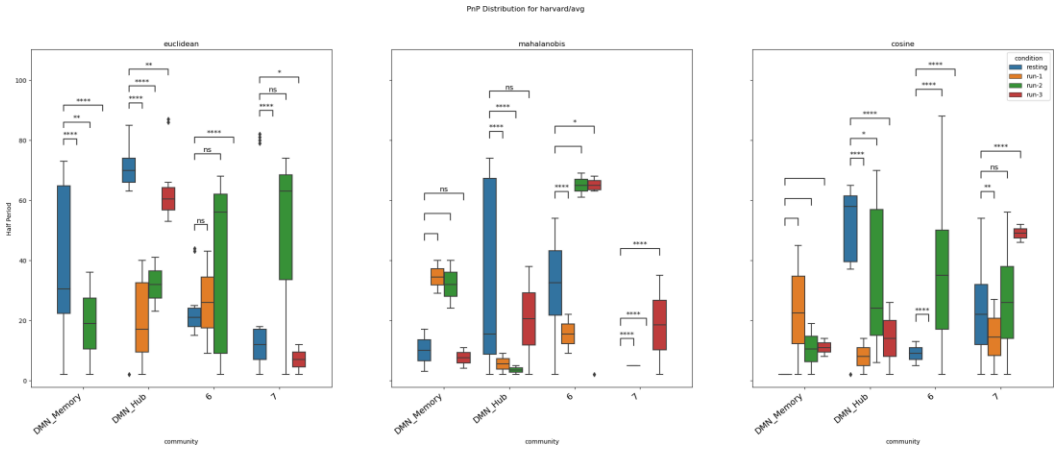

(a) Harvard atlas PnP Result.

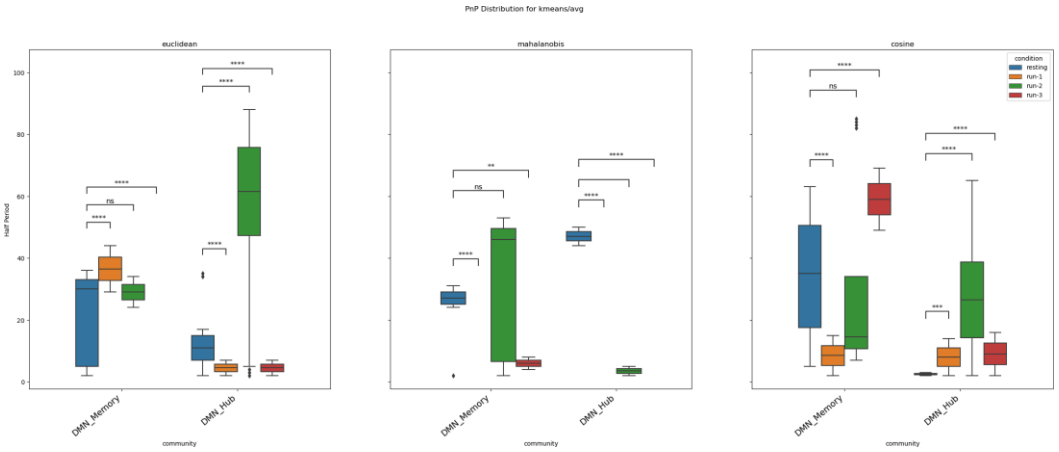

(b) K-Means parcellation PnP Result.

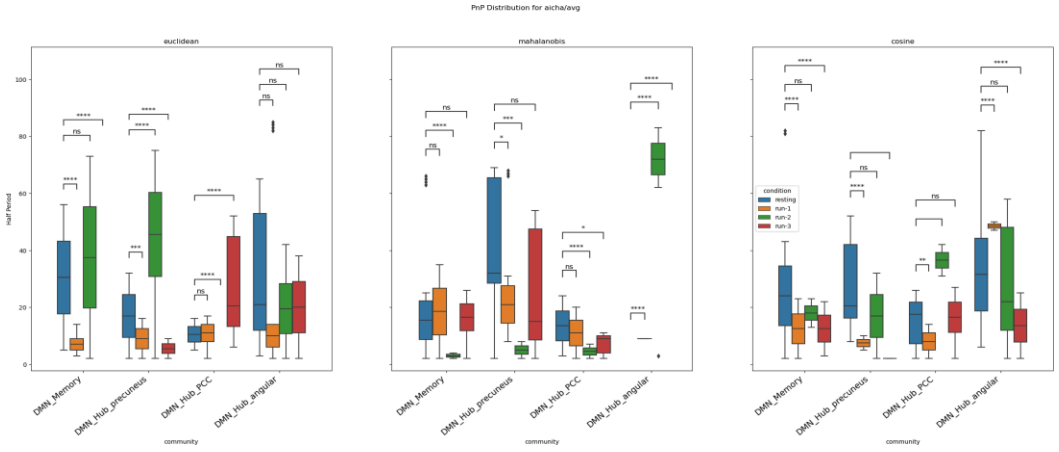

(c) Aicha atlas PnP Result.

Figure 43: Distributions of significant half periods (p<0.001) and differences between distributions of resting and task conditions in different brain parcellation schemes. Y-axis is the value of the identified half period. The X- axis is the condition. Blue: Resting State. Orange: run-1, Green: Run-2, Red: Run-3. For example, the leftmost
blue box in (a) means that in the DMN_Memory network, under resting-state condition, the median significant half-period is around 30, the 25th-percentile is around 25 and the 75th-percentile is almost 70.

8.2.3. Deep Learning Whole-brain Analysis

Deep learning combined with Dynamic Functional Connectivity (DFC) was also applied in the analysis. This analysis focused on the whole-brain state transition changes instead of single regions and networks in an effort to identify whole-brain-scale temporal pattern regularities.

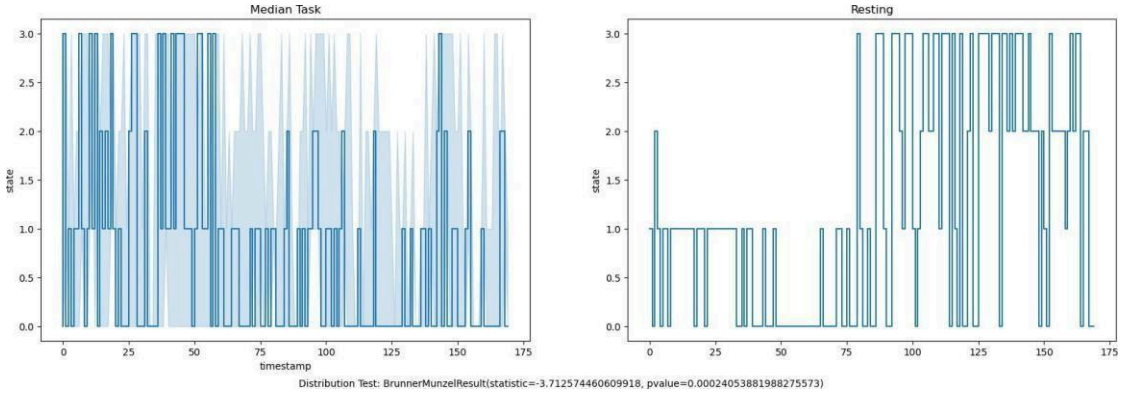

(a) Deep Clustering result for task conditions and resting state in Harvard atlas. Left: Median state distribution overtime for the morning routine/task condition. Right: State over time for resting state.

	MannWhitney	Permutation	Cosine	Euclidean
aicha	0.5395761574732842	0.5225477452254774	0.41875457447962083	16.062378404209
harvard	0.0002977849475190919	0.00019998000199980003	0.651162202462352	22.40535650240808
kmeans	0.04171234504012512	0.038396160383961604	0.449007048897483	20.2484567313166

(b). Distribution Test result for comparing the resting and median morning routine state results.

Fig.44 Deep Clustering analysis results for whole brain patterns.

The deep clustering analysis follows the pipeline introduced in Chapter.7.1.6 where DFC with a sliding window size of 10 frames was calculated for each condition. In this experiment, each session consists of 180 scans, meaning the resulting DFC sequence consists of 170 scans. The result indicated significant differences in whole-brain state distribution between task and resting conditions - the differences are significant enough to be visually detectable, as shown in Fig.44a. It should be noted that the results are both visible in the Harvard atlas and k-means parcellation but not in the Aicha atlas when extracting the median states of task conditions. This could change partially due to the fact that, while the Aicha atlas provides more parcellations to the brain, it covers a smaller percentage of the overall brain compared to the Harvard atlas and K-Means parcellation meaning that some signals in the brain are not accounted for - most importantly the cerebellum. This could indicate that the cerebellum is important in estimating the whole-brain states. It should also be noted that, as expected, the deep-clustering analysis loses some detection sensitivity when applied at a whole-brain scale. However, it is a powerful tool that can be used to explore the temporal transitions of the brain states at a granular scale. This topic is not in focus here but can be explored in future studies.

8.3. Summary

In this single case study, resting state and morning routine sessions were recorded using fMRI for a blind subject. The spatiotemporal regularity of fMRI data was explored using selected methods from the proposed pipeline. The results of analysis revealed that endogenously driven situations in memory recollection might represent a stable neural process resulting in consistent temporal regularities. In other words, during autobiographical memory recollection, humans can clearly recall not only the order of the events but also the durations. The results of the study also showed that we could reliably distinguish different brain states between resting state and morning routines. Analysis of the Default Mode Network (DMN), which is involved in episodic and autobiographical memory, revealed consistent temporal pattern differences between different tasks. Functional analysis revealed networks that are involved in this subject as well. One such network contains angular, supramarginal, and inferior frontal gyrus. These regions are known to be engaged in language processing and spatial recognition. Another network includes the bilateral occipital cortex, posterior cingulate cortex, and precuneus - which are involved in object recognition and episodic memory retrieval. This indicates that the subject used endogenous language cues to support memory retrieval and duration control.

In summary, endogenous stimuli could be effectively utilized as an experimental behavioral paradigm to control behavior when applied to long-duration episodic memory studies. It is also shown that we could identify the brain activity patterns that such a paradigm stimulates. In short, it is feasible to incorporate this endogenous paradigm into more fMRI studies.

9. Group Study: Leadership Experiment

The group study of the leadership experiment involves the endogenous control of emotions and retrieval of autobiographical memory. The subjects were not given particular instructions in the retrieval process other than general emotional guidance. Therefore, the endogenous stimuli (ES) in effect may include multiple channels, including visual, tactile, auditory, et cetera. In this study, I compared the spatial-temporal regularities of predefined and functional brain networks and resulting network differences between the two strong emotional conditions and examined group-level significance. By comparing the conditions, I can answer the question of whether emotional ES can be reliably used as experimental conditions.

9.1. Subject and Experiment

9.1.1. Subjects

The study included ten male subjects in successful leadership roles, marked as subject 2 to subject 11. Three subjects' data were removed from the analysis due to inconsistency and incomplete data collected (subjects 6, 7, 8). One subject was removed due to the incorrect data collected (9). The Ethics Committee of the Medical Faculty of the University of Munich has approved the fMRI experiment protocols.

9.1.2. Experimental Paradigm

During the experiment, subjects were instructed to recall extremely positive and negative experiences for 2 minutes. The experience could be leadership related. The positive experience was recorded first for all subjects except subject 2. The detailed content of the experience was not recorded nor kept due to ethics compliance considerations, and all data are anonymized so that they cannot be traced back to a single individual in the experiment.

Subjects	Condition 1	Condition 2	Duration
Subject 2	negative	positive	120s
Subject 3-11	positive	negative	120s

Table 1: Experimental Conditions

9.1.3. Data Acquisition

The fMRI data were collected using interleave order on a Siemens Skyra with 3 Tesla in the University Hospital of Ludwig Maximilian University in Großhadern (Siemens Healthineers). One session for each emotional state was recorded during the experiment.

The T1-weighted structural image was acquired with magnetization-prepared rapid gradient-echo sequence (MPRAGE) with the following arrangement: repetition time (TR) = 1.9s, echo time (TE) = 2.22 ms, flip angle (FA) = 9°, number of slices = 220, matrix = 256 x 256, slice spacing and slice thickness = 1 mm, in axial orientation. T2*-weighed functional images were acquired after the T1 session with an echo-planar image (EPI) sequence with the following arrangement: repetition time (TR) = 2500 ms, echo time (TE) = 30 ms, flip angle (FA) = 75°, number of slices = 44, matrix = 64*64, slice thickness = 3.5 mm, in-plane resolution = 3 x 3 mm, ascending sequential acquisition in axial orientation. Each condition (extremely positive and negative) consists of a total number of 48 volumes.

9.1.4. Data Reprocessing

The T1 and T2-weighted images collected were converted into Brain Imaging Data Structure (BIDS) format using the dcm2bids python package (https://github.com/UNFmontreal/Dcm2Bids/). The preprocessing of the converted BIDS data was performed using the fMRIPrep package, which is a NiPreps (NeuroImaging PREProcessing toolS) application (www.nipreps.org) for the preprocessing of task-based and resting-state functional MRI (fMRI). The preprocessing steps include motion correction, slice timing correction, realignment, unwrapping, skull stripping, segmentation, spatial normalization to MNI 152 space, and smoothing (https://fmriprep.org/en/stable/workflows.html). All slices are realigned in time to the middle of each TR. Motion-corrected images also have their motion confounds (three rotations, three translations) exported.

9.1.5. Pre-defined Brain Network

In this group study, I want to explore temporal regularities in selected brain regions known to be engaged in episodic memories and emotions. As a result, Default Mode Network (DMN) areas containing functional hubs and memory sub-network were included as predefined brain regions. In Dolcos et al. (2017), it was suggested that emotional episodic memories involve the interaction of the affective systems (such as the amygdala, medial orbitofrontal cortex, and insula) and memory systems (such as the hippocampus and fusiform face area). Therefore, these regions are also selected in the analysis as shown in Fig.45.

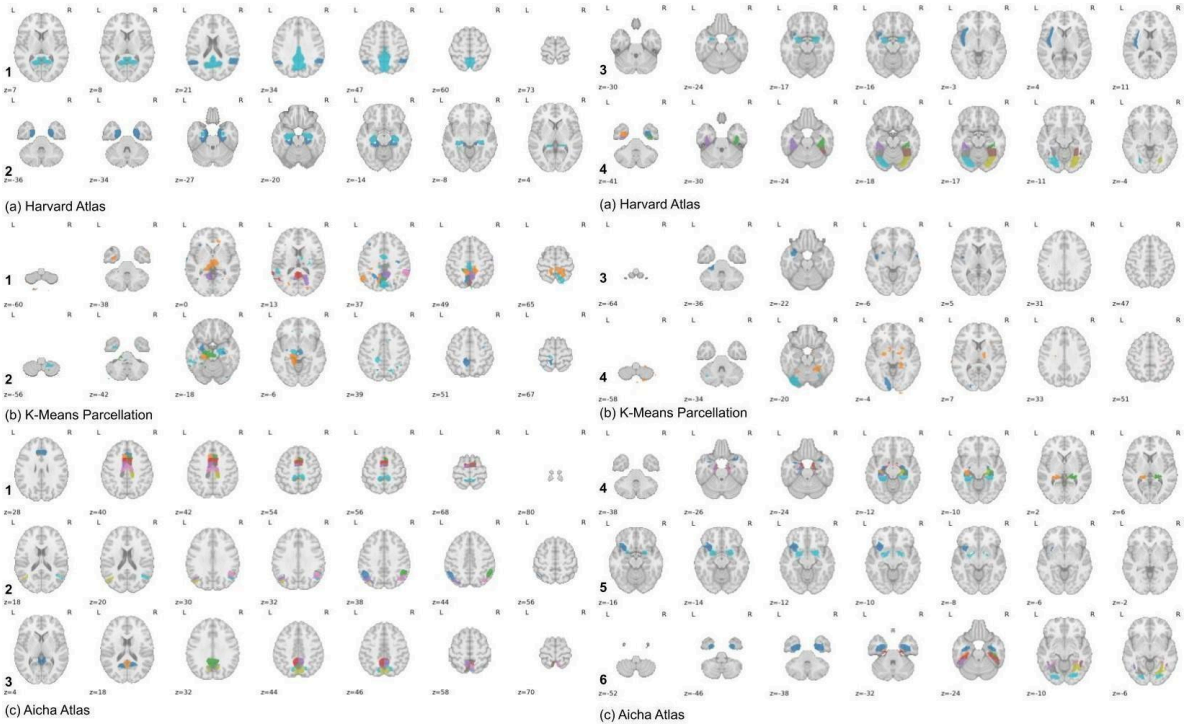

Figure 45: Selection of Predefined networks in this study. (a) DMN Network in Harvard Atlas. a.1 is the functional hub (PCC, angular gyrus, precuneus). a. 2, the memory hub (parahippocampal and hippocampus). a.3 Network for emotion (bilateral amygdala and insular cortex). q.4 Network for fusiform cortex related to face/facial expression recognition. (b) DMN Network in K-Means parcellation. The regions are selected based on overlap with Harvard regions - b.1-4 is based on a.1-4. (c) DMN Networks in Aicha Atlas. c.1 Posterior cingulate cortex (PCC). c.2 precuneus. c.3 angular gyrus. c.4 Memory hub including parahippocampal and hippocampus. c.5 Network for emotion (bilateral amygdala and insular cortex). c.6 Network for fusiform cortex related to face/facial expression recognition.

9.2. Results

The analysis followed the steps outlined in the pipeline, and the results are aggregated at the group level. A virtual subject consisting of the averaged signals of all the subjects after normalizing each subject to the MNI152 template is used to calculate the static Functional Connectivity (sFC) correlation matrix. Modularity-based community detection methods were applied to the resulting sFC correlation matrix, and networks were selected based on overlap with the predefined networks.

Again, the PnP method was applied, and the results were aggregated. Dynamic Functional connectivity (dFC) based deep clustering methods were also applied to the virtual subject for analysis. In addition to the pipeline results, a whole-brain voxel-wise analysis based on the general linear model (GLM) was applied using spm 12. A first-level analysis was done for each subject, and the results were aggregated to create a second-level (group-level) analysis.

9.2.1. Standard SPM Analysis

Fig.46 shows the relative activation detected from the (a) positive vs. negative condition and (b) negative vs. positive condition. The result indicates that brain regions in the negative emotional scenarios are more engaged in the right hemisphere. The lateralization in emotional stimuli processing has been reported (Gainotti, 2019). This includes regions like the right angular gyrus, right lateral occipital cortex, and right parietal operculum cortex. These regions are involved in complex cognitive processes such as object recognition, memory retrieval, and visual-spatial recognition (Măliia et al., 2018; Seghier, 2013).

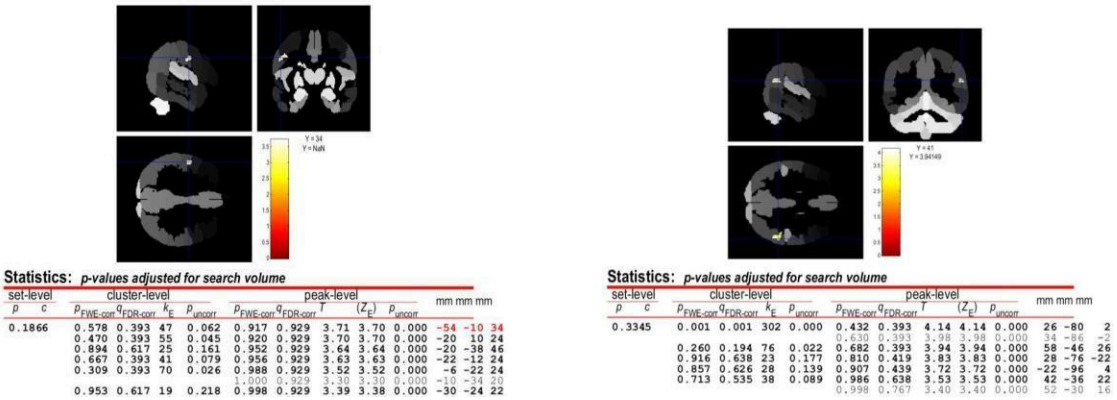

Figure 46: Whole-brain voxel-wise relative activation results using GLM and spm12. This is the stan- dard fMRI analysis pipeline used in over 70% of the studies (Yeung, 2018).

In positive scenarios, the left frontal pole is more engaged, which agrees with the existing findings that the left hemisphere is more involved when processing positive emotional stimuli (Root, Wong, & Kinsbourne, 2006). It should be noted in the study where lateralization in emotional stimuli processing was identified. The meta-study analyzed experiments mostly involving exogenous emotional cues (Cummings et al., 1994). In this experiment, however, the emotional stimuli are purely endogenous. The results indicated that endogenous emotional cues as stimuli could generate robust and consistent differences between positive and negative emotions at the group level. It should be noted that the traditional general linear model-based analysis using SPM does not consider the properties of brain networks and overlooks the temporal patterns at a functional level.

9.2.2. Functional Connectivity and Networks

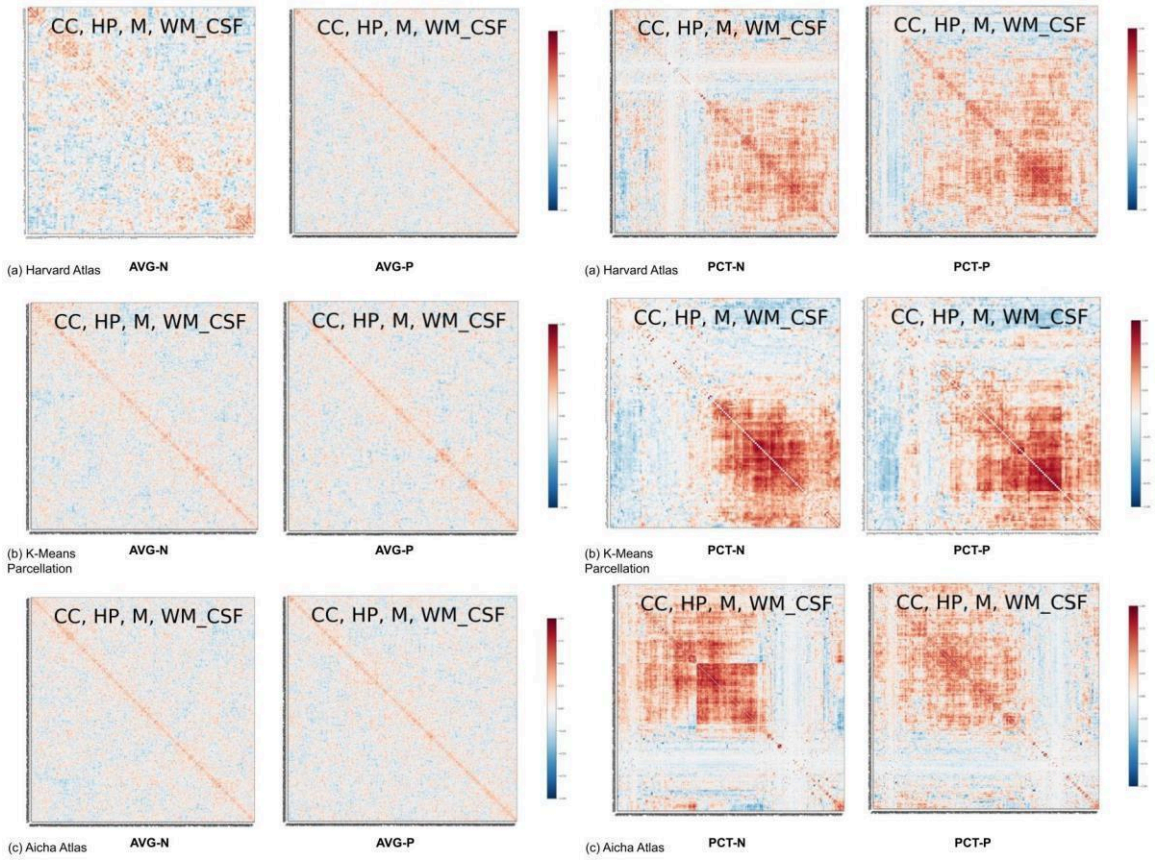

Figure 47: Functional connectivity matrices with confounds removed, including component correction, high-pass filter, motion, white matter, and cerebrospinal fluid. The FC matrix was calculated using the two conditions. *-N indicates the FC is calculated using negative sessions. *-P indicates that FC is calculated using positive sessions.

A virtual subject from averaged, normalized signals is created for the group study analysis pipeline. Similar to a single case pipeline, the signals are extracted from each ROI identified and aggregated. The whole-brain functional connectivity matrices are then calculated for each atlas and all the ROIs. Again, the Pearson correlation was computed between each ROI using averaged signals, the percentage change of averaged signals, and the principal components of each ROI.

Since this study focuses on the endogenously generated stimuli of strong positive and negative emotions, two types of FC matrices were calculated. As shown in Fig.47 (a)(b), correlation matrices for each atlas were calculated for both positive and negative conditions. Aicha atlas consisted of 384 ROIs, Harvard atlas had 132, and K-Means parcellation had 350 ROIs. The resulting FC matrices were then analyzed using community detection methods based on graph theory. Functional networks were extracted from the matrices using modularity-based graph theory methods described in Chapter.7.1.4.

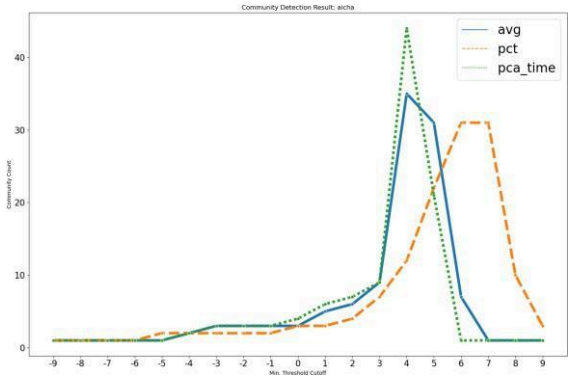

(a) Community count for aicha atlas: Negative

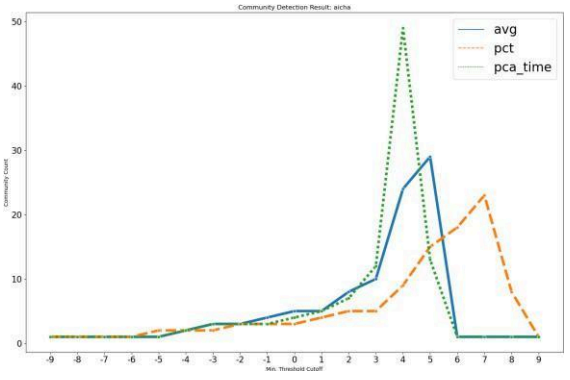

(b) Community count for aicha atlas: Positive

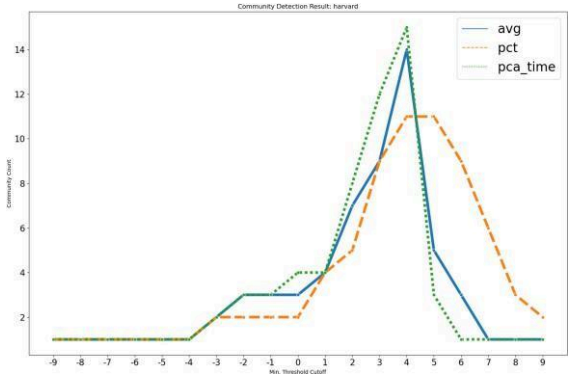

(c) Community count for harvard atlas: Negative

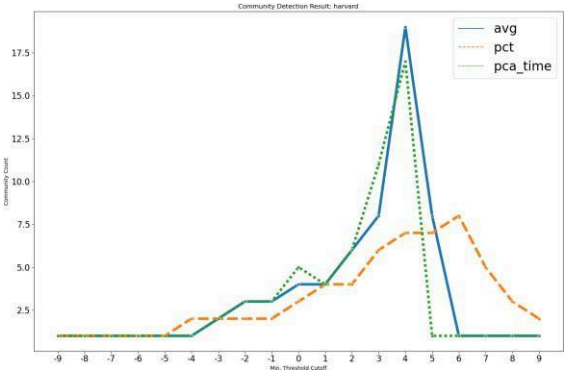

(d) Community count for harvard atlas: Negative

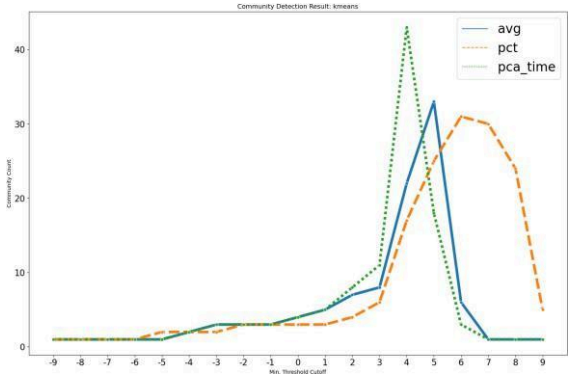

(e) Community count for k-means atlas: Negative

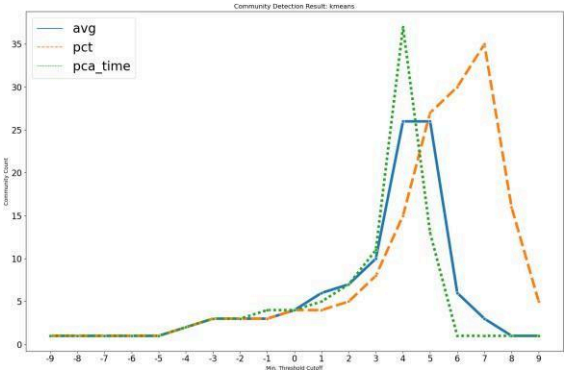

(f) Community count for k-means atlas: Negative

Figure 48: Total number of separated community distribution by threshold. The x-axis is the correlation value threshold used. A value of 5, for example, means that all values below 0.5 in the original FC matrix were removed from the calculation.

Fig.48 shows the Graph Theory-based network separation results. The y-axis indicates the total number of networks identified. This group study's average signal aggregation method had similar community separation performance in the Harvard atlas. However, in Aicha and K-Means atlas, the percentage-based parcellation provided better performance with higher confidence (stronger correlation). As a result, in this study, the average method will be used for the Harvard atlas, while the

percentage-based method will be used for K-Means and Aicha parcellation. Fig.49 shows the distribution of sizes (in the number of brain regions) for the communities that are identified using the different methods (average, percentage, PCA) and in different atlases (Harvard, K- Means, Aicha). The results showed that the percentage-based method provided a similar number of networks in the Aicha atlas and K-Means parcellation, likely due to the similar number of ROIs defined in each parcellation. However, this does not mean the networks identified are similar since the actual regions in each parcellation are different.

(a) Negative condition community size. (b) Positive condition community size.

Figure 49: Distributions of community sizes identified using Graph Theory. The Y-axis is the size of the community. Includes signal aggregation methods average, percentage and PCA.

(a) Negative condition community size. (b) Positive condition community size.

Figure 50: Size distribution of communities selected based on overlap with predefined networks. The Y-axis is the size of the community. Includes signal aggregation methods average, percentage.

Again, based on the analysis pipeline, additional brain networks were selected from the ones identified using FC. Similar to the previous analysis, only overlapping functional networks are selected using the same metric. Fig.50 showed the distribution of the community sizes for the networks that are selected based on their overlap with predefined brain networks. The average aggregation method provided networks of moderate sizes in the Harvard atlas regardless of emotional valence. The percentage method provided rather consistent performance.

9.2.3. Spatiotemporal Regularity

The multi-step temporal analysis demonstrated that consistent spatiotemporal regularities could be identified in different brain regions. As shown in Chapter.7.1.5, the temporal signals extracted from each brain network are further processed to identify dissimilarities between neighboring brain states. Three types of measures were used, including angle-based distances, distributional and non-distributional distances. The resulting temporal sequences are then analyzed using PnP methods introduced in Chapter.4.4 to identify potential temporal patterns.

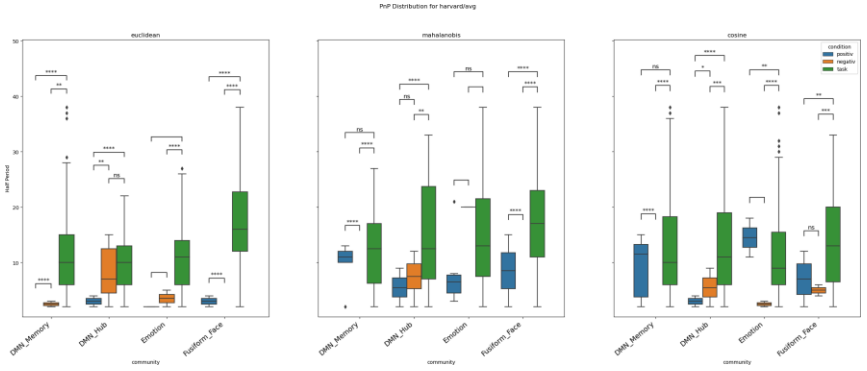

(a) Harvard atlas PnP Result for DMN.

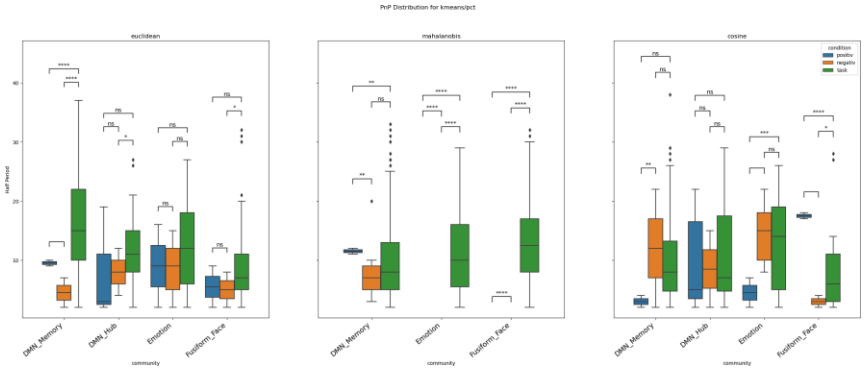

(b) K-Means parcellation PnP Result for DMN.

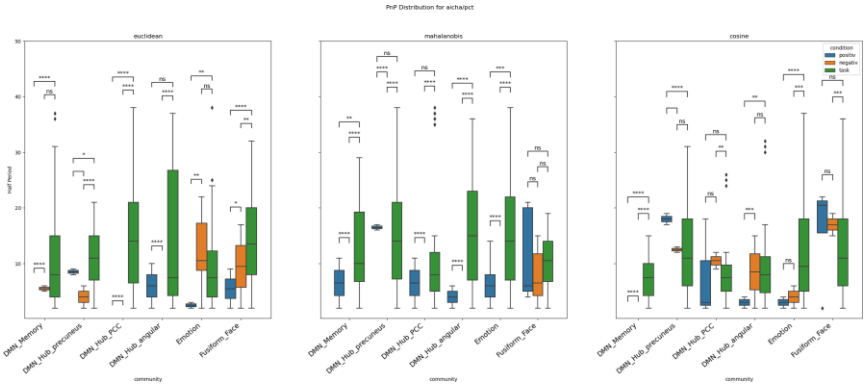

(c) Aicha atlas PnP Result for DMN.

Figure 51: Distributions of significant half periods (p<0.001) and differences between distributions of resting and control conditions in different brain parcellation schemes. Only the predefined networks are shown in this figure. Y- axis is the value of the identified half period. The X-axis are the conditions. Blue: Positive Condition. Orange: Negative Condition, Green: Control Condition. For example, the leftmost blue box in (a) means that in the DMN_Memory network, under positive conditions, no significant half-periods have been identified. The orange box means the half period identified for the positive condition is between 2-4 scans which are 5 to 10 seconds. empty: p=nan, *: p<0.05, **: p<1e-2, ***: p<1e-3, ****: p<1e-4

PnP Regularity Analysis The results of the PnP method, as shown in Fig.51, showed significant differences in temporal pattern distribution between the positive and negative emotional conditions in two-sided test results. There are significant differences between the positive and negative conditions in the memory hub of DMN across all three atlases and through the angle, distributional and non-distributional distances. Given such, I would like to suggest that the memory center (subnetwork) demonstrates robust and consistent differences in the endogenous emotional stimuli conditions employed in this study. In addition, stronger significance between the negative and control conditions is observed compared with that of the positive conditions, indicating a potentially stronger memory engagement in the case of strong negative emotions. This agrees with the previous finding that negative emotions are remembered more accurately in detail than positive experiences (Kensinger, 2009). In the DMN functional hubs, however, the results are less robust. No significant results were found in the K-Means parcellation, and weak significance (*, **) was observed in the Harvard atlas. As for the emotional hubs, however, the results are again significant across the atlases and distance measures. The difference between negative and control conditions is more significant and consistent

than positive conditions in the emotional hub. This could indicate that negative memories command more emotional involvement than positive ones.

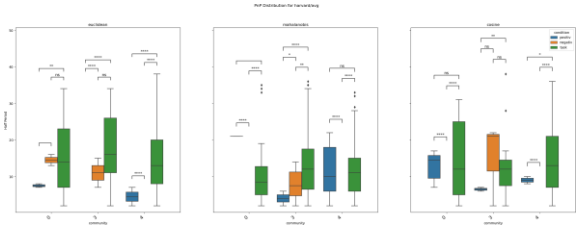

(a) Harvard atlas PnP Results for negative networks

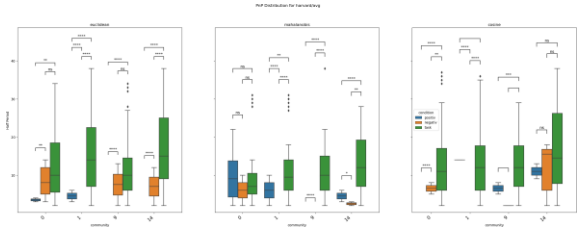

(b) Harvard atlas PnP Results for positive networks.

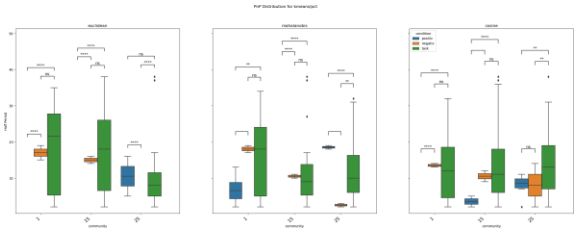

(c) K-Means parcellation PnP Results for negative networks

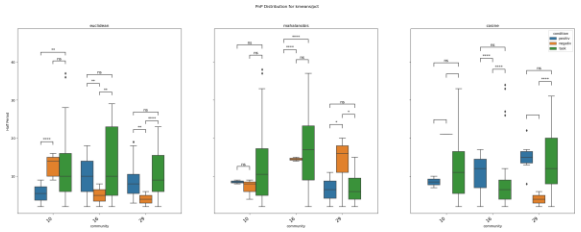

(d) K-Means parcellation PnP Results for positive networks.

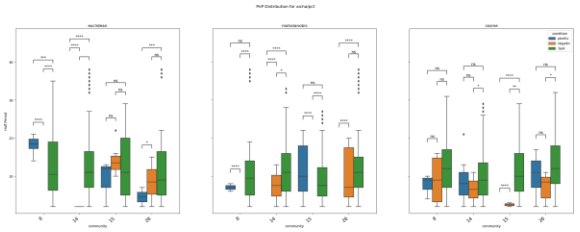

(e) Aicha atlas PnP Results for negative networks.

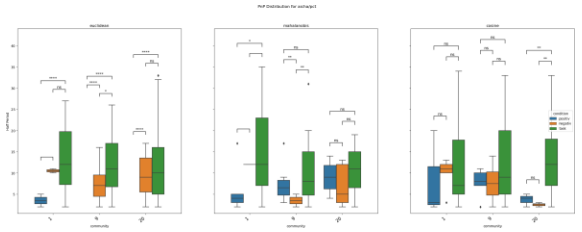

(f) Aicha atlas PnP Results for positive networks.

Figure 52: Distributions of significant half periods ($p<0.001$) for Harvard, K-Means, and Aicha parcellations in networks identified using negative (left) and positive conditions(right).

In addition to the networks selected, consistent temporal pattern regularity differences were also identified in the functional networks. Fig.52 provides detailed half-period distribution and testing results. It should be noted that the functional networks differ in each atlas. The functional network also differs based on the condition it was extracted from.

The results revealed differences across distance metrics in the temporal pole, medial prefrontal cortex (medial PFC), and posterior cingulate gyrus (PCC). These areas are found in various studies to be associated with the social and emotional process and memory retrieval, especially semantic processing (Kensinger, 2009). Further directional tests showed that these regions are more engaged in negative scenarios (Table.3). This indicates that in strong negative episodic memory sessions, subjects have stronger recollection and recall more semantic context than in positive scenarios. The directional results also showed that predefined fusiform networks and functional ones containing the right occipital fusiform cortex are more engaged in negative conditions. This could potentially indicate that for senior leadership, facial expressions of face registers are a large memory footprint in negative experiences.

In addition, the results in Aicha Atlas (Fig.51 (c)) showed that the precuneus subnetwork elicits consistent temporal regularity differences. Results in functional networks (Fig.52 (e)(f)) also showed that networks containing precuneus demonstrated consistent temporal regularity differences. The directional test further showed the precuneus is more engaged in positive conditions (Table.4). In An et al. (2018), precuneus was correlated with subjective happiness. This could indicate that in endogenous situations where strong positive stimuli were generated internally, it would engage similar brain regions and networks compared to exogenous stimuli.

condition	ttest_rel	distance	community
neg_v_pos	0.018807	cosine	4
neg_v_pos	0.020616	euclidean	7
neg_v_pos	0.009381	cosine	7
neg_v_pos	0.011324	euclidean	9
neg_v_pos	0.007500	cosine	9
neg_v_pos	0.046264	euclidean	Fusiform_Face
neg_v_pos	0.018024	cosine	Fusiform_Face

Table 2: Directional Test Results for functional networks identified based on negative condition.

condition	ttest_rel	distance	community
pos_v_neg	0.011250	euclidean	12
pos_v_neg	0.002965	cosine	12
pos_v_neg	0.005654	cosine	14

Table 3: Directional Test Results for functional networks identified based on positive condition.

condition	ttest_rel	distance	community
pos_v_neg	0.008846	euclidean	DMN_Hub_precuneus
pos_v_neg	0.021508	cosine	DMN_Hub_precuneus

Table 4: Directional Test Results for brain networks in positive > negative condition.

It can be observed from the result that a consistent temporal regularity was created in the emotional conditions compared with the control state in memory hubs of DMN and emotional hubs with high significance, as well as functional networks involving social-emotional processes and face/facial expression recognition. Lateralization of the emotional conditions was also observed. In addition, consistent spatial-temporal pattern differences were identified between positive and negative conditions. This suggests that different brain networks can be engaged in strong endogenous emotional stimuli sessions similar to those activated with exogenous stimuli. Further, consistent temporal regularity can be identified through the PnP method. In short, this indicates that endogenous modulation via emotions in short task sessions is a robust paradigm that can be used in addition to the traditional exogenous emotional inventory.

9.2.4. Deep Learning Whole-brain Analysis

Deep learning combined with Dynamic Functional Connectivity (DFC) was also applied in the analysis. This analysis focused on the whole-brain state transition change changes instead of single regions and networks to identify whole-brain-scale temporal pattern regularities.

The deep clustering analysis follows the pipeline introduced in Chapter.7.1.6 where DFC with a sliding window size of 10 frames was calculated for each condition. In this experiment, each session consists of 48 scans, meaning the resulting DFC sequence consists of 38 scans. The whole-brain deep- clustering did not identify any significant results comparing the positive and negative conditions. The results indicate that short-duration endogenous stimuli sessions cannot elicit consistent patterns at a whole-brain scale. In these scenarios, deep clustering for sub-networks should not be preferred to explore how the brain state changes over time.

atlas	Mann-Whitney	paired t-test	Euclidean Distance
Harvard	0.922510	0.928998	11.000000
Aicha	0.835564	0.565381	8.544004
K-Means	0.417608	0.416567	9.695360

Table 5: Test Results for deep clustering states.

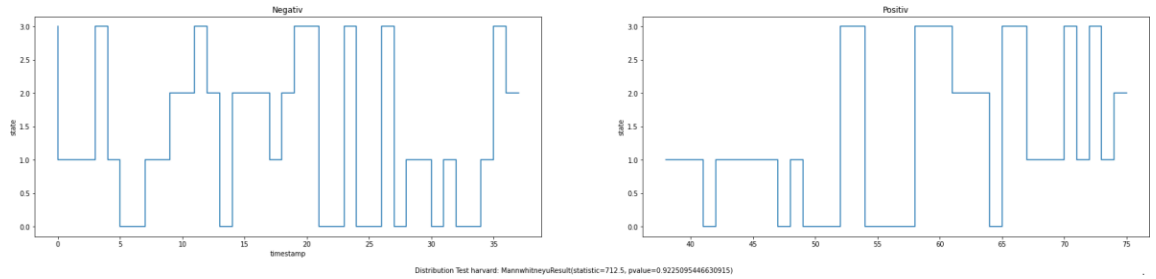

(a) Deep clustering results for positive and negative conditions in Harvard atlas.

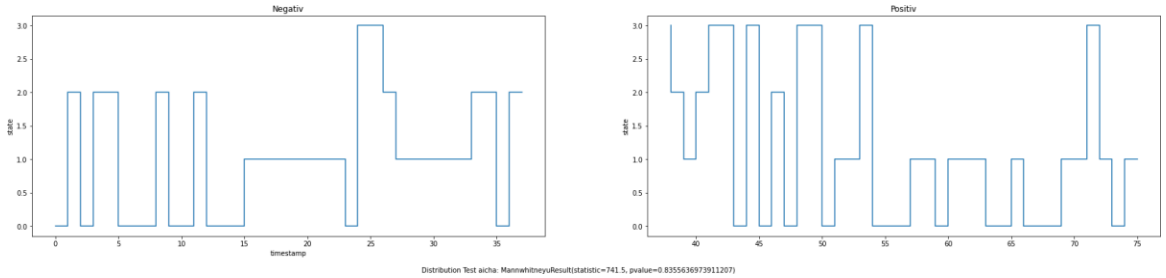

(b) Deep clustering results for positive and negative conditions in Aicha atlas.

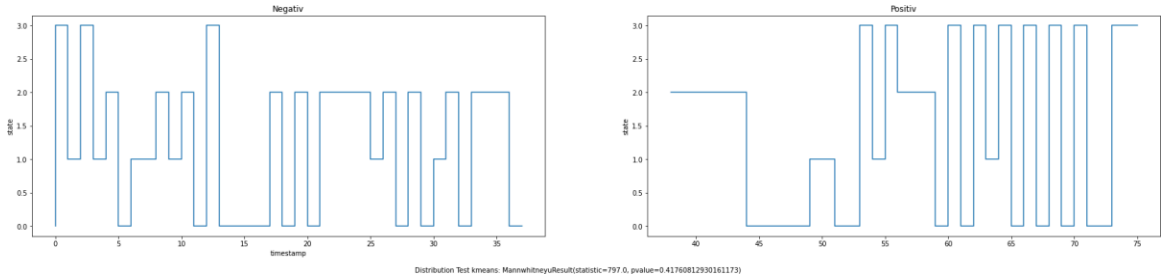

(c) Deep clustering results for positive and negative conditions in K-Means atlas.

Figure 53: Deep clustering states for positive and negative conditions.

9.3. Summary

In this group study, subjects in senior leadership positions were asked to recall extremely positive and negative experiences without informing experimenters of the content. The fMRI data were analyzed using both traditional SPM-based pipelines and analytical methods from the proposed pipeline. Both analyses indicated that the right hemisphere was more engaged during negative scenarios which aligns with observations from exogenous stimuli (Gainotti, 2019). Pipeline-based analysis using the PnP method revealed significant differences in temporal pattern distribution between positive and negative emotional conditions. For negative scenarios, the results identified strong activation in specific brain regions related to memory retrieval (autobiographical memory), semantic processing, inhibitory control (mPFC) etc. This indicates that negative emotions command stronger social-emotional responses and memory recollection. This also implies that senior leaderships focused more on context during negative experiences. Additionally, results showed that for senior leadership, facial expressions register a large memory footprint in negative experiences. For positive scenarios, results found regions like the left frontal pole and precuneus are more engaged. These regions are involved in positive emotional stimuli processing and subjective happiness (Toichi, 2015). It was also found that for senior leaderships, regions related to visual and sensory processing are more engaged in positive scenarios indicating they focused more on details and subjective feelings during positive experiences.

In summary, this experiment used purely endogenous emotional stimuli without explicit knowledge of the content. The analysis pipeline demonstrated that consistent temporal regularity differences could be identified between the scenarios in the memory center (subnetwork) and other functional networks. The results indicate that purely endogenous stimuli can elicit similar brain activation patterns as that of exogenous stimuli at the group level in short-duration episodic memory sessions. This means that paradigms using purely endogenous emotional stimuli can be reliably analyzed and extended to fMRI experiments. The results also showed that specific neural machinery can be extracted from the purely endogenous recollections without explicit knowledge of the content. It should be noted that deep-clustering techniques did not reveal meaningful results, likely due to the short duration of scenarios.

10. Single Case Study: Music Experiment

The single case study with the subject PS involves temporal perception, control, and auditory details recollections. This process requires imagination and manifestation of endogenous stimuli such as temporal and auditory channels. The reconstruction of auditory scenarios may pose a challenge for regular participants, but the subject is an experienced music conductor and can imagine music and tempo vividly and coherently. In this study, I want to examine the spatial-temporal regularities between different ES conditions (slow, normal, and fast tempo) to identify any consistent temporal dynamics of the underlying neural machinery.

10.1. Subject and Experiment

10.1.1. Subject

The subject PS is a male conductor with no known neural impairments at the time of the experiment. The subject can recollect vividly music pieces with a mostly accurate duration. PS can imagine hearing music fluently but has stated that imagining hearing music with a specific tempo is not a simple task. To quote from the talk with PS: ”When you conduct or perform, you will never jump from one point to another. When you are imagining hearing music, you will not be so sure, the music may be not so stable, and you may easily jump.” Despite the difficulty, musicians are trained to keep a steady tempo to perform. The Ethics Committee of the Medical Faculty of the University of Munich has approved the behavioral and fMRI experiment protocols.

10.1.2. Experimental Paradigm

The experiment was split into two parts. PS was instructed to imagine the situation where he sat in a cafe and listened to the selected music piece. As shown below, 5 music pieces were chosen for the study, with different optimal tempos.

Music Piece	Tact	Optimal Tempo	Slow Tempo	Fast Tempo
Beethoven, 7. Sinfonie, 2. Satz	27-34	74 bpm	60-66 bpm	110 bpm
Haydn Sinfonie Nr. 87 A-Dur 1. Satz	1-12	155 bpm	126 bpm	200 bpm
Stangel Lilith Concerto, 3. Satz	1-6	132 bpm	112 bpm	160 bpm
Beethoven Violin Concerto 1. Satz	1-9	100 bpm	80 bpm	120 bpm
Haydn Sinfonie Nr. 94, 3. Satz	1-19	58 bpm	42 bpm	80 bpm

Table 6: PS Music

PS was initially instructed to imagine a musical piece (Beethoven, 7. Sinfonie, 2. Satz) at different tempos. After the initial session, fMRI data were recorded over another session. PS was asked to imagine hearing five music pieces as shown in Table.6. The optimal, fast, and slow tempos were presented in random order. For each tempo, a short session was performed and recorded. Beats were shown to PS before each scenario. After the music session, an 8-minute resting state session was recorded.

10.1.3. Data Acquisition

The fMRI data were collected using ascending order on a 3T MRI Phillips scanner in the University Hospital of LMU, Munich. During the experiment, one session of 15 trials for music pieces and one trial of resting state was recorded. The last run was the resting state, in which PS was instructed not to focus on any topics. During the music runs, PS was instructed to recollect the details of the selected musical piece at a given tempo. The Beats/Tempo was presented to the participant via an App on an iPhone before each scenario. The selection of tempo for each music piece was randomized.

The T1-weighted structural image was acquired with magnetization-prepared rapid gradient-echo sequence (MPRAGE) with the following arrangement: repetition time (TR) = 8.2 ms, echo time (TE) = 3.76 ms, flip angle (FA) = 8°, number of slices = 220, matrix = 256 x 256, slice spacing and slice thickness = 1 mm, in axial orientation. T2*-weighed functional images were acquired after the T1 session with an echo-planar image (EPI) sequence with the following arrangement: repetition time (TR) = 2500 ms, echo time (TE) = 30 ms, flip angle (FA) = 90°, number of slices = 48, matrix = 144 x 144, slice spacing and slice thickness = 3 mm, ascending sequential acquisition in axial orientation. The resting-state condition contains a total of 180 volumes, while the volumes for each music condition vary based on duration.

10.1.4. Data Reprocessing

The T1 and T2-weighted images collected were converted into Brain Imaging Data Structure (BIDS) format using the dcm2bids python package (https://github.com/UNFmontreal/Dcm2Bids/). The preprocessing of the converted BIDS data was performed using the fMRIPrep package, which is a NiPreps (NeuroImaging PREProcessing toolS) application (www.nipreps.org) for the preprocessing of task-based and resting-state functional MRI (fMRI). The preprocessing steps include motion correction, slice timing correction, realignment, unwrapping, skull stripping, segmentation, spatial normalization to MNI 152 space, and smoothing (https://fmriprep.org/en/stable/workflows.html). All slices are realigned in time to the middle of each TR. Motion-corrected images also have their motion confounds (three rotations, three translations) exported.

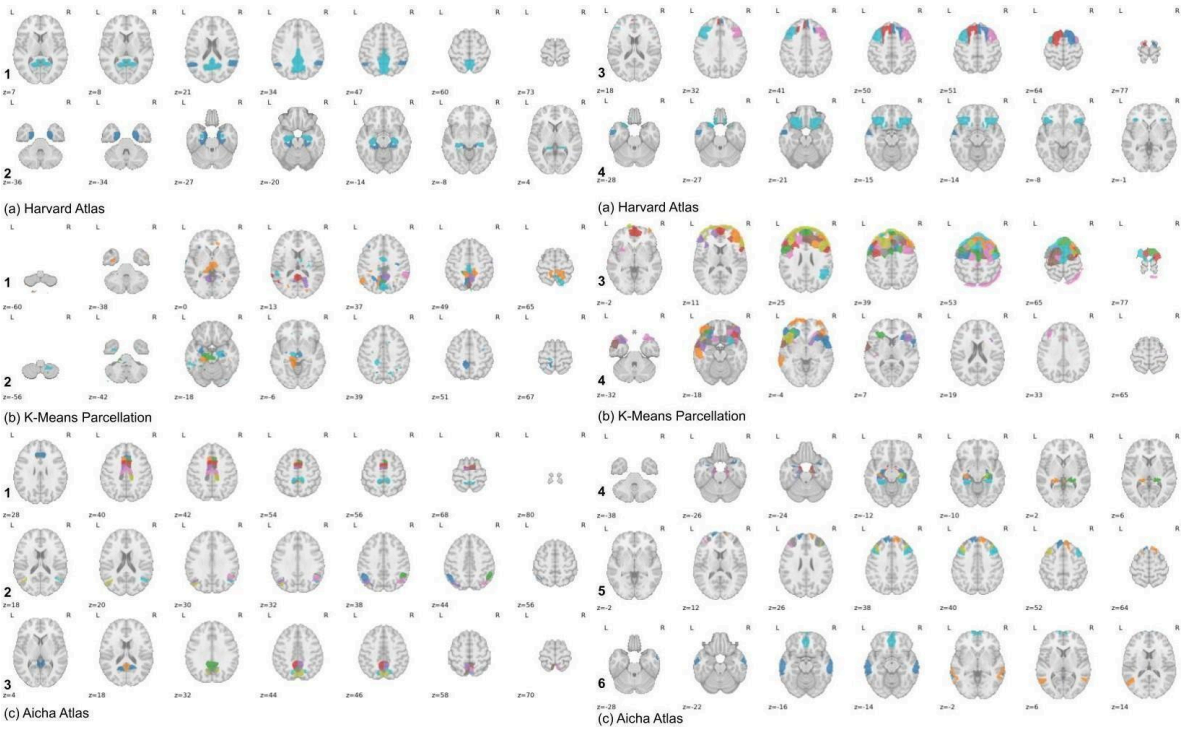

Figure 54: Selection of Pre-defined networks in this study. (a) DMN Network in Harvard Atlas. a.1 is the functional hub (PCC, angular gyrus, precuneus). a.2 the memory hub (parahippocampal and hippocampus). a.3 Network for episodic music memory (middle and superior frontal gyrus, precuneus). q.4 Network for semantic music memory (orbitofrontal cortex, middle temporal gyrus). (b) DMN Network in K-Means parcellation. The regions are selected based on overlap with Harvard regions - b.1-4 is based on a.1-4. (c) DMN Networks in Aicha Atlas. c.1 Posterior cingulate cortex (PCC). c.2 precuneus. c.3 angular gyrus. c.4 Memory hub including parahippocampal and hippocampus. c.5 Network for episodic music memory. c.6 Network for semantic music memory.

10.1.5. Pre-defined Brain Network

In this study, I want to explore temporal regularities in selected brain regions that are known to be engaged in episodic memories and musical experiences. Default Mode Network (DMN) areas containing functional hubs and memory sub-network were included as pre-defined brain regions. It was suggested that music episodic memories involve areas such as the middle and superior frontal gyrus region (with a left-sided preponderance), precuneus, while semantic music memories involve the medial and orbitofrontal cortex, the left angular gyrus, and the middle temporal cortex (Jäncke, 2008). Therefore, these regions are also selected in the analysis as shown in Fig.54.

10.2. Results

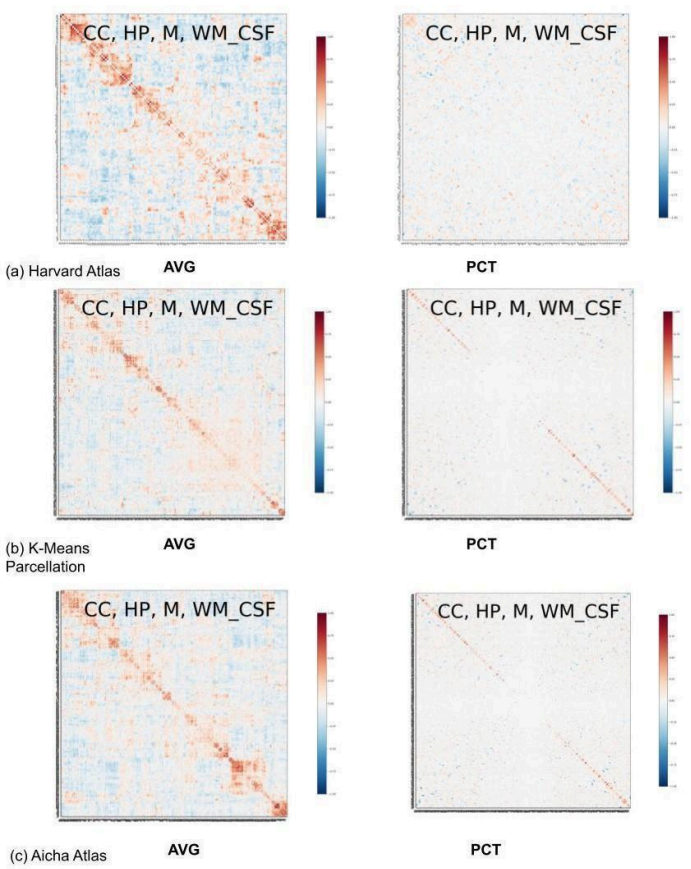

(a) Functional connectivity matrices.

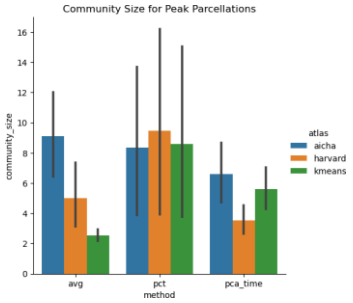

(b) Community size distribution for identified networks.

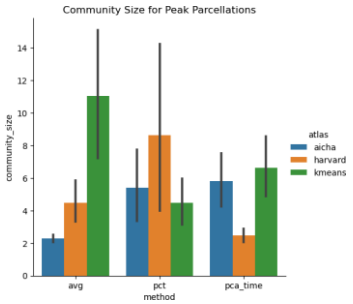

(c) Community size distribution for selected networks

Figure 55: a. Functional connectivity matrices with confounds removed, including component correction, high-pass filter, motion, white matter, and cerebrospinal fluid. a.(a) FC matrices for Harvard atlas averaged signals and percentage signals. a.(b) FC matrices for K-Means atlas averaged signals and percentage signals. a.c(c) FC matrices for Aicha atlas averaged signals and percentage signals. b.c. Community size distribution for brain networks. Counted in the number of regions included in each network.

The analysis followed the steps outlined in the pipeline, and the results are aggregated. The static functional connectivity-based network extraction results are combined with the pre-defined brain networks to identify regions that should be focused on in the analysis. Following the reduction of brain networks, the differences between the task conditions and resting state were compared from different perspectives. The PnP method was used to extract temporal regularities and identify discrepancies. The network-based PnP method was used to compare the spatial-temporal regulations in individual sub-networks. Further, The temporal similarities of different networks were compared through the dynamic time-warping method. Finally, I compared the whole-brain state transitions between different conditions combining deep learning and dynamic functional connectivity analysis.

10.2.1. Functional Connectivity and Networks

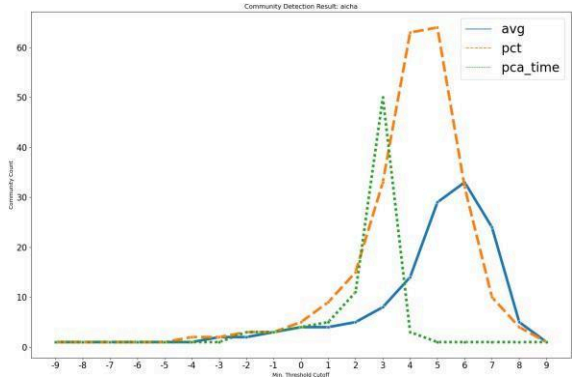

(a) Community count for aicha atlas

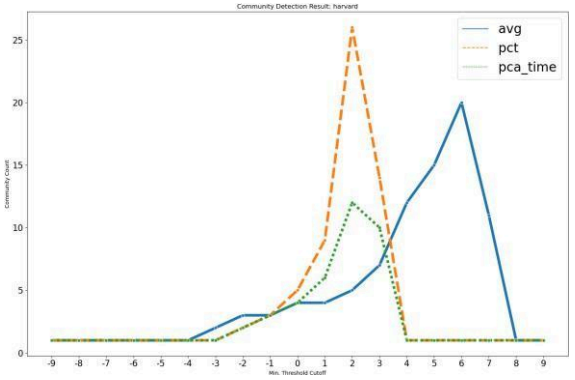

(b) Community count for harvard atlas

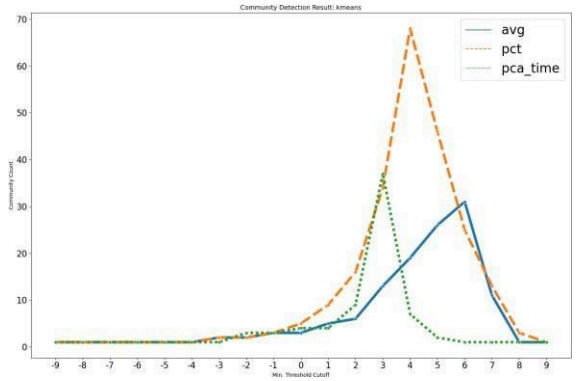

(a) Community count for k-means atlas

Figure 56: Total number of separated community distribution by threshold. The x-axis is the correlation value threshold used. A value of 5, for example, means that all values below 0.5 in the original FC matrix were removed from the calculation.

Based on the analysis pipeline for single case studies, the signals were extracted from each ROI defined in the atlases, and whole-brian functional connectivity matrices were calculated. Pearson correlation was used to define the correlation between each ROI identified from the atlases. For each atlas, the signals were extracted from each ROI using three different methods: average signals of each ROI, percentage change of averaged signal for each ROI, and principal components extracted from each ROI's raw signal using the principal component analysis (PCA) method (Fig.55a). The networks were extracted using resting state data due to the short-duration nature of the endogenous tempo modification sessions.

Fig.55b shows the distribution of sizes (in the number of brain regions) for the communities that are identified using the different methods (average, percentage, PCA) and in different atlases (Harvard, K- Means, Aicha). The results showed that the percentage-based method provided a similar number of networks in the Aicha atlas and K-Means parcellation, similar to that of previous studies.

Based on the analysis pipeline, additional brain networks were selected from the ones identified using FC. Similar to the previous analysis, only overlapping functional networks are selected using the same metric. Fig.55c showed the distribution of the community sizes for the selected networks based on their overlap with predefined brain networks. The Average aggregation method provided networks of moderate sizes in the Harvard atlas. The percentage method provided rather consistent performance in different conditions and atlases.

The functional network identification performance is shown in Fig.56. The result indicates that the average signal aggregation method tends to have better community separation performance when the threshold is higher, meaning the correlations are stronger. This means that the communities identified in the average method (and percentage) are more strongly correlated than those identified by PCA and percentage-based methods. Given these observations, the method that yields most networks at high correlation levels should be selected in each study. In the case of the Music experiment, average- based aggregation will be used.

10.2.2. Spatiotemporal Regularity

The multi-step temporal analysis results demonstrated that consistent spatiotemporal regularities could be identified in different brain regions. As shown in Chapter.7.1.5, the temporal signals extracted from each brain network are further processed to identify dissimilarities between neighboring brain states. Three types of measures were used in this thesis, including angle-based distances and non- distributional distances. Due to the short duration (small sample) of the music sessions, distributional distance like Mahalanobis distances cannot be calculated in some cases and is therefore excluded from the analysis in this experiment. The resulting temporal sequences are then analyzed using PnP methods introduced in Chapter.4.4 to identify potential temporal patterns. In addition, for the music experiment, the temporal sequences have internal similarities based on design (different tempos). Therefore, the dynamic time-warping (DTW) method was also applied to explore potential differences.

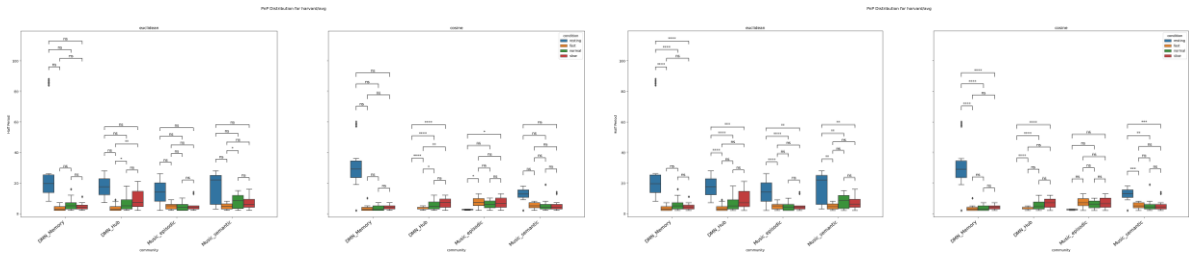

(a) Harvard atlas PnP results for DMN networks (less)

(b) Harvard atlas PnP results for DMN networks (more).

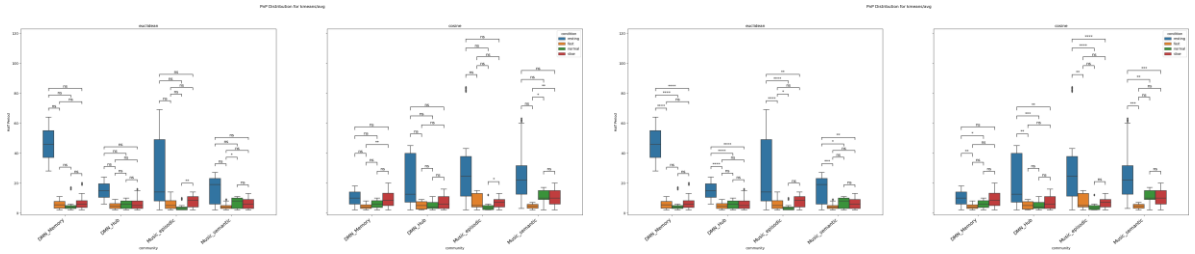

(c) KMeans parcellation PnP results for DMN networks (less).

(d) KMeans parcellation PnP results for DMN networks (more).

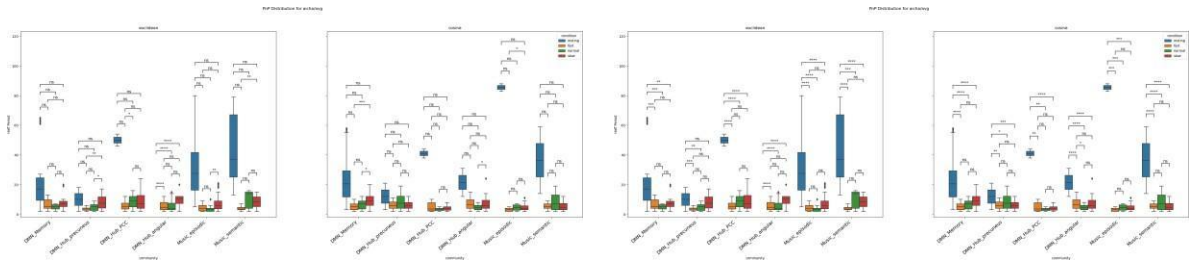

(e) Aicha atlas PnP results for DMN networks (less).

(f) Aicha atlas PnP results for DMN networks (more).

Figure 57: Distributions of significant half periods ($p<0.001$) for Harvard, K-Means, and Aicha parcellations in predefined networks with directional tests applied. (left: less, right: greater).

PnP Regularity Analysis The results of the PnP method in predefined networks, as shown in Fig.57, revealed significant differences in temporal pattern distribution between the music conditions and resting conditions in all atlases. When comparing the different music conditions, significant results were identified mostly in Default Mode Network (DMN) functional hubs. Fig.57a showed that the fast condition engaged less DMN functional hub than normal and slow conditions in both angle and non-distributional measures. In the Aicha atlas, results were further identified in sub-functional hubs involving precuneus (Fig.57e). Given such, I would like to suggest that the functional hubs are engaged more in normal and slow conditions, which could indicate slower scenarios requiring more internal modulation. In addition, in both Aicha and KMeans parcellations, significant results were found in the episodic music network (Fig.57e, Fig.57c). More specifically, the network has more engagement in slower conditions (slow -> normal, normal -> fast, slow -> fast), indicating that the slower the music or endogenously controlled tempo, the stronger the activation of the episodic memory retrieval process. The result could indicate that consistent temporal differences exist in functional hubs and music-related episodic memory networks and can be elicited by endogenously controlled tempo.

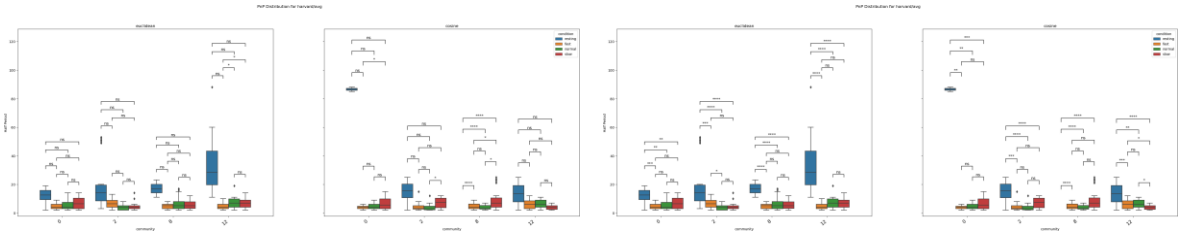

(a) Harvard atlas PnP results for functional networks (less).

(b) Harvard atlas PnP results for functional networks (more).

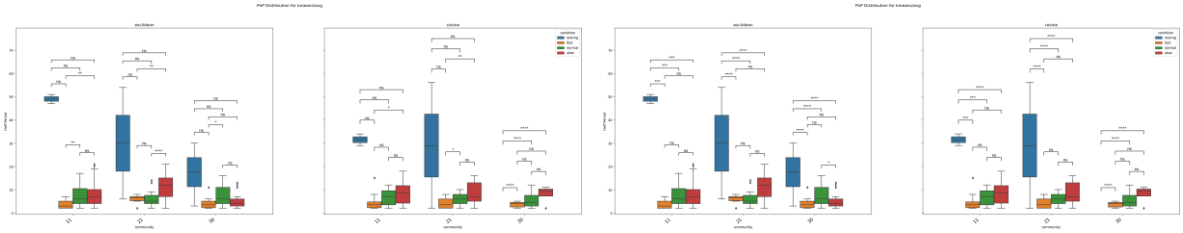

(c) KMeans parcellation PnP results for functional network (less).

(d) KMeans parcellation PnP results for functional network (more).

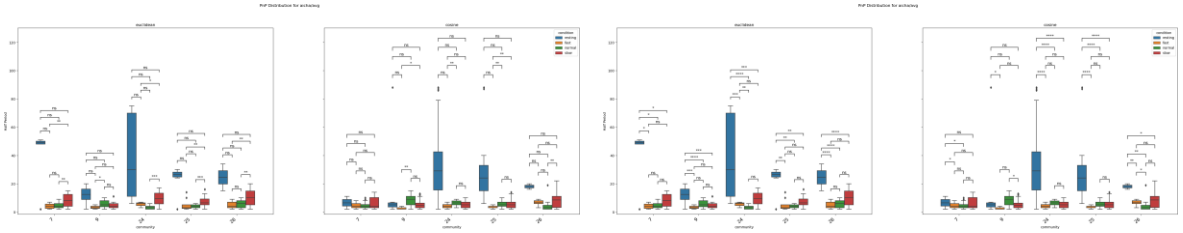

(e) Aicha atlas PnP results for functional networks (less).

(f) Aicha atlas PnP results for functional networks (more).

Figure 58: Distributions of significant half periods ($p<0.001$) for Harvard, K-Means, and Aicha parcellations in functional networks with directional tests applied. (left: less, right: greater).

In addition to the networks selected, consistent temporal pattern regularity differences were also identified in the functional networks. Fig.58 shows the distribution of half-periods identified from the PnP method and the corresponding one-sided test results[12]. The test results show that most regions are indifferent to the music conditions, with the exception of the posterior cingulate gyrus (PCC) and precuneus. Results in Fig.58f further supported this observation in that different sub-regions in the precuneus (community 25, 26) were found to demonstrate consistent temporal pattern differences in different tempos. More specifically, the precuneus engaged more in slower conditions than faster conditions during the musical retrieval (replay) process. It was suggested the precuneus is engaged more in episodic memory retrieval, mental image processing, and imaging future events (Tanaka & Kirino, 2016). I want to suggest that imagining the upcoming events and matching the correct tempo takes greater effort in the endogenously modulated tempo, resulting in precuneus engaging more in slower conditions. The results further indicate that consistent temporal pattern regularities and differences can be identified and observed in selected brain regions in endogenous scenarios.

Dynamic Time Warping Dynamic time warping (DTW) is a method to explore the similarities between temporal sequences. The distance calculated from DTW does not follow triangular inequality (Ruiz, Nolla, & Segovia, 1985) and is best used as a comparison statistic instead of a metric. This experiment calculates the DTW distance between the fast, normal, and slow conditions in pairs, using each condition as a reference. Its distance with the other two conditions was calculated. The metric provides an overall comparison of the conditions. A significant positive shift of DTW distance distribution has been identified in all atlases when using the fast as reference condition. As shown in Fig.59, the DTW distance distribution between slow and fast conditions shows a highly significant ($p<0.0001$) positive shift compared with the DTW distance distribution between normal and fast conditions. The positive shift means that the temporal dissimilarity between slow and fast conditions is stochastically greater

[12] A detailed community-to-brain area mapping can be found in the appendix.

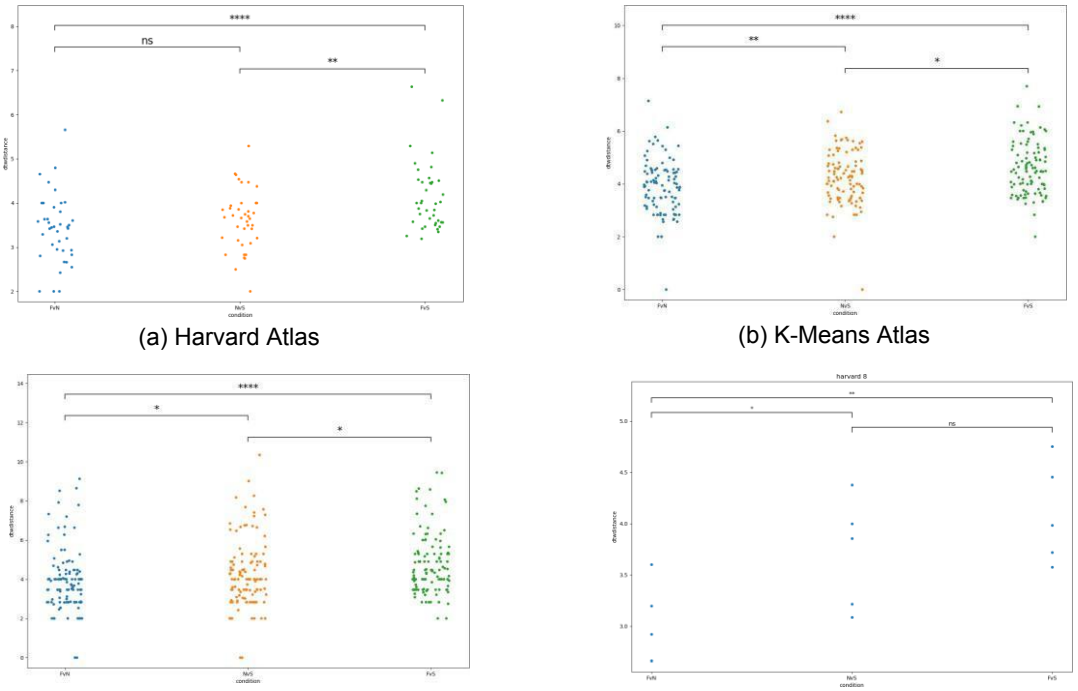

(a) Harvard Atlas

(b) K-Means Atlas

(c) Aicha Atlas

(d) Community 8 of Harvard Atlas

Figure 59: Distributions of dynamic time warping distances between fast, normal, and slow conditions for (a)Harvard, (b)K-Means, and (c)Aicha parcellations in all functional networks with one-sided Mann- Whiteney U test applied. (d) Result of a single community in Harvard atlas. (*: p< 0.05, **: p< 0.01, ***: p < 0.001, ****: p<0.0001)

atlas	community	hypothesis	significance
Harvard	8 (MTG r, SMG r, AG r, LOC r)	NvF < SvF	**
Aicha	21 (mOFC r)	NvF < SvF	*
hline Aicha	26 (Precuneus right)	NvF < SvF	*
K-Means	15 (precuneus right)	NvF < SvF	**

Table 7: Community with significant results by atlas using fast as reference

than that of normal and fast conditions. This could indicate that when slowing down the music internally, the endogenous process is more engaged the slower the tempo becomes. In other words, there are stronger consistent temporal regularity differences between the fast and slow conditions than the fast and normal conditions. No other highly significant results were found between the areas at a whole network level (p<0.001).

In addition to the overall analysis, sub-network level analysis was also performed, and specific regions were identified as shown in Table.7. Lateralization can be observed as most areas with significant differences are in the right hemisphere. For example, the regions showing differences include the right precuneus, right MTG, and right angular gyrus. The results agree with the tempo study using exogenous stimuli (Liu et al., 2018). Additional areas also surfaced in the case of the endogenous tempo scenario, like the medial orbitofrontal gyrus, which regulates sensitivity to outcome value or, in other words, compares desired output with actual output (Gourley et al., 2016). The DTW results indicate a consistent temporal regularity can be identified between tempo conditions, and an endogenous process with memory retrieval and modification process can be reliably utilized.

10.2.3. Deep Learning Whole-brain Analysis

Deep learning combined with Dynamic Functional Connectivity (DFC) was also applied to explore whole-brain state transition change changes instead of single regions and networks to identify whole-brain-scale temporal pattern regularities. Fig.60 shows the comparison of the median states for different tempo conditions. Same as the previous analysis, a sliding window size of 10 frames were used. The results showed no consistent results across the different conditions in all atlases. This agrees with the results in the previous group study. Again, deep clustering for sub-networks should not be preferred in these scenarios to explore how the brain state changes over time.

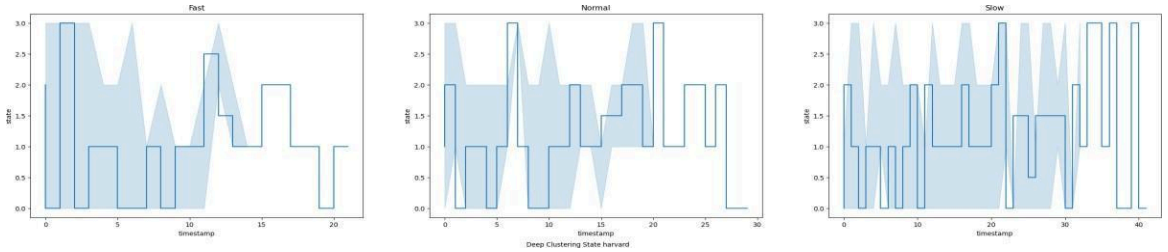

(a) Deep clustering results for fast, normal and slow conditions in Harvard atlas

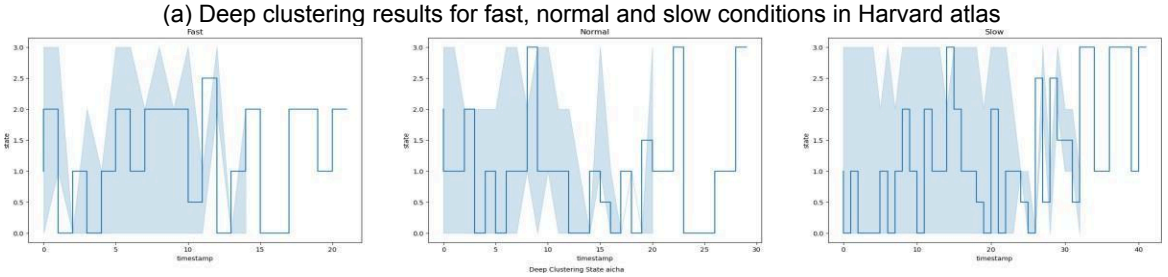

(b) Deep clustering results for fast, normal and slow conditions in Aicha atlas.

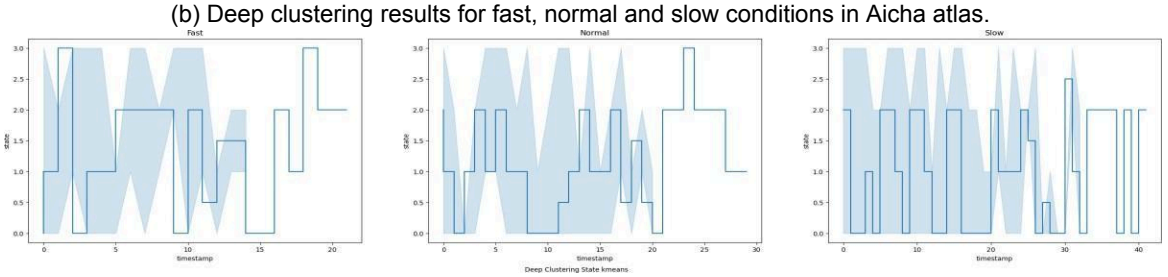

(c) Deep clustering results for fast, normal and slow conditions in K-Means atlas.
Figure 60: Deep clustering states for tempo conditions**.**

atlas	Fast Against Normal	Normal Against Slow	Fast Against Normal
Harvard	0.45347	0.93857	0.50882
Aicha	0.28663	0.27120	0.95371
K-Means	0.37972	0.47001	0.27857

Table 8: Test Results for deep clustering states.

10.3. Summary

In this single case study, the subject was asked to recall music pieces while altering their tempo internally during the recollection. Five musical pieces were selected, including Beethoven, Haydn, and Stangel. Three different tempos (fast, normal, slow) were incorporated. The spatiotemporal regularity of fMRI data was explored using selected methods from the proposed pipeline including PnP and DTW Method. The results showed that significant temporal pattern differences could be identified between music conditions and resting states in all scenarios and atlases. Further, significant brain pattern differences were identified when comparing different tempos. The functional hub of the Default Mode Network (DMN) was found to be engaged less during fast conditions compared with normal and slow conditions. Similar phenomena were also observed in episodic music networks - the slower the tempo, the higher the engagement. This indicates that a slower tempo requires more internal modulation and invokes a stronger episodic memory retrieval process. Additionally, consistent temporal pattern regularity differences were also identified in the functional networks, including regions like the right precuneus, right MTG, and right angular gyrus. This lateralization during music recollection is also observed in studies using exogenous stimuli. Analysis using DTW also revealed a similar engagement increase in a slower tempo.

Overall, the results indicate consistent temporal pattern regularities and differences can be identified and observed in selected brain networks in endogenous scenarios. In addition, the analysis found that the slower the tempo becomes, the greater the mental effort it needs. Results also identified consistent spatiotemporal pattern differences for different tempo conditions across music pieces. The study showed that purely endogenous stimuli could be reliably used to alter memory retrieval and its temporal properties in short-duration tasks. It also showed that similar brain activations can be observed across exogenous and endogenous stimuli. This means that the endogenous stimuli in short-duration tasks with conscious temporal control can be used as a reliable experimental paradigm and extended to other fMRI studies.

11. Group Study: Random Item Generation

The group study of Random Item Generation (RIG) involves the endogenous process of generating random sequences based on different types of items. The subjects were instructed to generate items (sampled from numbers and Chinese characters) at different time intervals (500ms and 1500ms) using different sequences (random or sequential). This study combines the exogenous stimuli - timing control - with endogenous stimuli of item choice and random generation process. The items are retrieved from long-term semantic memory instead of autobiographical memory. By comparing temporal regularities and different brain states, I aim to examine the endogenous random process involved and identify common spatial-temporal structures at the group level.

11.1. Subjects and Experiment

11.1.1. Subjects

A total of 20 subjects were included in the study, including 10 females and 10 males. Three subjects were discarded due to invalid trials. The final subjects include 10 females and 7 males (mean age: 27.46, SD: 1.61, Range: 23-29). All subjects have normal or corrected visual and no neurological disease history. Subjects were instructed to avoid any performance-impairing substance use, including caffeine and medicines, in the 24 hours prior to the study. The selected subjects have a basic understanding of probability, and consent was collected from all the subjects. The Ethics Committee of the Medical Faculty of Ludwig Maximillian University Munich approved the behavioral and fMRI experiment protocols.

11.1.2. Experimental Paradigm

The experiment was designed with three variables in mind – item, duration (gap duration) and sequence. The gap duration included 500 ms (fast) and 1500 ms (slow), while the item type included numbers and words. For the number condition, 1-5 was used. For the words, 5 Chinese characters were selected, which represent different animals (sheep, monkey, mouse, dog, and chicken). The item selection was rooted in the consistency of categories, word frequency, and the number of syllables. All the items are from the traditional Chinese zodiac and do not have a semantic linkage with each other - like the association people tend to create between a mouse and a cat. In addition, all characters are single syllables that match the phonetic property of the numbers 1 through 5 in Chinese. Each random sequence condition was coupled with a control condition consisting of sequential counting. This forms the third variable (sequence) corresponding to the task and control condition. During the control condition, subjects were instructed to count numbers in ascending order in a loop. For the words, subjects were instructed to recite a predefined character sequence of 5 animals given to them one day prior to the study. Overall, 8 experimental conditions were conducted, while each condition includes six thirty seconds blocks (12 volumes per block, 72 volumes in total).

11.1.3. Data Acquisition

The fMRI data were collected using ascending order on a 3T MRI Phillips scanner in the University Hospital of LMU, Munich. Localizer images were first collected to align the field of view centered on each participant's brain. The T1-weighted structural image was acquired with magnetization-prepared rapid gradient-echo sequence (MPRAGE) with the following arrangement: (1 mm × 1 mm × 1 mm; 240
× 240 matrices, field-of view = 220 mm) before the experimental EPI runs. For functional imaging, a gradient echo-planar sequence was used (repetition time (TR) = 2500 ms; echo time (TE) = 30 ms; flip angle = 90◦; acquisition matrix = 80×80; 49*3 mm slices, no gap between slices). For each valid subject, the resting state contains 360 functional volumes, and the task condition recording consists of 800 functional volumes.

Figure 61: Selection of Predefined networks in this study. (a) DMN Network in Harvard Atlas. a.1 is the functional hub (PCC, angular gyrus, precuneus). a. 2, the memory hub (parahippocampal and hippocampus). a.3 Left superior, middle, and inferior frontal gyrus, as well as left caudate and thalamus. a.4 Right superior, middle, and inferior frontal gyrus, as well as left caudate and thalamus. a.5 Dorsolateral prefrontal cortex (DLPFC) (b) DMN Network in K-Means parcellation. The regions are selected based on overlap with Harvard regions - b.1-5 is based on a.1-5. (c) DMN Networks in Aicha Atlas. c.1 Posterior cingulate cortex (PCC). c.2 precuneus. c.3 angular gyrus. c.4 Memory hub including parahippocampal and hippocampus. c.5-7 is the same network as a.3- 5.

11.1.4. Pre-defined Brain Network

In this group study, I want to explore temporal regularities in selected brain regions engaged in the random generation processes and memory retrieval processes. As a result, Default Mode Network (DMN) areas containing functional hubs and memory sub-network were included as predefined brain regions. In Jahanshahi et al. (2000), it was suggested that the random number generation process involves the dorsolateral prefrontal cortex (DLPFC) regions in the brain. Therefore, these regions are also selected in the analysis, as shown in Fig.61.

11.2. Results

The analysis followed the steps outlined in the pipeline, and the results are aggregated at the group level. A virtual subject consisting of the averaged signals of all the subjects after normalizing each subject to the MNI152 template is used to calculate the static Functional Connectivity (sFC) correlation matrix. Modularity-based community detection methods were applied to the resulting sFC correlation matrix, and networks were selected based on overlap with the predefined networks. In this study, the PnP method does not quite fit the case but was conducted still for completeness. In addition to PnP, a pooled data analysis was done to identify temporal pattern differences. Dynamic Functional Connectivity (dFC) based deep clustering methods were also applied to the virtual subject for analysis. In addition to the pipeline results, a whole-brain voxel-wise analysis based on the general linear model (GLM) was applied using SPM 12. A first-level analysis was done for each subject, and the results were aggregated to create a second-level (group-level) ANOVA analysis.

11.2.1. Standard SPM Analysis

Traditional SPM-based analysis was performed for the group study. ANOVA analysis was first performed for each subject, testing the interactions between the variables and the main effects of each variable. In this study, the three variables are defined as tempo/duration (short and long time gap between each random generation), item (whether the generated content is a number or word), and sequence (generates a random sequence or a predefined counting sequence). After the first-level analysis, the results are aggregated and tested using a one-sample t-test in the 2nd-level analysis to identify any consistent activation for different interactions and effects across subjects.

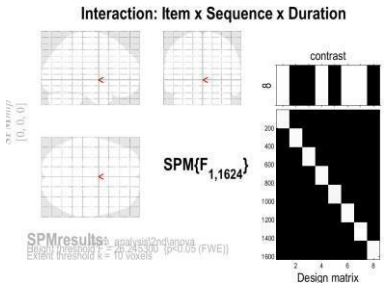

(a)Three-way Interaction Between the variables

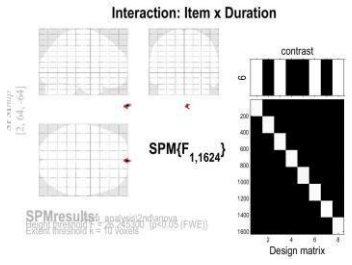

(b) Interaction between item and duration (tempo)

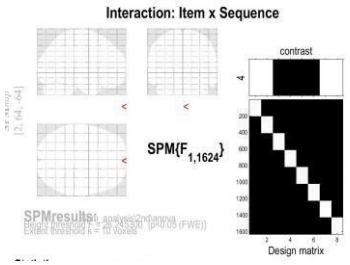

(c) Interaction between item and sequence

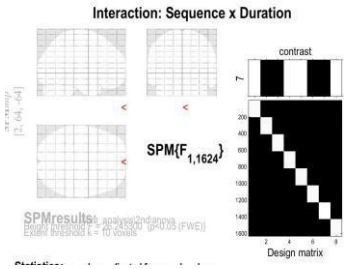

(d) Interaction between duration and sequence

Figure 62: ANOVA interaction results between the variables. (a) three-way interaction. (b)(c)(d) two-way interactions.

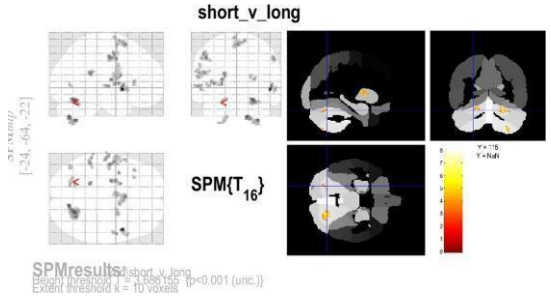

(a) Example activation: (cerebellum.

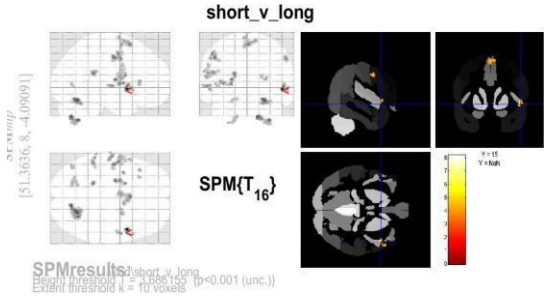

(b) Example activation: precuneus.

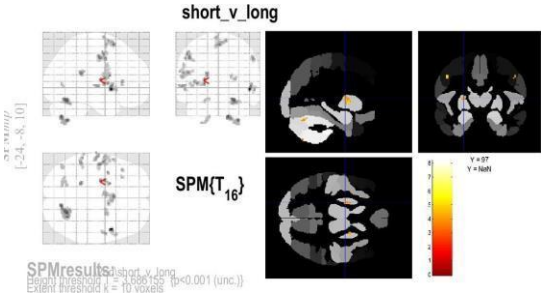

(c) Example activation: left putamen

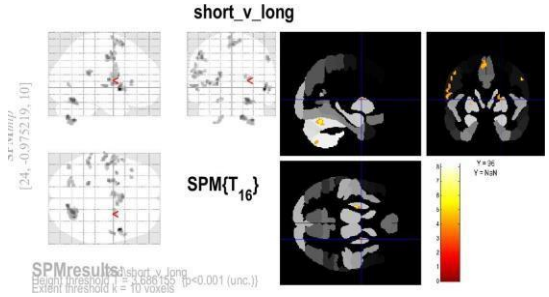

(d) Example activation: right putamen.

Figure 63: Whole-brain voxel-wise relative activation results for the duration (tempo) condition.

For the three-way ANOVA, interactions between the variables are tested - tempo(duration) and item, sequence, and item, as well as tempo(duration) and sequence. As shown in Fig.62(a), no significant

voxels were identified in three-way interaction scenarios. When an interaction is not found, this means that there is no effect of one variable's levels on another variable. In this scenario, it means the type of duration, item, and sequence has no impact on one another. As shown in Fig.62(b)(c)(d), no significant two-way interactions were observed. With this in mind, I can examine each variable's main effects.

Fig.63 shows the example regions identified from the relative activation between the short and long time gap condition. Bilateral putamen were activated along with precuneus. It was shown that a fair portion of the cerebellum was activated in these scenarios. The right temporal pole (rTP) was also identified from the test. Jahanshahi et al. (2000) showed that bilateral precuneus and cerebellum were associated with random number generation. In addition, compared with random number generation, random item generation engages more precuneus region and temporal pole.

The results of this study indicate that similar activation patterns can also be found for random item generation between random number generation. Still, random item generation involves more cognitive processes than random number generation.

11.2.2. Functional Connectivity and Networks

A virtual subject from averaged, normalized signals is created for the group study analysis pipeline. Like the single case pipeline, the signals are extracted from each ROI identified and aggregated. The whole-brain functional connectivity matrices are then calculated for each atlas and all the ROIs. Again, the Pearson correlation was computed between each ROI using averaged signals, the percentage change of averaged signals, and the principal components of each ROI.

Since the study was designed with a resting state coupled with a continuous task state with shuffled conditions over time, functional connectivity matrices were created using the resting state data.
Fig.64 shows the example of functional connectivity matrices calculated.

Fig.64b shows the distribution of sizes of the networks identified using graph theory based on different signal aggregation methods (average, percentage, PCA) and in different atlases (Harvard, K-Means, Aicha). Based on the analysis pipeline, additional brain networks were selected based on overlapping with predefined brain networks. Fig.64c showed the distribution of the community sizes for the selected brain networks. The average aggregation method provided networks of moderate sizes in the Harvard atlas regardless of emotional valence. The percentage method provided rather consistent performance in different conditions and atlases.

Fig.65 is the Graph Theory-based network separation results. The y-axis indicates the total number of networks identified. As shown in Fig.65, the average signal aggregation method provided the highest network separation performance at a high correlation threshold. This means that when looking at strongly correlated brain regions, using the average aggregation method can provide the best network detection. In Aicha and K-Means atlas, the average aggregation-based method provides the highest number of networks at a stronger correlation threshold. As a result, in this study, the average method will be used in the subsequent analysis in all atlases.

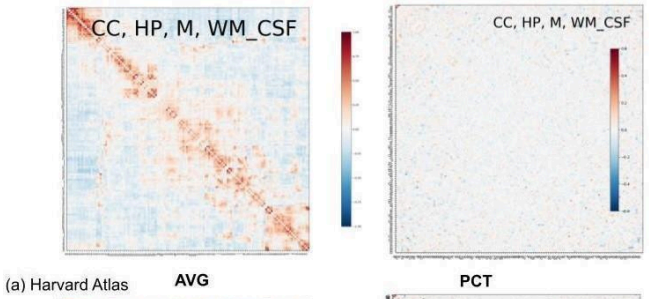

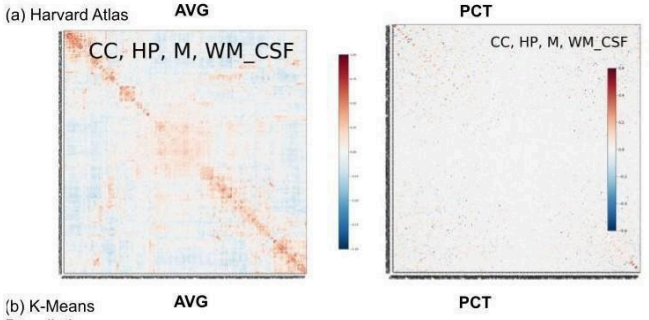

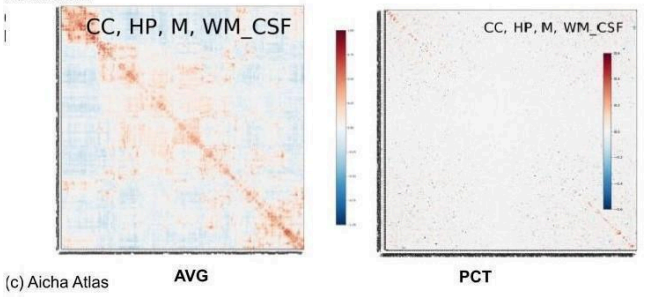

(a) Functional connectivity matrices.

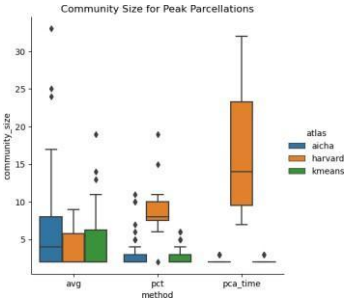

(b) Community size for identified networks.

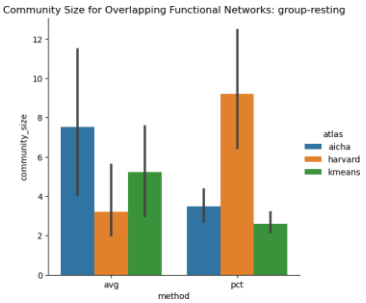

(c) Community size for selected networks.

Figure 64: a. Functional connectivity matrices with confounds removed, including component correction, high-pass filter, motion, white matter, and cerebrospinal fluid. a.(a) FC matrices for Harvard atlas averaged signals and percentage signals. a.(b) FC matrices for K-Means atlas averaged signals and percentage signals. a.(c) FC matrices for Aicha atlas averaged signals and percentage signals. b. and c. Community size distribution for identified and selected brain networks. Counted in the number of regions included in each network.

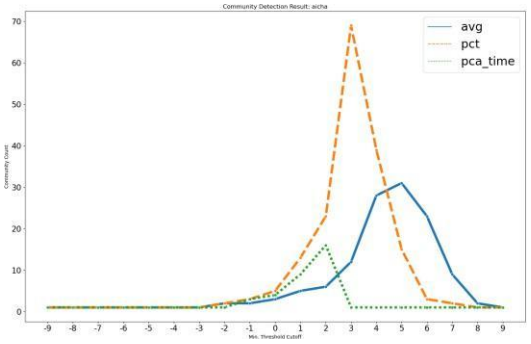

(a) Community count for aicha atlas

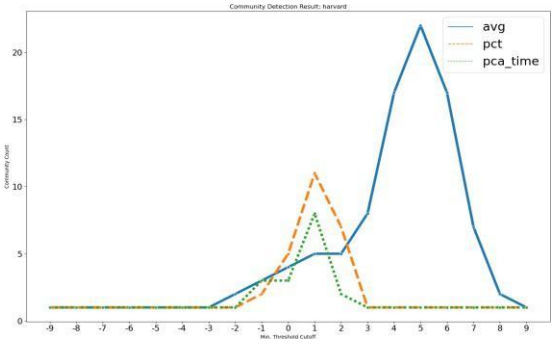

(a) Community count for harvard atlas

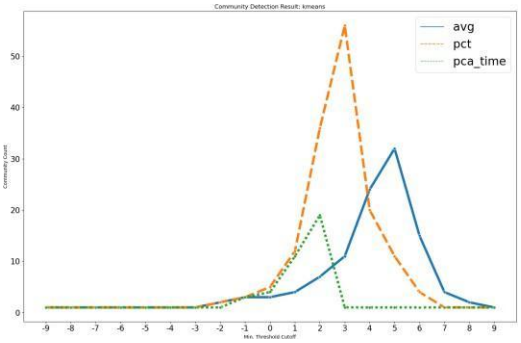

(a) Community count for K-means atlas

Figure 65: Total number of separated community distribution by threshold. The x-axis is the correlation value threshold used. A value of 5, for example, means that all values below 0.5 in the original FC matrix were removed from the calculation.

11.2.3. Spatiotemporal Regularity

The multi-step temporal analysis results demonstrated that consistent spatiotemporal regularities could be identified in different brain regions. As shown in 7.1.5, the temporal signals extracted from each brain network are further processed to identify dissimilarities between neighboring brain states. I have used three types of measures: angle-based distances, distributional and non-distributional distances. In this group study, applying PnP methods in the analysis was not feasible since each task condition (a combination of the tempo, item, and sequence) was short in terms of recording (30 seconds). Given such, additional methods like pooled time series data tests (ordinary least squares, OLS), and Generalized Estimating Equation (GEE) were selected to explore the temporal pattern differences between different conditions.

PnP Regularity Analysis As mentioned, the duration of the task condition is only 30 seconds for each scenario. For example, when generating a random number sequence with a long gap between each prompt, the duration is 30 seconds, translating to 12 scans. In the case of PnP methods, this means I can only test the half-period from two to five scans which do not offer sufficient distributional differences between the conditions. It should be noted that it does not mean the PnP method cannot be applied and tested; it simply means the resulting half-period does not offer enough variations.

The half-period can be calculated for each task condition for all sessions of the condition in each subject and then summed up across all subjects to create a distribution of the temporal regularities. The distribution can then be compared across conditions, as shown in Fig.66.

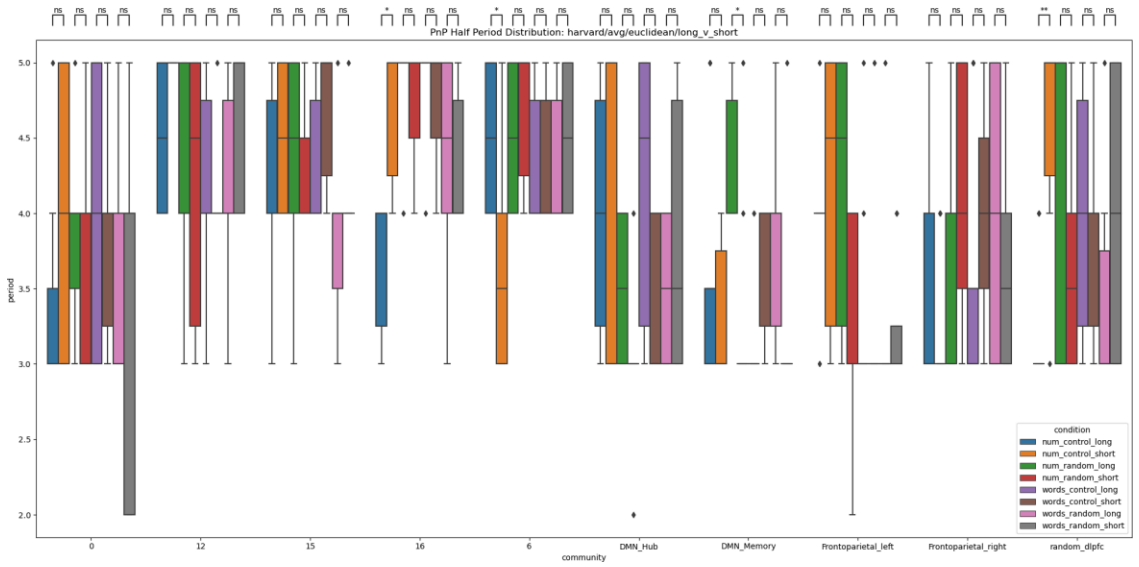

Figure 66: Distributions of significant half periods (p<0.001) for different brain networks in Harvard atlas. Y-axis is the value of the identified half period. The X-axis are the conditions. For example, the green and red bars represent random number generation with a long and short time gap. The test is performed between the half-period distributions aggregated across the subjects (e.g., summing up the total number of one significant half-period across all sessions in all subjects). empty: p=nan, *: p<0.05, **: p<1e-2, ***: p<1e-3, ****: p<1e-4

Pooled Time Series Analysis Since each task session is exactly 30 seconds or 12 scans in length, the timestamp of each session can be matched, and the time series data can be naturally pooled together to create a form of panel data for subsequent analysis. Table.9 gives an example of how the data is organized for analysis. In the example, the condition given is word/short/random and word/long/random. Directly comparing the differences between the two across all subjects will examine the relationship between different gap duration in the random item generation scenario.

In this study, the distribution of panel data for different scenarios was tested. A significant p-value would allow us to conclude that the variable is significantly different from the dependent variable. In addition, given the correlated nature of the observations, the General Estimating Equations method was used to examine the temporal pattern differences.

condition	timestamp	network	subject
word_short_random	0	DMN_Hub	A
word_short_random	1	DMN_Hub	A
word_short_random	0	DMN_Hub	B
word_short_random	1	DMN_Hub	B
...	...	...	...
word_long_random	0	DMN_Hub	A
word_long_random	1	DMN_Hub	A
word_long_random	0	DMN_Hub	B
word_long_random	1	DMN_Hub	B

Table 9: Example illustration of pooled panel data for time series across subjects.

Directional distribution test revealed that the dorsolateral prefrontal cortex (DLPFC) network is activated less when compared with the control condition in both number and words scenario, as shown in Table.10 and Table.11. This indicates a reduction of neighboring state variations or a potential inhibition in the DLPFC networks in the random generation scenario. Like what was found in Jahanshahi et al. (2000) using PET analysis where DLPFC showed suppression of activities during the random generation process. Further, when comparing the scenarios under the words condition, the right frontal regions were found to be suppressed in addition to the DLPFC networks, more specifically, the superior and middle frontal gyrus. The brain's frontal areas involve various functions, from cognitive control to response modulation. In Hu et al. (2016), it was suggested that the superior frontal gyrus, right in particular, is associated with response inhibition and control of impulsive responses. The results could indicate the scenario of generating random items and suppressing habitual responses as shown in DLPFC. The brain also opted for less control of the impulsive responses.

The GEE results as shown in Table.10 also indicated interactions between the variables. When duration is short (500ms), the random scenario elicits lower activation (negative coefficient) in bilateral caudate and higher activation in precuneus and PCC (positive coefficient). The caudate was associated with language and has been shown to be crucial for language control (Hannan et al., 2010). PCC and precuneus are associated with awareness and many other functions. This indicates that the language regions are suppressed when generating random words, and awareness heightened. One potential explanation is that subjects are suppressing the processing of words' meaning for random production.

Further, when comparing words against numbers in control conditions, as shown in Table.10 and Table.12, the memory hubs of DMN were more involved in the process. More specifically, the results showed that at short duration (500ms), words engage higher activation than numbers. This indicates that during the control condition of words, the memory retrieval process is more active, which corresponds with expectation - since the sequence of the words was not a counting task but rather a collection of previously remembered sequences.

The results also revealed temporal pattern differences between words and numbers in the random generation process and a 3-way interaction was found for the left frontal parietal network. When generating random sequences with short gaps / faster tempo, the left frontal regions (left SFG, middle frontal cortex, and left inferior temporal gyrus) and memory hubs are more engaged in words than numbers scenarios. These regions are involved in working memory (Boisgueheneuc et al., 2006) and language and semantic memory processing. However, when the temporal gap is longer, only the right frontal regions are more engaged in words against numbers. This could indicate that when reducing temporal gaps or increasing tempos, the brain needs to be more engaged when generating random words compared to random numbers.

In short, consistent temporal pattern differences were observed in random item generation processes, and strong differences were also found when comparing randomly generated words and numbers. Inhibition of the dorsolateral prefrontal cortex was consistent with previous studies. The results indicated that the endogenous random generation process could reliably induce differences in

different item generation scenarios. It also means that the endogenous random process can be reliably combined with exogenous stimuli and non-episodic memory experiments.

p-value	Coefficient	Effect	network
*	-0.0718	item[T.words]:sequence[T.random]	DLPFC
***	-0.0860	duration[T.short]: sequence [T.random]	Caudate
*	0.2772	duration[T.short]: sequence [T.random]	Precuneous, PCC
*	0.0416	item[T.words]:duration[T.short]	DMN Memory Hub
*	0.0583	item[T.words]:duration[T.short]: sequence [T.random]	Left Frontal Parietal Network

Table 10: GEE test result for the three variables. (*: p<0.05, **: p<0.01, ***: p<0.001)

p-value	measure	network atlas	
*	mahalanobis	DLPFC	Aicha
*	mahalanobis	Right Frontal Parietal Network	Harvard
*	mahalanobis	DLPFC	Harvard
**	mahalanobis	Right Frontal Parietal Network	KMeans
***	mahalanobis	DLPFC	KMeans

Table 11: Distribution test of random generation against control condition in words. (*: p<0.05, **: p<0.01, ***: p<0.001)

p-value	measure	network	atlas
*	Mahalanobis	DMN_Memory	Aicha
*	cosine	DMN_Memory	Aicha
**	cosine	DMN_Memory	Harvard
**	Mahalanobis	DMN_Hub	KMeans
**	euclidean	DMN_Memory	KMeans
***	cosine	DMN_Memory	KMeans

Table 12: Distribution test of words against number scenario in the control condition. (*: p<0.05, **: p<0.01, ***: p<0.001)

11.2.4. Deep Learning Whole-brain Analysis

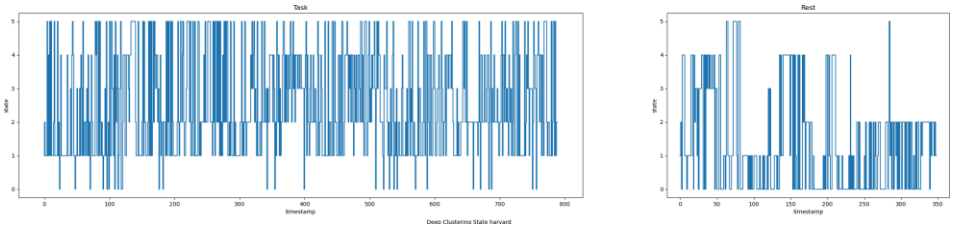

(a) Deep clustering results for resting and task conditions in Harvard atlas.

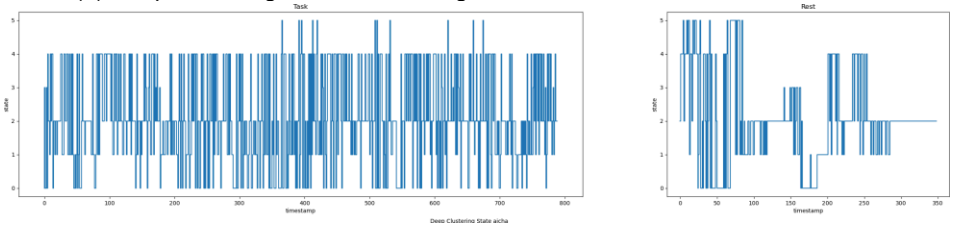

(b) Deep clustering results for resting and task conditions in Aicha atlas.

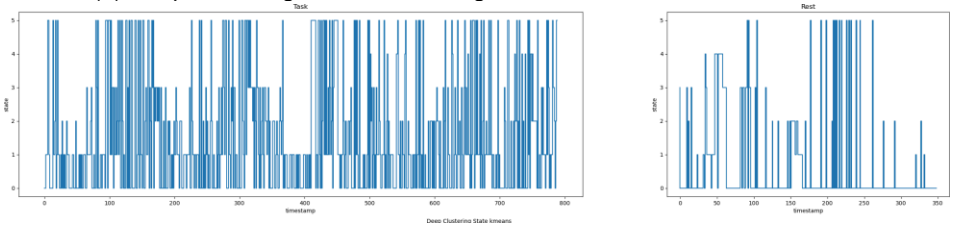

(c) Deep clustering results for resting and task conditions in K-Means atlas.
Figure 67: Deep clustering states for resting and task conditions.

Deep learning combined with Dynamic Functional Connectivity (DFC) was also applied in the analysis. This analysis focused on the whole-brain state transition changes instead of single regions and networks to identify whole-brain-scale temporal pattern regularities. The deep clustering method was applied to the overall task and resting conditions.

atlas	Mann-Whitney Stats	Mann-Whitney P Value
Harvard	197018.5	2.229e-32
Aicha	139381	7.28e-1-*
K-Means	185509	9.841e-24

Table 13: Test Results for deep clustering states.

The deep clustering analysis follows the pipeline introduced in 7.1.6 where DFC with a sliding window size of 10 frames was calculated for each condition. In this experiment, the resting state consisted of 360 scans, and the task condition consisted of 800 scans, meaning the resulting DFC sequences are 350 and 790, respectively. The result indicated significant differences in whole-brain state distribution between task and resting conditions - the differences are substantial enough to be visually detectable, as shown in Fig.67 in K-Means and Harvard atlas. The distribution test result, as shown in Fig.13, also demonstrated highly significant differences between the deep clustering result of task and resting condition in Harvard and K-Means atlases. It should be noted that the results are not visible in the Aicha atlas when extracting the median states of different conditions. This could partially be due to the fact that, while the Aicha atlas provides more parcellations to the brain, it covers a smaller percentage of the overall brain compared to the Harvard atlas and K-Means parcellation meaning that some signals in the brain are not accounted for - most importantly the cerebellum. Again, this could indicate that the cerebellum plays an important role in estimating the whole-brain states.

11.3. Summary

In this group study, subjects were asked to produce a sequence (either random or in a fixed order) of items (words or numbers) at a specific duration (500ms/1500ms gap duration). The fMRI data were first analyzed using traditional SPM methods and ANOVA. The ANOVA analysis was performed first at the individual level and then at the group level. The results found no significant interaction (three-way and two-way) between the variables but identified main effects of tempo. This means that SPM FWE analysis was unable to identify the effect of sequence on the other variables. Compared with random number generation, generating random items shows more engagement in the left temporal pole, left paracingulate gyrus, and precuneus areas. It showed that some common activation could be identified for the random generation of both contents, but random word generation requires more cognitive processing.

For spatiotemporal regularity analysis, data are pooled together to create panel data for distribution analysis and GEE test. The results showed that the dorsolateral prefrontal cortex (DLPFC) is less engaged during random item generation sessions. In addition, the results showed that the right frontal regions, including the superior and middle frontal gyrus, were suppressed in addition to DLPFC. This indicates that during random item generation, habitual responses and control of impulsive responses were suppressed. Additionally, the results showed that the brain regions involved in memory and awareness are more engaged when generating random words. This means creating arbitrary words demands more cognitive exertion compared to numbers. Deep clustering analysis in this study identified consistent temporal pattern differences between task and resting state conditions.

In summary, the study identified consistent differences comparing the generation of different types of endogenous stimuli. The results indicate that endogenous stimuli would elicit similar brain activation patterns like that of exogenous stimuli in the random generation process. Further, the results mean that at group level, endogenous alteration of stimulus types, tempo and processes in generation of contents for short-duration tasks can be used as a reliable experimental paradigm. In short, the endogenous stimuli paradigm can be combined with exogenous stimuli and used to study the different brain modulation processes for different stimulus types.

12. General Discussion

In neuroscience studies, one important question is whether experimental paradigms with endogenous stimuli can be reliably used. Previous experiments have adopted endogenous stimuli in their approaches (Avram et al., 2013; Vedder et al., 2015), but a systematic examination is yet to be performed.

More specifically, whether endogenous stimuli can elicit consistent spatiotemporal regularities and whether these neural patterns can be reliably detected using analytical methods needs to be examined. This expands to whether the endogenous stimuli can be reliably used in long-duration and short- duration episodic memory tasks as well as retrieval and modification of episodic and semantic memory in short-duration tasks. In addition, whether the endogenous stimuli can be used in scenarios where exogenous stimuli is included.

These questions are examined in the four experiments using comparative approaches. To explore the validity of the endogenous paradigms, the temporal regularities of different cognitive processes are compared in endogenous stimuli scenarios with resting state or baseline scenarios to identify neural pattern activations. To extract the brain patterns from the vast number of spatiotemporal signals from the fMRI recordings, I compared the temporal regularities at the brain-network level of different scenarios and conditions. Despite the fMRI inherent limitations (Logothetis, 2008), there are still many analytical methods that can be used to extract information from these data. To establish a standardized analysis infrastructure, a pipeline is proposed that can serve as the framework of analysis where the techniques can be picked and chosen given different experiment conditions at different stages. The findings of the presented studies are discussed in the following sections.

12.1. Endogenous stimuli as a paradigm

The four studies followed the framework outlined in Fig.34 in 6.2. The first set of studies focused on the endogenous stimuli application in episodic memory sessions of different duration and whether a consistent and robust spatiotemporal regularity can be identified in these cases. The second set of studies focused on endogenous stimuli and processes combined with exogenous stimuli and memory retrieval and modification. The studies explored whether a consistent and robust spatiotemporal regularity can be identified in these complex scenarios to examine the endogenous paradigm's validity and extensibility.

In the first single case study, the subject was asked to recall her daily morning routine after giving a verbal description and was recorded in fMRI. The morning routine sessions were repeated with precise temporal control. It was found that when the subject used endogenous stimuli during the episodic memory sessions, a high level of temporal control was elicited. This observation implies that when humans are asked to recall past events, they apparently can remember the order of events and the duration of these events, if one accepts this single case study as typical, and that the “internal events” correspond to the sequence and duration of events in reality. The analysis of this experiment focused on the brain networks and regions that are known to be heavily engaged in episodic memory and autobiographical memory sessions, namely the Default Mode Network (DMN). The DMN is split into specific sub-networks, such as functional hubs and memory networks. The result of the study revealed significant temporal regularity differences in these networks. In addition, functional parcellation identified functional networks that are more engaged in morning-routine sessions than resting state sessions. One network contains brain regions such as the angular, supramarginal, and inferior frontal gyrus. The regions in this network are known to be engaged in language processing and spatial recognition. Another identified network contains regions such as the bilateral occipital cortex, posterior cingulate cortex, and precuneus. These regions are known to be recruited during object recognition and episodic memory retrieval. Previous studies (Biesbroek, Weaver, & Biessels, 2017; Tulving et al., 2002) have found that DMN is engaged early in episodic memory sessions, and sensory-related regions are more engaged towards the later part of an episodic memory session. The findings suggest that using the endogenous stimuli paradigm can be a reliable method in long duration episodic memory studies. Furthermore, the results demonstrate our capability to identify the patterns of brain activity stimulated by such experimental paradigms.

In the second leadership group study, participants recalled both extremely positive and negative experiences for 2 minutes without sharing specifics. The traditional SPM12-based analysis results indicate that brain regions in the negative emotional scenarios are more engaged in the right hemisphere. This includes regions like the right angular gyrus, right lateral occipital cortex, and right parietal operculum cortex. These regions are involved in complex cognitive processes such as object

recognition, memory retrieval, and visual-spatial recognition. Experiments using exogenous stimuli have also reported lateralization in emotional stimuli processing (Gainotti, 2019). In positive scenarios, the left frontal pole is more engaged, which agrees with the findings that the left hemisphere is more involved when processing positive emotional stimuli (Root, Wong, & Kinsbourne, 2006). The meta- study by Gainotti analyzed experiments mostly involving exogenous emotional cues. In this experiment, however, the emotional stimuli are purely endogenous.

The temporal regularity results using the PnP method revealed significant differences in temporal pattern distribution between positive and negative emotional conditions. The results show that strong negative memories command more emotional involvement than positive memories. Results also suggest that senior leaderships had more focus on context during negative experiences. Additionally, results showed that for senior leadership, facial expressions register a large memory footprint in negative experiences. For positive scenarios, regions involved in positive stimuli processing and subjective happiness were identified, as well as regions involved in visual and sensory processing. This could indicate that senior leaderships focused more on visual details and subjective feelings during strong positive experiences. It should be noted that the traditional general linear model-based analysis using SPM does not consider the properties of brain networks and overlooks the temporal patterns at a functional level.

To summarize, the group study explored neural activation patterns in emotional imaginations without any knowledge of the content. The results suggest that imaginations can elicit similar patterns of brain activation as exogenous stimuli during short episodic memory measurements. Furthermore, the study demonstrated that a specific neural machinery can be extracted from purely endogenous recollections without knowledge of the content at group level. This suggests we might be able to identify strong emotional brain states without having knowledge of the details of the endogenous stimuli. To further verify this, a study involving more subjects could be conducted. It should be noted that these findings are based on senior, western (Caucasian) males. As a future direction we could consider including more female, non-western subjects and create a balanced group in terms of gender, culture, and race.

In the third music single-case experiment, the subject was asked to recollect five different music pieces at different tempos (fast, normal and slow). The PnP method and the dynamic time warping (DTW) method were applied to explore spatiotemporal regularity between music and resting conditions as well as across different tempo and music pieces. The PnP results showed significant differences in temporal pattern distribution between the music and resting conditions. When comparing the different music conditions, significant results were found in the Default Mode Network (DMN) functional hubs. It was shown that the fast condition engaged less DMN functional hub than the normal and slow conditions. In the Aicha atlas, results were further identified in sub-functional hubs involving the precuneus, suggesting that slower scenarios require more internal modulation. Furthermore, in both Aicha and KMeans parcellations, significant results were found in the episodic music network. This indicates that purely endogenous music stimuli can elicit identifiable, consistent neural pattern differences in DMN functional hub and episodic music networks. Additionally, consistent temporal pattern regularity differences were identified in the functional networks containing posterior cingulate gyrus and precuneus. The study suggests that the precuneus is more engaged in slower conditions during the musical retrieval process. This means that imagining upcoming events and matching the correct tempo takes greater effort the slower the tempo. The DTW method was employed to calculate and compare the dissimilarity between different conditions. Similarly, it was found that the temporal dissimilarity between slow and fast music conditions was greater than that of normal and fast conditions. This again indicates that the effort to slow down the music endogenously increases as the tempo slows down. The study also found right lateralization in the brain regions that were involved, such as the right precuneus, right MTG, and right angular gyrus. Studies using exogenous tempo stimuli have shown similar lateralization (Liu et al., 2018). In summary, the findings show that consistent spatiotemporal patterns differences in functional brain networks can be reliably identified during endogenous scenarios. The analysis revealed an inverse relationship between tempo speed and mental effort required. Additionally, noticeable spatiotemporal pattern variations were found across musical pieces with different tempos. The experiment showed that the endogenous stimuli in short-duration tasks with conscious temporal control can be used as a reliable experimental paradigm in fMRI studies.

The last group study involved asking subjects to produce either random or sequential items at different temporal gaps. Traditional SPM analysis and spatiotemporal regularity analysis methods were used for analysis. In SPM, ANOVA (Analysis of Variance) was first performed for each subject, testing the interactions between the variables and the main effects of each variable. The three variables were defined as duration (short and long-time gap duration), item (number or words), and sequence (random sequence or a predefined sequence). The results of the ANOVA analysis found

no significant three-way and two-way interaction. However, main effects were found for tempo. The study found that random item generation engages more cognitive processes than random number generation, showing significant engagement in regions such as the precuneus and left temporal pole. For spatiotemporal regularity, data were pooled and analyzed using distribution analysis and GEE test. The analysis focused on the networks involving memory retrieval (DMN and sub- networks), random sequence generation (DLPFC) as well as improvisation (frontal-parietal regions). The study found temporal pattern differences in random generation conditions, with the dorsolateral prefrontal cortex (DLPFC) network being activated less when compared with the control condition in both number and word scenarios. This indicates a potential inhibition in the DLPFC networks in the random generation scenario. The study also found that when comparing the scenarios under the words condition, the right frontal regions were suppressed in addition to the DLPFC networks, specifically the superior and middle frontal gyrus. The results could indicate the scenario of generating random items and suppressing habitual responses in DLPFC and less control of impulsive responses. The study also found regions that showed stronger activation in random sequence, more specifically, the left frontal networks and functional hubs, precuneus, and caudate regions. These findings are consistent with previous studies using the random number generation paradigm (Jahanshahi et al., 2000; Hu et al., 2016). The results also revealed temporal pattern differences between words and numbers in the random generation process, with more engagement of left frontal regions and memory hubs in words than numbers. In short, the research identified consistent spatiotemporal regularity differences at group level when subjects are asked to generate endogenously modulated contents of different types in conjunction with exogenous stimuli. In other words, the paradigm can not only be used reliably, but also can be extended to include different stimulus types as well as exogenous stimuli. It also means that the pipeline is robust and can be applied to diverse scenarios.

The four studies compared the spatiotemporal regularities of different brain networks to explore the validity of the endogenous stimuli paradigm. The findings suggest that at both individual and group level, consistent neural patterns elicited by endogenous stimuli can be observed and identified. This can be further supported by the fact that identified networks coincide with brain regions and networks activated by exogenous stimuli in previous studies.

This indicates that endogenous stimuli can be a reliable source of stimuli in fMRI studies. Furthermore, the findings suggest that endogenous stimuli can elicit similar responses as exogenous stimuli in scenarios such as strong emotional experiences and music experiences. The overall results suggest that the endogenous stimuli paradigm can be used in research and that this paradigm can even be extended to experiments where exogenous stimuli is included or in experiments that involve non-episodic memory. It implies that the approach can be valid and valuable in multiple research fields.

12.2. Deep clustering as a method

The deep learning technique was also explored as a way to extrapolate information from the whole-brain level in this study. The goal is to examine whether the method can identify consistent temporal regularity differences at a large scale. In the experiments, a sliding window size of 10 frames was applied to four different studies. The first study yielded significant differences in whole-brain state distribution between task and resting conditions, visible in the Harvard atlas and k-means parcellation but not in the Aicha atlas. This could indicate that the cerebellum is important in estimating the whole-brain states. The second and third studies did not yield consistent results across conditions at a whole- brain scale. More specifically, the temporal patterns of the whole-brain states in short-duration experiments may not contain sufficient data for deep learning clustering to train an accurate model for classification. The fourth study also yielded significant differences in whole-brain state distribution between task and resting conditions, visible in the Harvard atlas and k-means parcellation but not in the Aicha atlas, again indicating that cerebellum plays an important role in estimating the whole-brain states.

The findings in this analysis indicate the cerebellum plays an important role when evaluating brain states, especially at the whole-brain level. As a matter of fact, previous studies (Fontes et al., 2016; Ivry & Spencer, 2004) have found that the cerebellum plays a critical role in our internal understanding and representation of time. This indicates that in memory experiments, to consistently identify whole- brain scale temporal regularity differences and use the brain states as an indicator, the cerebellum should be included in the atlas mask used to extract brain signals. The result also suggests that temporal perception and control are crucial in episodic memory sessions. Deep clustering as a method is most useful when there is sufficient recorded data to train the model on. For single case studies, repeated long resting-state recordings would be sufficient to provide robust data. Further studies could be conducted to explore the accuracy of the method at various functional

networks to provide an easy- to-interpret granular signal.

12.3. Analysis Pipeline as a tool

An analysis pipeline of fMRI data has been introduced, which provides a wide range of analytical tools to extrapolate information from brain signals. The results show that not all methods can be applied to all experiments in all scenarios. Therefore, I would like to suggest that a subset of analytical tools should be applied based on the experiment designs. This should be the baseline infrastructure pipeline for experiment analysis. For example, a study with a very short task duration might not be a suitable candidate for dynamic functional connectivity or deep clustering analysis. The pipeline also included tools to examine the spatiotemporal regularities of the brain signals. Tools like functional connectivity (FC) and graph-theory-based community detection would be able to reduce the dimension of consideration by identifying functional networks. Temporal data can then be extracted from the identified functional networks and be further analyzed using temporal regularity analysis tools such as the PnP method.

Overall, the pipeline has introduced tools that are proven to be robust in detection - identifying brain networks and regions that coincide with previous studies and those that could not be identified using the traditional SPM method. There are, however, limitations associated with the methods mentioned, and careful choice is needed. The DTW method, for example, appears as a powerful tool for analyzing the time series similarities. However, the method should only be used when a relationship between the time series is expected - such as the same music piece but with a different tempo.

The selection of distance measures in the fMRI analysis is also an important topic. The pipeline examined different distance measures such as angle-based measure (Cosine), distribution (Euclidean), and non-distribution distance (Mahalanobis). Mahalanobis distance is a measure of distance between two points in a multivariate space that considers the correlation between the variables. It is defined as the distance between two points in a multivariate space, adjusted for the covariance of the data. This distance is particularly useful when the variables in the space are correlated, as it provides a more robust measure of distance than the Euclidean or cosine distance. The Euclidean distance is the traditional straight-line distance between two points in multivariate space, but it does not consider the correlation between the variables. This can be problematic when the variables are correlated, leading to over or underestimating the distance between points. The cosine distance, which is also known as the cosine similarity, is a measure of similarity between two non-zero vectors of an inner product space that measures the cosine of the angle between them. It ranges from -1, indicating exactly opposite, to 1, indicating exactly the same, with 0 indicating orthogonality. Cosine distance may be less robust than Mahalanobis distance in handling correlated variables. In summary, Mahalanobis distance is more robust than Euclidean distance and Cosine distance when handling correlated variables because it adjusts for the covariance in the data, which can give more accurate distance measurements. This feature makes it useful in various applications such as pattern recognition, multivariate statistical analysis, or cluster analysis. It should be noted that these distances describe relationships from different perspectives. Meaning that significant differences in one measure does not necessarily mean there are significant differences in other measurements. Therefore, it’s important to cross-examine the relationship between the patterns using different distance measures.

The analysis pipeline also suggested that functional connectivity of the brain should be examined closely in fMRI studies. More specifically, temporal pattern analysis could be performed at functional network level. The argument here is that lots of our brain activities are related to certain brain networks. Most notable one is the default mode network. There have been many studies exploring these methods but are often overlooked. The accompanying python library that was created along with the pipeline provides streamlined functional network processing, including dynamic functional connectivity and networks.

The pipeline also included a suite of methods that have been used to explore temporal pattern regularities in fMRI experiments and many other fields. For comparatively short sequences, we have a trend agnostic period detection algorithm (PnP). For related temporal sequences we can use Dynamic Time Warping to explore its similarities and differences. We can also use a whole suite of methods such as Discrete wavelet transform, Fourier transform, power spectrum etc to explore the temporal properties of the time series. Again, it is important to mention that not all methods apply to all scenarios. As for under what circumstances a method can be applied, a golden standard is yet to be established. Nonetheless, researchers should be able to understand the analytical means, but also have an accessible way of implementing them.

13. Conclusion and Outlook

In conclusion, the endogenous stimuli can evoke a stable and reliable neurological process capable of producing consistent temporal regularity differences that can be reliably identified. The results also indicate that endogenous stimuli can elicit comparable reactions to exogenous stimuli. The research implies that utilizing an endogenous stimuli paradigm can be useful in various research fields, including combining it with exogenous stimuli or in experiments involving non-episodic memory. Overall, it suggests that this approach can be a valid and valuable method in multiple research areas. There have already been studies that compare cultural differences (Yang, et al. 2019), those that employ emotional and intrinsic judgment of beauty and emotions (Vedder, et al. 2015), and those that employ endogenous temporal control patterns (Zhou, B, et al, 2014). The results presented here validate the paradigm and suggest that a wider integration of the paradigm could be done in future studies.

The analyses presented here also suggest that using traditional methods only such as Statistical Parametric Mapping (SPM) with GLM may not provide enough information. This implies that such traditional methods have limitations in uncovering important details. This means that there is a need for alternative methods or techniques and that the limitations of SPM must be considered when interpreting results obtained through this method only (Logothetis, 2008).

While the experiments presented here explored different endogenous stimuli-based paradigms, subsequent studies should also be conducted to overcome specific limitations. The fMRI recordings' low temporal resolution (2.5s) limited the temporal regularity analysis, especially when trying to establish differences on the functional network or whole-brain level state. Advanced imaging methods (such as EEG, high-temporal-resolution fMRI, and MEG) can be used to explore the validity of this paradigm in more detail. In addition, this can be applied to real-time fMRI where the subject's endogenous activity is controlled. An increased temporal resolution can surface more information about the temporal regularities and help to identify more detailed brain functions. Furthermore, a suite of methods for spatiotemporal regularity analyses has been presented. The suggested pipeline has been shown to have equal if not better analytical power than traditional methods. The future direction of studies could focus on comparing more experimental paradigms and employing endogenous stimuli in various experiments. Furthermore, using different techniques and designs, a cross-modality analytical pipeline could establish a potentially consistent framework for neuroimaging analyses, especially when analyzing spatiotemporal regularities.

A Appendix: Terminologies

Significance Level Significance Level, often represented as α (alpha) in studies, quantifies the probability of a study rejecting its null hypothesis. Most neuroscience studies use a significance level of 0.05 (5%). However, recent studies have pointed out that this level provides more false positives and claim that all studies should use a much lower significance level, namely 0.001 or (0.1%).

A.1 Granger Causality

The granger causality test examines whether one time series is useful for forecasting another. When applied to fMRI, this would translate to if signals from one brain region can be used for forecasting another brain region. As such, this is a common method used in fMRI effective connectivity analysis to see if one area impacts the neural patterns of another.

A.2 Clustering Coefficient

The clustering coefficient is defined as the number of actual connections divided by all possible connections between the nodes. In an undirected graph, the number of actual connections is doubled since each edge is bidirectional.

A.3 Graph Modularity

The modularity of a graph refers to the density of edges within and outside communities. Optimizing the modularity would result in an optimal clustering of the nodes as the density is high within each subgroup, while the density is very low across subgroups.

A.4 Different Clustering Methods

A.4.1 K-Means Clustering

K-Means clustering is designed to separate the data points into K clusters based on the distances between each data point. The points that are close to each other will be assigned to the same cluster. K-Means clustering has many variations with respect to the choice of distance statistics and the way the data points are represented.

A.4.2 Hierarchical Clustering

Hierarchical clustering creates a hierarchy of clusters from the given data points in one of two ways: bottom-up or top-down. The bottom-up clustering will start with each data point representing its own cluster and gradually merge the clusters as the hierarchy moves up. The top-down clustering will start with all data points in a single cluster and gradually split the data points into separate clusters as the hierarchy moves down.

A.4.3 Ward Clustering

Ward clustering is an applied bottom-up version of hierarchical clustering. The method Ward's minimum variance method is used to merge the two closest clusters as the hierarchy moves up. The distance metric used between two clusters is the sum total of all squared distances between points from one cluster to another.

A.4.4 Spectral Clustering

Spectral clustering method groups similar data points together by extracting patterns from the similarity matrix calculated between all data points. The concept is similar to that of Functional Connectivity based parcellation. Spectral clustering can be used when traditional methods are hard to separate the data points.

A.5 PCA and ICA

A.5.1 Principal Component Analysis (PCA)

Principal component analysis (PCA) simplifies high-dimensional data by extracting the main components that can explain the dataset and reducing the number of variables. The PCA method identifies the directions in which the data has the most variations and projects the data to the direction - these directions are termed principal components. The components are ordered so that the first component explains the most amount of variations within the dataset and the rest in descending order. The components in PCA are usually selected to explain a combined variation of over 80% for subsequent analysis. In short, PCA reduces the dimension of the dataset and finds the variables that can explain most of the dataset.

A.5.2 Independent Component Analysis (ICA)

Independent Component Analysis (ICA) separates the high-dimensional, multivariate signals into independent, non-Gaussian components. ICA assumes the original signal is a linear combination of the independent components and then estimates those components. In short, ICA breaks down signals into different underlying independent components. In fMRI studies, this usually means breaking down the overall signals from the brain into individual collections of voxels (sub-networks).

B Appendix: Selected Functional Networks

B.1 Blind Lady Functional Networks

atlas	network_id	regions
aicha	12	G_Parietal_Sup-2-R,G_Parietal_Sup-3-R,G_Parieta...
aicha	16	S_Intraparietal-3-L,G_Precuneus-9-L
aicha	26	S_Cingulate-2-L,S_Cingulate-3-L,S_Cingulate-4-L
aicha	27	S_Cingulate-6-R,S_Cingulate-7-L
aicha	28	G_Cingulum_Post-2-L,G_Precuneus-2-R,G_Precuneus...
aicha	29	G_Angular-3-L,G_Occipital_Mid-2-R,G_Occipital_M... table
aicha	30	G_Precuneus-7-R,G_Precuneus-8-L
harvard	2	IFG oper I ,aMTG I ,pMTG I , toMTG I ,alTG I ,AG...
harvard	6	IFG oper r,aSMG r ,pSMG r,AG r,CO r ,PO r , P...
harvard	7	sLOC r , sLOC I ,PC ,Precuneous

The table above shows the Functional Networks identified based on the resting condition.

B.2 Leadership Experiment Functional Networks

atlas	network_id	regions
aicha	0	G_Frontal_Sup-1-R,S_Sup_Frontal-3-R,G_Frontal_M...
aicha	10	S_Rolando-2-R,S_Rolando-3-L,S_Cingulate-3-R
aicha	16	S_Sup_Temporal-2-L,G_Fusiform-6-R
aicha	18	S_Sup_Temporal-4-L,S_Cingulate-1-R
aicha	24	S_Cingulate-3-L,N_Thalamus-5-R
aicha	25	S_Cingulate-6-L,G_Cingulum_Post-1-L
aicha	26	S_Cingulate-7-L,G_Hippocampus-2-L
aicha	28	S_Parietooccipital-4-R,G_ParaHippocampal-5-R
harvard	0	FP r ,FP l ,SFG r ,IFG oper r ,pITG l ,PostCG l...
harvard	1	IC l ,MidFG l ,PaCiG r ,AC ,aTFusC r ,FO l ,PO ...
harvard	4	TP r ,TP l ,iLOC l ,Hippocampus r
harvard	9	SPL r ,iLOC r ,TOFusC r ,Cereb6 l
harvard	11	AG r ,sLOC r ,aPaHC r ,aTFusC l ,Thalamus r,Amy...
harvard	12	tolTG l ,pPaHC r ,CO r ,Cereb3 l ,Cereb3 r ,Cer...
harvard	13	pPaHC l ,Ver9
harvard	14	OFusG l ,FO r ,Brain-Stem,Cereb8 l ,Cereb9 l ,C...
harvard	17	LG r ,OFusG r ,Cereb1 r ,Cereb6 r

The table above shows the Functional Networks identified based on the positive conditions at the group level.

atlas	network_id	regions
aicha	1	S_Sup_Frontal-1-L,G_Frontal_Mid_Orb-1-L,S_Prece...
aicha	5	S_Inf_Frontal-2-R,G_ParaHippocampal-2-L,G_ParaH...
aicha	6	G_Frontal_Sup-1-L,G_Frontal_Sup-1-R,S_Inf_Front...
aicha	7	S_Intraparietal-2-L,S_Intraoccipital-1-L,G_Occi...
aicha	10	nom_l,S_Sup_Frontal-2-L,S_Sup_Frontal-2-R,S_Sup...
aicha	11	S_Inf_Frontal-1-L,S_Orbital-2-R,G_Parietal_Sup-...
aicha	12	S_Rolando-1-L,S_Cingulate-6-L
aicha	14	S_Rolando-2-L,S_Postcentral-1-L,S_Cingulate-7-L...
aicha	16	S_Sup_Frontal-3-R,S_Sup_Frontal-4-R,S_Sup_Front...
aicha	17	S_Sup_Frontal-4-L,G_Frontal_Inf_Orb-2-R,G_Parie...
aicha	18	G_Frontal_Mid_Orb-2-L,G_Parietal_Sup-1-R,G_Pari...
aicha	19	G_Parietal_Sup-2-R,G_Supramarginal-1-L,G_SupraM...
aicha	20	G_Supramarginal-1-R,S_Cingulate-1-R
aicha	21	G_Frontal_Sup-3-R,G_Frontal_Mid-1-L,S_Olfactory...
aicha	22	S_Orbital-1-L,S_Orbital-2-L,S_Precentral-6-L,S_...
aicha	24	S_Sup_Frontal-1-R,S_Sup_Frontal-6-R,G_SupraMarg...
aicha	25	G_Occipital_Mid-2-R,G_Hippocampus-2-L
aicha	27	S_Orbital-1-R,G_Parietal_Sup-4-R,G_SupraMargina...
aicha	32	G_Lingual-2-L,G_Fusiform-7-R
aicha	33	G_ParaHippocampal-1-R,N_Thalamus-9-L
aicha	34	G_Fusiform-3-R,G_Fusiform-7-L
harvard	0	FP r ,FP l ,SFG r ,SFG l ,MidFG r ,MidFG l ,pST...
harvard	3	TP l ,MedFC ,PC ,Cereb1 r ,Cereb2 r
harvard	4	pMTG r ,aITG r ,AG l ,HG r ,SCC l ,Caudate r
harvard	7	IFG oper r ,SPL r ,sLOC r ,sLOC l ,ICC r ,ICC l...
harvard	9	TOFusC r ,OP r ,OP l ,Hippocampus r,Cereb7 l

The table above shows the Functional Networks identified based on the negative conditions at the group level.

B.3 Music Experiment Functional Networks

atlas	network_id	regions
aicha	0	G Frontal Sup-1-R.G Frontal Sup-2-L.G Frontal S...
aicha	2	S^{-}Sup Frontal-3-R,S Sup Frōntal-4-R, G $^{-}$Frontal M ...
aicha	4	S Postcentral-3-R,G Parietal Sup-1-L,G Parietal...
aicha	7	G^{-}Angular-1-L,G Anqular-2-L,G Precunēus-8-L,S P...
aicha	8	G^{-}Angular-1-R,G Angular-3-R, S^{-}Intraparietal-1-R...
aicha	9	G^{-}Angular-2-R, G^{-}Occipital Mid-3- R
aicha	10	G-Angular-3-L,S Sup Temporal-5-L,G Precuneus-2-...
aicha	16	S Intraoccipital-1-R.G Occipital Pole-1-L.G Occ...
aicha	21	G^{-}Frontal Med Orb-1-R,G Frontal Med Orb-2-L
aicha	24	S Rolando-3-R,S Cingulate-6-R,S Cingulate-7-L,G...
aicha	25	G- Paracentral Lobule-4-R,G Precuneus-1-L,G Prec...
aicha	26	G Precuneus-2-R,G Precuneus-6-R,G Precunèss-7-R
aicha	28	G_Calcarine-3-R,G_ParaHippocampal-4-R
aicha	31	G'ParaHippocampāl-3-R.G ParaHippocampal-4-L
harvard	0	FP r.MidFG r
harvard	2	SFG r,SFG l,MidFG l
harvard	8	toMTG $r, pSMGr, AGr, sLOCr$
harvard	12	PC Precuneous

The table above shows the Functional Networks identified based on the resting condition.

B.4 Random Item Generation Functional Networks

atlas	network_id	regions
aicha	0	G_Frontal_Sup-1-R,G_Frontal_Sup-2-L,S_Sup_Front...
aicha	2	G_Frontal_Mid-4-L,G_Frontal_Mid-5-L
aicha	6	S_Rolando-2-R,S_Rolando-3-R,S_Rolando-4-L,S_Pos...
aicha	9	S_Precentral-6-R,S_Rolando-1-L,S_Rolando-3-L,S_...
aicha	19	S_Cingulate-5-R,_Cingulate-6-L
aicha	20	G_Supp_Motor_Area-3-R,S_Cingulate-1-L,S_Cingula...
aicha	23	G_Cingulum_Post-1-R,G_Cingulum_Post-2-L,G_Parac...
aicha	24	G_Precuneus-3-R,G_Precuneus-4-L
aicha	25	G_Parietal_Sup-4-R,G_Parietal_Sup-5-L,G_Precune...
aicha	26	G_ParaHippocampal-3-R,G_ParaHippocampal-4-L
aicha	27	N_Amygdala-1-R,N_Caudate-1-R
aicha	28	N_Caudate-3-R,N_Caudate-5-R
aicha	29	N_Caudate-4-L,N_Caudate-4-R,N_Caudate-5-L,N_Cau... table
harvard	0	FP r , FP l ,SFG r,SFG l ,MidFG r,MidFG l,pSM...
harvard	6	pSMG l ,AG l
harvard	12	PC ,Precuneous
harvard	15	Thalamus r,Thalamus l
harvard	16	Caudate r,Caudate l

The table above above shows the Functional Networks identified based on the resting condition at the group level.

References

Abraham, A., Milham, M. P., Di Martino, A., Craddock, R. C., Samaras, D., Thirion, B., and Varoquaux, G. (2017). “Deriving reproducible biomarkers from multi-site resting-state data: An Autism-based example”. *NeuroImage* 147, 736–745.

Abrams, R. A. and Dobkin, R. S. (1994). “Inhibition of return: effects of attentional cuing on eye movement latencies.” *Journal of Experimental Psychology: Human Perception and Performance* 20.3, 467.

Aggarwal, C. C., Hinneburg, A., and Keim, D. A. (2001). “On the surprising behavior of distance metrics in high dimensional space”. *International conference on database theory*. Springer, 420–434.

Ahlheim, C. and Love, B. C. (2018). “Estimating the functional dimensionality of neural representations”. *NeuroImage* 179, 51–62.

Allen, E. A., Damaraju, E., Plis, S. M., Erhardt, E. B., Eichele, T., and Calhoun, V. D. (2014). “Tracking whole-brain connectivity dynamics in the resting state”. *Cerebral cortex* 24.3, 663–676.

An, S., Han, X., Wu, B., Shi, Z., Marks, M., Wang, S., Wu, X., and Han, S. (2018). “Neural activation in response to the two sides of emotion”. *Neuroscience letters* 684, 140–144.

Andrews-Hanna, J. R. (2012). “The brain’s default network and its adaptive role in internal mentation”. *The Neuroscientist* 18.3, 251–270.

Andrews-Hanna, J. R., Smallwood, J., and Spreng, R. N. (2014). “The default network and self-generated thought: Component processes, dynamic control, and clinical relevance”. *Annals of the new York Academy of Sciences* 1316.1, 29–52.

Arielli, E. and Manovich, L. (2022). “Ai-Aesthetics and the Anthropocentric Myth of Creativity”. *NODES* 1.19-20.

Avram, M., Gutyrchik, E., Bao, Y., Pöppel, E., Reiser, M., and Blautzik, J. (2013). “Neurofunctional correlates of esthetic and moral judgments”. *Neuroscience Letters* 534, 128–132. DOI: https://doi.org/10.1016/j.neulet.2012.11.053.

Babaeeghazvini, P., Rueda-Delgado, L. M., Gooijers, J., Swinnen, S. P., and Daffertshofer, A. (2021). “Brain Structural and Functional Connectivity: A Review of Combined Works of Diffusion Magnetic Resonance Imaging and Electro-Encephalography”. *Frontiers in human neuroscience*, 585.

Bauer, P. J. and Dugan, J. A. (2020). “Chapter 18 - Memory development”. *Neural Circuit and Cognitive Development (Second Edition)*. Ed. by J. Rubenstein, P. Rakic, B. Chen, and K. Y. Kwan. Second Edition. Academic Press, 395–412. ISBN: 978-0-12-814411-4. DOI: https://doi.org/10.1016/B978-0-12-814411-4.00018-4.

Behrens, T. E. and Sporns, O. (2012). “Human connectomics”. *Current opinion in neurobiology* 22.1, 144–153.

Biesbroek, J. M., Weaver, N. A., and Biessels, G. J. (2017). “Lesion location and cognitive impact of cerebral small vessel disease”. *Clinical Science* 131.8, 715–728.

Bird, C. M. and Burgess, N. (2008). “The hippocampus and memory: insights from spatial processing”. *Nature Reviews Neuroscience* 9.3, 182–194. DOI: 10.1038/nrn2335.

Bobadilla-Suarez, S., Ahlheim, C., Mehrotra, A., Panos, A., and Love, B. C. (2020). “Measures of Neural Similarity”. *Computational Brain and Behavior* 3.4, 369–383. DOI: 10.1007/s42113-019-00068-5.

Boisgueheneuc, F. d., Levy, R., Volle, E., Seassau, M., Duffau, H., Kinkingnehun, S., Samson, Y., Zhang, S., and Dubois, B. (2006). “Functions of the left superior frontal gyrus in humans: a lesion study”. *Brain* 129.12, 3315–3328.

Braunlich, K. and Love, B. C. (2019). “Occipitotemporal representations reflect individual differences in conceptual knowledge.” *Journal of Experimental Psychology: General* 148.7, 1192.

Buckner, R. L., Andrews-Hanna, J. R., and Schacter, D. L. (2008). “The brain’s default network: anatomy, function, and relevance to disease”. *Annals of the New York Academy of Sciences* 1124.1, 1–38.

Bullmore, E. and Sporns, O. (2009). “Complex brain networks: graph theoretical analysis of structural and functional systems”. *Nature Reviews Neuroscience* 10.3, 186–198. DOI: 10.1038/nrn2575.

Cabeza, R. and St Jacques, P. (2007). “Functional neuroimaging of autobiographical memory”. *Trends in cognitive sciences* 11.5, 219–227.

Casagrande, M., & Mereu, S. (2009). Unconsciously perceived arrows yield an endogenous, automatic orienting of attention. In Proceedings of the Annual Meeting of the Cognitive Science Society (Vol. 31, No. 31).

Chen, H.-Y., Gilmore, A. W., Nelson, S. M., and McDermott, K. B. (2017). “Are There Multiple Kinds of Episodic Memory? An fMRI Investigation Comparing Autobiographical and Recognition Memory Tasks”. *Journal of Neuroscience* 37.10, 2764–2775. DOI: 10.1523/JNEUROSCI.1534-16.2017.

Chen, W.-L., Wagner, J., Heugel, N., Sugar, J., Lee, Y.-W., Conant, L., Malloy, M., Heffernan, J., Quirk, B., Zinos, A., Beardsley, S. A., Prost, R., and Whelan, H. T. (2020). “Functional Near-Infrared Spectroscopy and Its Clinical Application in the Field of Neuroscience: Advances and Future Directions”. *Frontiers in Neuroscience* 14, 724. DOI: 10.3389/fnins.2020.00724.

Chen, Y., Wang, S., Hilgetag, C. C., and Zhou, C. (2013). “Trade-off between multiple constraints enables simultaneous formation of modules and hubs in neural systems”. *PLoS computational biology* 9.3, e1002937.

Conover, W. J. (1999). *Practical nonparametric statistics*. Vol. 350. john wiley & sons.

Conway, M. A. and Pleydell-Pearce, C. W. (2000). “The construction of autobiographical memories in the self-memory system.” *Psychological review* 107.2, 261.

Crossley, N. A., Mechelli, A., Vértes, P. E., Winton-Brown, T. T., Patel, A. X., Ginestet, C. E., McGuire, P., and Bullmore, E. T. (2013). “Cognitive relevance of the community structure of the human brain functional coactivation network”. *Proceedings of the National Academy of Sciences* 110.28, 11583– 11588.

Cummings, J. L., Mega, M., Gray, K., Rosenberg-Thompson, S., Carusi, D. A., and Gornbein, J. (1994). “The Neuropsychiatric Inventory: comprehensive assessment of psychopathology in dementia”. *Neurology* 44.12, 2308–2308.

D’Argembeau, A., Comblain, C., and Van der Linden, M. (2003). “Phenomenal characteristics of autobiographical memories for positive, negative, and neutral events”. *Applied Cognitive Psychology: The Official Journal of the Society for Applied Research in Memory and Cognition* 17.3, 281–294.

D’Argembeau, A. and Van der Linden, M. (2008). “Remembering pride and shame: Self-enhancement and the phenomenology of autobiographical memory”. *Memory* 16.5, 538–547.

Datar, M., Gionis, A., Indyk, P., and Motwani, R. (2002). “Maintaining stream statistics over sliding windows”. *SIAM journal on computing* 31.6, 1794–1813.

De Boer, D., Johnston, P., Kerr, G., Meinzer, M., and Cleeremans, A. (2020). “A causal role for the right angular gyrus in self-location mediated perspective taking”. *Scientific reports* 10.1, 1–10.

De Puy, W. H. (1879). *The People’s Cyclopedia of Universal Knowledge: With Numerous Appendixes Invaluable for Reference in All Departments of Industrial Life. The Whole Brought Down to the Year 1883. With the Pronunciation and Orthography Conformed to Webster’s Unabridged Dictionary. Illustrated with Numerous Colored Maps and Over Five Thousand Engravings*. Vol. 1. Jones Brothers.

Deffieux, T., Demene, C., Pernot, M., and Tanter, M. (2018). “Functional ultrasound neuroimaging: a review of the preclinical and clinical state of the art”. *Current Opinion in Neurobiology* 50, 128–135. DOI: https://doi.org/10.1016/j.conb.2018.02.001.

Dewalle, A., Betrouni, N., Steinling, M., Vermandel, M., Rousseau, J., and Vasseur, C. (2007). “Comparison between shifted Spearman rank correlation test and SPM in fMRI”. *2007 29th Annual International Conference of the IEEE Engineering in Medicine and Biology Society*, 3400–3403. DOI: 10.1109/IEMBS.2007.4353061.

Diedrichsen, J. and Kriegeskorte, N. (2017). “Representational models: A common framework for understanding encoding, pattern-component, and representational-similarity analysis”. *PLoS computational biology* 13.4, e1005508.

Dimsdale-Zucker, H. R. and Ranganath, C. (2018). “Chapter 27 - Representational Similarity Analyses: A Practical Guide for Functional MRI Applications”. Handbook of Behavioral Neuroscience 28. Ed. by D. Manahan-Vaughan, 509–525. DOI: https://doi.org/10.1016/B978-0-12-812028-6.00027-6.

Dolcos, F., Katsumi, Y., Weymar, M., Moore, M., Tsukiura, T., and Dolcos, S. (2017). “Emerging directions in emotional episodic memory”. *Frontiers in Psychology* 8, 1867.

Dugué, L., Merriam, E. P., Heeger, D. J., and Carrasco, M. (2020). “Differential impact of endogenous and exogenous attention on activity in human visual cortex”. *Scientific reports* 10.1, 1–16.

Dundoo, S. D. (2015). *‘Astu’, a state of acceptance.* The Hindu

Ehlers, A., Maercker, A., and Boos, A. (2000). “Posttraumatic stress disorder following political imprisonment: the role of mental defeat, alienation, and perceived permanent change.” *Journal of abnormal psychology* 109.1, 45.

Eickhoff, S. and Müller, V. (2015). “Functional Connectivity”. *Brain Mapping*. Ed. by A. W. Toga. Waltham: Academic Press, 187–201. ISBN: 978-0-12-397316-0. DOI: https://doi.org/10.1016/B978-0-12-397025-1.00212-8.

Einstein, G. O., Mullet, H. G., and Harrison, T. L. (2012). “The testing effect: Illustrating a fundamental concept and changing study strategies”. *Teaching of Psychology* 39.3, 190–193.

Ekhtiari, H., Nasseri, P., Yavari, F., Mokri, A., and Monterosso, J. (2016). “Chapter 7 - Neuroscience of drug craving for addiction medicine: From circuits to therapies”. *Neuroscience for Addiction Medicine: From Prevention to Rehabilitation - Constructs and Drugs*. Ed. by H. Ekhtiari and M. Paulus. Vol. 223. Progress in Brain Research. Elsevier, 115–141. DOI:

https://doi.org/10.1016/bs.pbr.2015.10.002.

Eklund, A., Nichols, T., and Knutsson, H. (2015). “Can parametric statistical methods be trusted for fMRI based group studies?” *arXiv preprint arXiv:1511.01863*.

Farahani, F. V., Karwowski, W., and Lighthall, N. R. (2019). “Application of graph theory for identifying connectivity patterns in human brain networks: a systematic review”. *frontiers in Neuroscience* 13, 585.

Farnsworth, B. (2019). *EEG vs. MRI vs. fMRI – What are the Differences?* https://imotions.com/blog/eeg-vs-mri-vs-fmri-differences/

Felleman, D. J. and Van Essen, D. C. (1991). “Distributed hierarchical processing in the primate cerebral cortex.” *Cerebral cortex (New York, NY: 1991)* 1.1, 1–47.

Fontes, R., Ribeiro, J., Gupta, D. S., Machado, D., Lopes-Júnior, F., Magalhães, F., Bastos, V. H., Rocha, K., Marinho, V., Lima, G., et al. (2016). “Time perception mechanisms at central nervous system”. *Neurology international* 8.1, 5939.

Fox, M. D., Snyder, A. Z., Vincent, J. L., Corbetta, M., Van Essen, D. C., and Raichle, M. E. (2005). “The human brain is intrinsically organized into dynamic, anticorrelated functional networks”. *Proceedings of the National Academy of Sciences* 102.27, 9673–9678.

Franklin, S., Baars, B. J., Ramamurthy, U., and Ventura, M. (2005). “The role of consciousness in memory”. *http://ccrg. cs. memphis. edu/assets/papers/wrcm-bmm. pdf* 1.

Friedland, R. P. and Iadecola, C. (1991). “Roy and Sherrington (1890)”. *Neurology* 41, 10–10.

Friston, K. J. (1994). “Functional and effective connectivity in neuroimaging: a synthesis”. *Human brain mapping* 2.1-2, 56–78.

Friston, K. J. (2011). “Functional and effective connectivity: a review”. *Brain connectivity* 1.1, 13–36.

Fulcher, B. D., Little, M. A., and Jones, N. S. (2013). “Highly comparative time-series analysis: the empirical structure of time series and their methods”. *Journal of the Royal Society Interface* 10.83, 20130048.

Gainotti, G. (2019). “The role of the right hemisphere in emotional and behavioral disorders of patients with frontotemporal lobar degeneration: an updated review”. *Frontiers in aging neuroscience* 11, 55.

Galdi, P., Fratello, M., Trojsi, F., Russo, A., Tedeschi, G., Tagliaferri, R., and Esposito, F. (2019). “Stochastic rank aggregation for the identification of functional neuromarkers”. *Neuroinformatics* 17.4, 479–496.

Glover, G. H. (2011). “Overview of functional magnetic resonance imaging”. *Neurosurgery Clinics* 22.2, 133–139.

Gourley, S. L., Zimmermann, K. S., Allen, A. G., and Taylor, J. R. (2016). “The medial orbitofrontal cortex regulates sensitivity to outcome value”. *Journal of Neuroscience* 36.16, 4600–4613.

Greicius, M. D., Krasnow, B., Reiss, A. L., and Menon, V. (2003). “Functional connectivity in the resting brain: A network analysis of the default mode hypothesis”. *Proceedings of the National Academy of Sciences of the United States of America* 100.1, 253–258. DOI: 10.1073/pnas.0135058100.

Hannan, K. L., Wood, S. J., Yung, A. R., Velakoulis, D., Phillips, L. J., Soulsby, B., Berger, G., McGorry, P. D., and Pantelis, C. (2010). “Caudate nucleus volume in individuals at ultra-high risk of psychosis: a cross-sectional magnetic resonance imaging study”. *Psychiatry Research: Neuroimaging* 182.3, 223–230.

Hassabis, D. and Maguire, E. A. (2007). “Deconstructing episodic memory with construction”. *Trends in cognitive sciences* 11.7, 299–306.

Hausfeld, L., Valente, G., and Formisano, E. (2014). “Multiclass fMRI data decoding and visualization using supervised self-organizing maps”. *NeuroImage* 96, 54–66.

Havlicek, M., Ivanov, D., Roebroeck, A., and Uludağ, K. (2017). “Determining excitatory and inhibitory neuronal activity from multimodal fMRI data using a generative hemodynamic model”. *Frontiers in neuroscience* 11, 616.

Havlicek, M., Roebroeck, A., Friston, K., Gardumi, A., Ivanov, D., and Uludag, K. (2015). “Physiologically informed dynamic causal modeling of fMRI data”. *Neuroimage* 122, 355–372.

Henriques, T., Ribeiro, M., Teixeira, A., Castro, L., Antunes, L., and Costa-Santos, C. (2020). “Nonlinear methods most applied to heart-rate time series: a review”. *Entropy* 22.3, 309.

Al-Hiyali, M. I., Yahya, N., Faye, I., Khan, Z., and Alsaih, K. (2021). “Classification of BOLD FMRI signals using wavelet transform and transfer learning for detection of autism spectrum disorder”. *2020 IEEE-EMBS Conference on Biomedical Engineering and Sciences (IECBES)*. IEEE, 94–98.

Hobson, J. A., Pace-Schott, E. F., and Stickgold, R. (2000). “Dreaming and the brain: toward a cognitive neuroscience of conscious states”. *Behavioral and brain sciences* 23.6, 793–842.

Hodgkin, A. L. and Huxley, A. F. (1952). “A quantitative description of membrane current and its application to conduction and excitation in nerve”. *The Journal of Physiology* 117.4, 500–544. DOI: https://doi.org/10.1113/jphysiol.1952.sp004764.

Honey, C. J., Thivierge, J.-P., and Sporns, O. (2010). “Can structure predict function in the human brain?” *Neuroimage* 52.3, 766–776.
Hopfield, J. J. (1982). “Neural networks and physical systems with emergent collective computational abilities.” *Proceedings of the national academy of sciences* 79.8, 2554–2558.
Hu, S., Ide, J. S., Zhang, S., and Chiang-shan, R. L. (2016). “The right superior frontal gyrus and individual variation in proactive control of impulsive response”. *Journal of Neuroscience* 36.50, 12688–12696.
Hubel, D. H. and Wiesel, T. N. (1959). “Receptive fields of single neurones in the cat’s striate cortex”. *The Journal of physiology* 148.3, 574.
Hutchison, R. M., Womelsdorf, T., Allen, E. A., Bandettini, P. A., Calhoun, V. D., Corbetta, M., Della Penna, S., Duyn, J. H., Glover, G. H., Gonzalez-Castillo, J., et al. (2013). “Dynamic functional connectivity: promise, issues, and interpretations”. *Neuroimage* 80, 360–378.
Inman, C. S., James, G. A., Vytal, K., and Hamann, S. (2018). “Dynamic changes in large-scale functional network organization during autobiographical memory retrieval”. *Neuropsychologia* 110, 208–224.
Ivry, R. B. and Spencer, R. M. (2004). “The neural representation of time”. *Current opinion in neurobiology* 14.2, 225–232.
Jahanshahi, M., Dirnberger, G., Fuller, R., and Frith, C. D. (2000). “The role of the dorsolateral prefrontal cortex in random number generation: a study with positron emission tomography”. *Neuroimage* 12.6, 713–725.
Jäncke, L. (2008). “Music, memory and emotion”. *Journal of biology* 7.6, 1–5.
Jeong, W., Chung, C. K., and Kim, J. S. (2015). “Episodic memory in aspects of large-scale brain networks”. *Frontiers in human neuroscience* 9, 454.
Jeunehomme, O. and D’Argembeau, A. (2019). “The time to remember: Temporal compression and duration judgements in memory for real-life events”. *Quarterly Journal of Experimental Psychology* 72.4, 930–942.
Johnson, K. (June 2022). *LAMDA and the sentient ai trap*.
Joliot, M., Jobard, G., Naveau, M., Delcroix, N., Petit, L., Zago, L., Crivello, F., Mellet, E., Mazoyer, B., and Tzourio-Mazoyer, N. (2015). “AICHA: An atlas of intrinsic connectivity of homotopic areas”. *Journal of Neuroscience Methods* 254, 46–59. DOI: https://doi.org/10.1016/j.jneumeth.2015.07.013.
Jones, O. P., Alfaro-Almagro, F., and Jbabdi, S. (2018). “An empirical, 21st century evaluation of phrenology”. *bioRxiv*. DOI: 10.1101/243089.
Juslin, P. N., Liljeström, S., Västfjäll, D., and Lundqvist, L.-O. (2010). “How does music evoke emotions? Exploring the underlying mechanisms.”
Kandel, E. R., Schwartz, J. H., Jessell, T. M., Siegelbaum, S. A., and Hudspeth, A. J. (Dec. 2000). *Principles of neural science, fifth edition*. 5th ed. New York, NY: McGraw-Hill Medical.
Kauppi, J.-P., Pajula, J., Niemi, J., Hari, R., and Tohka, J. (2017). “Functional brain segmentation using inter-subject correlation in fMRI”. *Human Brain Mapping* 38.5, 2643–2665.
Keightley, M. L., Winocur, G., Graham, S. J., Mayberg, H. S., Hevenor, S. J., and Grady, C. L. (2003). “An fMRI study investigating cognitive modulation of brain regions associated with emotional processing of visual stimuli”. *Neuropsychologia* 41.5, 585–596. DOI: https://doi.org/10.1016/S0028- 3932(02)00199-9.
Kensinger, E. A. (2009). “Remembering the details: Effects of emotion”. *Emotion review* 1.2, 99–113.
Kim, B., Andrews-Hanna, J. R., Han, J., Lee, E., and Woo, C.-W. (2021). “When self comes to a wandering mind: Brain representations and dynamics of self-generated concepts in spontaneous thought”. *bioRxiv*.
Knockaert, V., Geerardyn, F., and Van de Vijver, G. (2002). “Anticipation, Memory and Attention in the Early Works of Freud” ().
Kriegeskorte, N. (2015). “Deep neural networks: a new framework for modelling biological vision and brain information processing”. *biorxiv*, 029876.
Kriegeskorte, N. and Douglas, P. K. (2018). “Cognitive computational neuroscience”. *Nature Neuroscience* 21.9, 1148–1160. DOI: 10.1038/s41593-018-0210-5.
Kriegeskorte, N., Goebel, R., and Bandettini, P. (2006). “Information-based functional brain mapping”. *Proceedings of the National Academy of Sciences* 103.10, 3863–3868.
Kriegeskorte, N., Mur, M., and Bandettini, P. (2008). “Representational similarity analysis - connecting the branches of systems neuroscience”. *Frontiers in Systems Neuroscience* 2.NOV, 1–28. DOI: 10.3389/neuro.06.004.2008.
Kriegeskorte, N., Mur, M., Ruff, D. A., Kiani, R., Bodurka, J., Esteky, H., Tanaka, K., and Bandettini, P. A. (2008). “Matching categorical object representations in inferior temporal cortex of man and monkey”. *Neuron* 60.6, 1126–1141.
Kuyken, W. and Howell, R. (2006). “Facets of autobiographical memory in adolescents with major depressive disorder and never-depressed controls”. *Cognition and Emotion* 20.3-4, 466–487.

Lawrence, R. M., Bridgeford, E. W., Myers, P. E., Arvapalli, G. C., Ramachandran, S. C., Pisner, D. A., Frank, P. F., Lemmer, A. D., Nikolaidis, A., and Vogelstein, J. T. (2021). “Standardizing human brain parcellations”. *Scientific data* 8.1, 1–9.

Ledoit, O. and Wolf, M. (2004). “A well-conditioned estimator for large-dimensional covariance matrices”. *Journal of Multivariate Analysis* 88.2, 365–411. DOI: https://doi.org/10.1016/S0047-259X(03)00096-4.

Lettvin, J. Y., Maturana, H. R., McCulloch, W. S., and Pitts, W. H. (1959). “What the frog’s eye tells the frog’s brain”. *Proceedings of the IRE* 47.11, 1940–1951.

Li X, Pöppel E, Bao Y. Nonparametric extraction of oscillations in short time series. Psych J. 2018 Dec;7(4):225-226. doi: 10.1002/pchj.221. Epub 2018 Jul 20. PMID: 30028907.

Liang, X., Zou, Q., He, Y., and Yang, Y. (2016). “Topologically reorganized connectivity architecture of default-mode, executive-control, and salience networks across working memory task loads”. *Cerebral cortex* 26.4, 1501–1511.

Liu, Y., Liu, G., Wei, D., Li, Q., Yuan, G., Wu, S., Wang, G., and Zhao, X. (2018). “Effects of musical tempo on musicians’ and non-musicians’ emotional experience when listening to music”. *Frontiers in Psychology* 9, 2118.

Logothetis, N. K. (2008). “What we can do and what we cannot do with fMRI”. *Nature* 453.7197, 869–878. DOI: 10.1038/nature06976.

Lowe, M. (1936). “The application of the balance to the study of the bodily changes occurring during periods of volitional activity”. *British Journal of Psychology* 26.3, 245.

Lutz, A., Slagter, H. A., Dunne, J. D., and Davidson, R. J. (2008). “Attention regulation and monitoring in meditation”. *Trends in Cognitive Sciences* 12.4, 163–169. DOI: 10.1016/j.tics.2008.01.005.

Mahalanobis, P. (1936). “”On the Generalised Distance in Statistics””. *Proceedings of the National Institute of Science of India*. DOI: 10.1007/s13171-019-00164-5.

Mahmoudi, A., Takerkart, S., Regragui, F., Boussaoud, D., and Brovelli, A. (2012). “Multivoxel pattern analysis for fMRI data: A review”. *Computational and Mathematical Methods in Medicine* 2012.June 2014. DOI: 10.1155/2012/961257.

Măliia, M.-D., Donos, C., Barborica, A., Popa, I., Ciurea, J., Cinatti, S., and Mındruţă, I. (2018). “Functional mapping and effective connectivity of the human operculum”. *Cortex* 109, 303–321.

Mann, H. B. and Whitney, D. R. (1947). “On a test of whether one of two random variables is stochastically larger than the other”. *The annals of mathematical statistics*, 50–60.

Massot-Tarrús, A., White, K., and Mirsattari, S. M. (2019). “Comparing the Wada test and functional MRI for the presurgical evaluation of memory in temporal lobe epilepsy”. *Current neurology and neuroscience reports* 19.6, 1–14.

McDermott, K. B., Szpunar, K. K., and Christ, S. E. (2009). “Laboratory-based and autobiographical retrieval tasks differ substantially in their neural substrates”. *Neuropsychologia* 47.11, 2290–2298.

McKeown, M. J., Hansen, L. K., and Sejnowsk, T. J. (2003). “Independent component analysis of functional MRI: what is signal and what is noise?” *Current opinion in neurobiology* 13.5, 620–629.

McKeown, M. J. and Sejnowski, T. J. (1998). “Independent component analysis of fMRI data: Examining the assumptions”. *Human Brain Mapping* 6.5-6, 368–372.

Medaglia, J. D. (Nov. 2017). “Graph Theoretic Analysis of Resting State Functional MR Imaging”. *Neuroimaging Clinics of North America* 27.4, 593–607. DOI: 10.1016/j.nic.2017.06.008.

Meunier, D., Achard, S., Morcom, A., and Bullmore, E. (2009). “Age-related changes in modular organization of human brain functional networks”. *Neuroimage* 44.3, 715–723.

Miescke, K.-J. and Pöppel, E. (1982). “A nonparametric procedure to detect periods in time series”. *Stochastic Processes and their Applications* 13.3, 319–325. DOI: https://doi.org/10.1016/0304-4149(82)90018-7.

Milgram, S. (1967). “The small world problem”. *Psychology today* 2.1, 60–67. Minsky, M. L. and Papert, S. A. (1988). “Perceptrons: expanded edition”.

Moghimi, P., Dang, A. T., Netoff, T. I., Lim, K. O., and Atluri, G. (2021). “A Review on MR Based Human Brain Parcellation Methods”. *arXiv preprint arXiv:2107.03475*.

Monti, M. M. (2011). “Statistical analysis of fMRI time-series: A critical review of the GLM approach”. *Frontiers in Human Neuroscience* 5.MARCH, 1–13. DOI: 10.3389/fnhum.2011.00028.

Nakao, T., Sanematsu, H., Yoshiura, T., Togao, O., Murayama, K., Tomita, M., Masuda, Y., and Kanba, S. (2011). “fMRI of patients with social anxiety disorder during a social situation task”. *Neuroscience Research* 69.1, 67–72. DOI: https://doi.org/10.1016/j.neures.2010.09.008.

Newman, M. E. and Girvan, M. (2004). “Finding and evaluating community structure in networks”. *Physical review E* 69.2, 026113.

Nichols, T. E. and Holmes, A. P. (2001). “Nonparametric Permutation Tests For Functional Neuroimaging: A Primer with Examples”. *Human Brain Mapping* 25.August 1999, 1–25.

Nikolaou, F., Orphanidou, C., Papakyriakou, P., Murphy, K., Wise, R. G., and Mitsis, G. D. (2016). “Spontaneous physiological variability modulates dynamic functional connectivity in resting-state functional magnetic resonance imaging”. *Philosophical Transactions of the Royal Society A: Mathematical, Physical and Engineering Sciences* 374.2067, 20150183.

Nili, H., Wingfield, C., Walther, A., Su, L., Marslen-Wilson, W., and Kriegeskorte, N. (2014). “A toolbox for representational similarity analysis”. *PLoS computational biology* 10.4, e1003553.

O’Sullivan, S., Jeanquartier, F., Jean-Quartier, C., Holzinger, A., Shiebler, D., Moon, P., and Angione, C. (2020). “Developments in AI and Machine Learning for Neuroimaging”. *Artificial Intelligence and Machine Learning for Digital Pathology*, 307–320.

Ogawa, S., Lee, T.-M., Kay, A. R., and Tank, D. W. (1990). “Brain magnetic resonance imaging with contrast dependent on blood oxygenation.” *proceedings of the National Academy of Sciences* 87.24, 9868–9872.

Patihis, L., Frenda, S. J., LePort, A. K., Petersen, N., Nichols, R. M., Stark, C. E., McGaugh, J. L., and Loftus, E. F. (2013). “False memories in highly superior autobiographical memory individuals”. *Proceedings of the National Academy of Sciences* 110.52, 20947–20952.

Pauling L, Coryell CD. The Magnetic Properties and Structure of Hemoglobin, Oxyhemoglobin and Carbonmonoxyhemoglobin. Proc Natl Acad Sci U S A. 1936 Apr;22(4):210-6. doi: 10.1073/pnas.22.4.210. PMID: 16577697; PMCID: PMC1076743.

Pereira, F. (2009). “Machine learning classifiers and fMRI: a tutorial overview”. *NeuroImage* 28.48, 1947–1953. DOI: 10.1016/j.neuroimage.2008.11.007.Machine.

Persaud, N. (2005). “Humans can consciously generate random number sequences: A possible test for artificial intelligence”. *Medical hypotheses* 65.2, 211–214.

Petrican, R., Palombo, D. J., Sheldon, S., and Levine, B. (2020). “The neural dynamics of individual differences in episodic autobiographical memory”. *Eneuro* 7.2.

Pillet, I., Op de Beeck, H., and Lee Masson, H. (2020). “A Comparison of Functional Networks Derived From Representational Similarity, Functional Connectivity, and Univariate Analyses”. *Frontiers in Neuroscience* 13.January, 1–14. DOI: 10.3389/fnins.2019.01348.

Poldrack, R. A. (2007). “Region of interest analysis for fMRI”. *Social cognitive and affective neuroscience* 2.1, 67–70.

Poldrack, R. A., Huckins, G., and Varoquaux, G. (2020). “Establishment of best practices for evidence for prediction: a review”. *JAMA psychiatry* 77.5, 534–540.

Pöppel, E. (Jan. 1970). “Frequency measurement in time series data”. *Life sciences and space research* 8, 234.

Pöppel, E., Avram, M., Bao, Y., Graupmann, V., Gutyrchik, E., Lutz, A., Park, M., Reiser, M., Russell, E., Silveira, S., et al. (2013). “Sensory processing of art as a unique window into cognitive mechanisms: evidence from behavioral experiments and fMRI studies”. *Procedia-Social and Behavioral Sciences* 86, 10–17.

Preti, M. G., Bolton, T. A., and Van De Ville, D. (2017). “The dynamic functional connectome: State-of- the-art and perspectives”. *NeuroImage* 160, 41–54. DOI: https://doi.org/10.1016/j.neuroimage.2016.12.061.

Puzicha, J., Hofmann, T., and Buhmann, J. M. (1997). “Non-parametric similarity measures for unsupervised texture segmentation and image retrieval”. *Proceedings of IEEE Computer Society Conference on Computer Vision and Pattern Recognition*. IEEE, 267–272.

Raichle, M. E., MacLeod, A. M., Snyder, A. Z., Powers, W. J., Gusnard, D. A., and Shulman, G. L. (2001). “A default mode of brain function”. *Proceedings of the National Academy of Sciences of the United States of America* 98.2, 676–682. DOI: 10.1073/pnas.98.2.676.

Rana, M., Varan, A. Q., Davoudi, A., Cohen, R. A., Sitaram, R., and Ebner, N. C. (2016). “Real-time fMRI in neuroscience research and its use in studying the aging brain”. *Frontiers in aging neuroscience* 8, 239.

Rashid, M., Singh, H., and Goyal, V. (2020). “The use of machine learning and deep learning algorithms in functional magnetic resonance imaging—A systematic review”. *Expert Systems* 37.6, e12644.

Rényi, A. et al. (1961). “On measures of entropy and information”. *Proceedings of the fourth Berkeley symposium on mathematical statistics and probability*. Vol. 1. 547-561. Berkeley, California, USA.

Reybrouck, M., Vuust, P., and Brattico, E. (2018). “Brain connectivity networks and the aesthetic experience of music”. *Brain Sciences* 8.6, 107.

Robinson, J. A. (1976). “Sampling autobiographical memory”. *Cognitive psychology* 8.4, 578–595.

Root, J. C., Wong, P. S., and Kinsbourne, M. (2006). “Left hemisphere specialization for response to positive emotional expressions: A divided output methodology.” *Emotion* 6.3, 473.

Rovee-Collier, C. K., Hayne, H., and Colombo, M. (2001). *The development of implicit and explicit memory*. John Benjamins Publishing Company Amsterdam.
Rugg, M. D. and Vilberg, K. L. (2013). "Brain networks underlying episodic memory retrieval". *Current opinion in neurobiology* 23.2, 255–260.
Ruiz, E. V., Nolla, F. C., and Segovia, H. R. (1985). "Is the DTW "distance" really a metric? An algorithm reducing the number of DTW comparisons in isolated word recognition". *Speech Communication* 4.4, 333–344.
Sakoe, H. and Chiba, S. (1978). "Dynamic programming algorithm optimization for spoken word recognition". *IEEE transactions on acoustics, speech, and signal processing* 26.1, 43–49.
Sandrone, S., Bacigaluppi, M., Galloni, M. R., and Martino, G. (2012). "Angelo Mosso (1846–1910)". *Journal of neurology* 259.11, 2513–2514.
Sandrone, S., Bacigaluppi, M., Galloni, M. R., Cappa, S. F., Moro, A., Catani, M., Filippi, M., Monti, M. M., Perani, D., and Martino, G. (May 2013). "Weighing brain activity with the balance: Angelo Mosso's original manuscripts come to light". *Brain* 137.2, 621–633. DOI: 10.1093/brain/awt091.
Scalabrini, A., Esposito, R., and Mucci, C. (2021). "Dreaming the unrepressed unconscious and beyond: repression vs dissociation in the oneiric functioning of severe patients". *Research in Psychotherapy: Psychopathology, Process, and Outcome* 24.2.
Scarapicchia, V., Brown, C., Mayo, C., and Gawryluk, J. R. (2017). "Functional Magnetic Resonance Imaging and Functional Near-Infrared Spectroscopy: Insights from Combined Recording Studies". *Frontiers in Human Neuroscience* 11, 419. DOI: 10.3389/fnhum.2017.00419.
Schwartz, E. L. (1993). *Computational neuroscience*. Mit Press.
Seghier, M. L. (2013). "The angular gyrus: multiple functions and multiple subdivisions". *The Neuroscientist* 19.1, 43–61.
Sejnowski, T. J. (2018). *The deep learning revolution*. London, England: MIT Press.
Shakil, S., Lee, C.-H., and Keilholz, S. D. (2016). "Evaluation of sliding window correlation performance for characterizing dynamic functional connectivity and brain states". *Neuroimage* 133, 111–128.
Sheldon, S., Fenerci, C., and Gurguryan, L. (2019). "A neurocognitive perspective on the forms and functions of autobiographical memory retrieval". *Frontiers in systems neuroscience* 13, 4.
Silveira, S., Fehse, K., Vedder, A., Elvers, K., and Hennig-Fast, K. (2015). "Is it the picture or is it the frame? An fMRI study on the neurobiology of framing effects". *Frontiers in human neuroscience* 9, 528.
Slough, C., Masters, S. C., Hurley, R. A., and Taber, K. H. (2016). "Clinical Positron Emission Tomography (PET) Neuroimaging: Advantages and Limitations as a Diagnostic Tool". *Journal of Neuropsychiatry* 28.2, a4–71. DOI: 10.1176/appi.neuropsych.16030044.
Smith, D. M. and Mizumori, S. J. (2006). "Hippocampal place cells, context, and episodic memory". *Hippocampus* 16.9, 716–729.
Spencer, A. P. and Goodfellow, M. (2022). "Using deep clustering to improve fMRI dynamic functional connectivity analysis". *NeuroImage* 257, 119288. DOI: https://doi.org/10.1016/j.neuroimage.2022.119288.
Sporns, O. (2022). "Graph theory methods: applications in brain networks". *Dialogues in clinical neuroscience*.
Spreng, R. N. (2012). "The fallacy of a "task-negative" network". *Frontiers in psychology* 3, 145.
Squire, L. R. (2009). "The legacy of patient HM for neuroscience". *Neuron* 61.1, 6–9.
Stuss, D. T. and Alexander, M. P. (2000). "Executive functions and the frontal lobes: a conceptual view". *Psychological research* 63.3, 289–298.
Suckling, J., Wink, A. M., Bernard, F. A., Barnes, A., and Bullmore, E. (2008). "Endogenous multifractal brain dynamics are modulated by age, cholinergic blockade and cognitive performance". *Journal of Neuroscience Methods* 174.2, 292–300. DOI: https://doi.org/10.1016/j.jneumeth.2008.06.037.
Sugar, J. and Moser, M.-B. (2019). "Episodic memory: Neuronal codes for what, where, and when". *Hippocampus* 29.12, 1190–1205.
Tanaka, S. and Kirino, E. (2016). "Functional connectivity of the precuneus in female university students with long-term musical training". *Frontiers in human neuroscience* 10, 328.
Taya, F., Souza, J. de, Thakor, N. V., and Bezerianos, A. (2016). "Comparison method for community detection on brain networks from neuroimaging data". *Applied Network Science* 1.1, 1–20.
Thirion, B., Varoquaux, G., Dohmatob, E., and Poline, J.-B. (2014). "Which fMRI clustering gives good brain parcellations?" *Frontiers in neuroscience* 8, 167.
Thome, J., Terpou, B. A., McKinnon, M. C., and Lanius, R. A. (2020). "The neural correlates of trauma- related autobiographical memory in posttraumatic stress disorder: A meta-analysis". *Depression and Anxiety* 37.4, 321–345.
Tilani, J. and Najamuddin, M. (2014). "A Review of Adaptive Bayesian Modeling for Time Series Forecasting". *Journal of Applied Environmental and Biological Sciences* 4, 99–106.

Trimble, M. R. and Cavanna, A. E. (2008). “Chapter 3.7 The role of the precuneus in episodic memory”. *Handbook of Episodic Memory*. Ed. by E. Dere, A. Easton, L. Nadel, and J. P. Huston. Vol. 18. Handbook of Behavioral Neuroscience. Elsevier, 363–377. DOI: https://doi.org/10.1016/S1569- 7339(08)00220-8.Tulving, E. (1972). “Episodic and semantic memory.”

Toichi, M., Sato, W., Uono, S., Sawada, R., Yoshimura, S., Kochiyama, T., & Kubota, Y. (2015). The structural neural substrate of subjective happiness. *Scientific Reports*.

Tulving, E. (2002). “Episodic memory: From mind to brain”. *Annual review of psychology* 53.1, 1–25.

Turner, B. M., Miletić, S., and Forstmann, B. U. (2020). “Deep Neural Networks in Computational Neuroscience”. *NeuroImage* 180, 117–118. DOI: 10.1016/j.neuroimage.2017.12.078.

Turner, R. (2016). “Uses, misuses, new uses and fundamental limitations of magnetic resonance imaging in cognitive science”. *Philosophical Transactions of the Royal Society B: Biological Sciences* 371.1705. DOI: 10.1098/rstb.2015.0349.

Vago, D. R. and Silbersweig, D. A. (2012). “Self-awareness, self-regulation, and self-transcendence (S-ART): a framework for understanding the neurobiological mechanisms of mindfulness”. *Frontiers in human neuroscience* 6, 296.

Vedder, A., Smigielski, L., Gutyrchik, E., Bao, Y., Blautzik, J., Pöppel, E., Zaytseva, Y., and Russell, E. (2015) “Neurofunctional Correlates of Environmental Cognition: An fMRI Study with Images from Episodic Memory”. *PLOS ONE* 10.4, 1–11. DOI: 10.1371/journal.pone.0122470.

Vértes, P. E., Alexander-Bloch, A. F., Gogtay, N., Giedd, J. N., Rapoport, J. L., and Bullmore, E. T. (2012). “Simple models of human brain functional networks”. *Proceedings of the National Academy of Sciences* 109.15, 5868–5873.

Vessel, E., Starr, G. G., and Rubin, N. (2012). “The brain on art: intense aesthetic experience activates the default mode network”. *Frontiers in Human Neuroscience* 6. DOI: 10.3389/fnhum.2012.00066.

Walker, W. R., Vogl, R. J., and Thompson, C. P. (1997). “Autobiographical memory: Unpleasantness fades faster than pleasantness over time”. *Applied Cognitive Psychology: The Official Journal of the Society for Applied Research in Memory and Cognition* 11.5, 399–413.

Wammes, J. D., Lin, Q., Norman, K. A., and Turk-Browne, N. B. (2021). “Studying episodic memory using real-time fMRI”. *fMRI Neurofeedback*. Elsevier, 107–130.

Wang, F., Li, Y., and Gu, Z. (2017). “An MVPA method based on sparse representation for pattern localization in fMRI data analysis”. *Neurocomputing* 269, 206–211.

Wang, J., Ren, Y., Hu, X., Nguyen, V. T., Guo, L., Han, J., and Guo, C. C. (2017). “Test–retest reliability of functional connectivity networks during naturalistic fMRI paradigms”. *Human brain mapping* 38.4, 2226–2241.

Wang, S. (2010). *The neuroscience of everyday life. [Part 2 of 3]*. Teaching.

Weaverdyck, M. E., Lieberman, M. D., and Parkinson, C. (Apr. 2020). “Tools of the Trade Multivoxel pattern analysis in fMRI: a practical introduction for social and affective neuroscientists”. *Social Cognitive and Affective Neuroscience* 15.4, 487–509. DOI: 10.1093/scan/nsaa057.

Whitfield-Gabrieli, S., & Nieto-Castanon, A. (2012). Conn: a functional connectivity toolbox for correlated and anticorrelated brain networks. *Brain connectivity*, *2*(3), 125-141.

Wiesner, J. B. (1961). *The Thinking Machine, Tomorrow*. CBS News.

Yang, T., Silveira, S., Formuli, A., Paolini, M., Pöppel, E., Sander, T., & Bao, Y. (2019). Aesthetic experiences across cultures: neural correlates when viewing traditional Eastern or Western landscape paintings. *Frontiers in psychology*, *10*, 798.

Yeung, A. W. (2018). “An updated survey on statistical thresholding and sample size of fMRI studies”. *Frontiers in human neuroscience* 12, 16.

Yu, Q., Cheval, B., Becker, B., Herold, F., Chan, C. C., Delevoye-Turrell, Y. N., Guérin, S. M., Loprinzi, P., Mueller, N., and Zou, L. (2021). “Episodic Memory Encoding and Retrieval in Face-Name Paired Paradigm: An fNIRS Study”. *Brain Sciences* 11.7, 951.

Zhou, B., Pöppel, E., & Bao, Y. (2014). In the jungle of time: the concept of identity as a way out. *Frontiers in Psychology*, *5*, 844.

Acknowledgements

I would like to convey my sincere gratitude to those who have been critical in the pursuit of this thesis. The journey of this research would not have been possible without their invaluable understanding and support.

Firstly, I extend my utmost respect and deep appreciation to my esteemed advisor, Prof.Ernst Pöppel. His remarkable guidance and wisdom have served as a beacon during this research journey, illuminating the path and aiding me in navigating the challenges that arose. His continuous support has played an essential role in the successful completion of this thesis.

My colleagues and fellow students deserve a special mention for their contributions to this thesis. The enlightening discussions we had sparked numerous ideas and brought valuable insights to this work. Our collaborative spirit enriched this endeavor, fostering a conducive learning environment that facilitated the exchange of knowledge.

I extend my heartfelt gratitude to my family and parents. Their understanding, support, and unyielding faith in my capabilities have been a constant source of strength. Their unwavering belief in me has been critical in reaching this significant milestone in my academic journey. Also, a special thanks to my daughter, Aria, whose presence made the journey even more meaningful.

The journey of completing this thesis has been long, challenging, but incredibly rewarding. I am truly grateful for the opportunity to learn, grow, and develop as a researcher along the way. I look forward to exploring this field further, carrying forward the wisdom gained from this research.

In conclusion, I express my profound gratitude to everyone who has contributed to this journey, for their support and dedication have made the completion of this thesis possible. The knowledge and experiences I have gained are invaluable and will undoubtedly guide me in my future academic pursuits.

Affidavit

Affidavit

Gu, Yu_____

Surname, first name

_____

Street

_____

Zip code, town, country

I hereby declare, that the submitted thesis entitled:

Spatiotemporal regularities in the Brain: using endogenous stimuli in Functional Magnetic Resonance Imaging Studies

is my own work. I have only used the sources indicated and have not made unauthorized use of services of a third party. Where the work of others has been quoted or reproduced, the source is always given.

I further declare that the submitted thesis or parts thereof have not been presented as part of an examination degree to any other university.

Munich, 02.12.2024 _____Yu Gu_____

place, date Signature doctoral candidate